AD_____

Award Number: W81XWH-05-1-0470

TITLE: Genomic Instability and Breast Cancer

PRINCIPAL INVESTIGATOR: Junjie Chen, Ph.D.

CONTRACTING ORGANIZATION: Yale University
New Haven, CT 06520-8047

REPORT DATE: October 2007

TYPE OF REPORT: Annual

PREPARED FOR: U.S. Army Medical Research and Materiel Command
Fort Detrick, Maryland 21702-5012

REPORT DOCUMENTATION PAGE

Form Approved
OMB No. 0704-0188

1. REPORT DATE *(DD-MM-YYYY)*	**2. REPORT TYPE**	**3. DATES COVERED** *(From - To)*
01-10-2007	Annual	5 SEP 2006 - 4 SEP 2007

4. TITLE AND SUBTITLE

Genomic Instability and Breast Cancer

5a. CONTRACT NUMBER

5b. GRANT NUMBER
W81XWH-05-1-0470

5c. PROGRAM ELEMENT NUMBER

6. AUTHOR(S)
Junjie Chen, Ph.D.

E-Mail: Junjie.Chen@yale.edu

5d. PROJECT NUMBER

5e. TASK NUMBER

5f. WORK UNIT NUMBER

7. PERFORMING ORGANIZATION NAME(S) AND ADDRESS(ES)

Yale University
New Haven, CT 06520-8047

8. PERFORMING ORGANIZATION REPORT NUMBER

9. SPONSORING / MONITORING AGENCY NAME(S) AND ADDRESS(ES)
U.S. Army Medical Research and Materiel Command
Fort Detrick, Maryland 21702-5012

10. SPONSOR/MONITOR'S ACRONYM(S)

11. SPONSOR/MONITOR'S REPORT NUMBER(S)

12. DISTRIBUTION / AVAILABILITY STATEMENT
Approved for Public Release; Distribution Unlimited

13. SUPPLEMENTARY NOTES

14. ABSTRACT
Genomic instability is one of the key initiating events that lead to breast cancer development. We would like to gain further insights into the regulation of genomic stability and how the disruption of this regulation contributes to tumorigenesis. In the past year, we have identified several new components in the DNA damage pathway that act upstream of BRCA1.We have also discovered a novel link between aging and breast cancer development. In addition, we have established a platform for large-scale purification of protein complexes for the study of networks involved in breast cancer development. On top of these, we are also interested in developing novel agents for cancer treatment. In this arena, we have set up ascreen for cytotoxic agents that would target Chfr-deficient tumor cells. In a collaborative study, we identified compounds that would disrupt the interaction between BRCA1 and itsbinding partners for potential use as radiation sensitizer. Moreover, we have initiated acollection of stable cell lines expressing various protein kinases for the screening ofspecific kinase inhibitors. Together, these studies will help us understand breast cancer

15. SUBJECT TERMS
Tumor suppressor, Oncology, Cell signaling, DNA repair, cell biology

16. SECURITY CLASSIFICATION OF:			**17. LIMITATION OF ABSTRACT**	**18. NUMBER OF PAGES**	**19a. NAME OF RESPONSIBLE PERSON**
					USAMRMC
a. REPORT	**b. ABSTRACT**	**c. THIS PAGE**			**19b. TELEPHONE NUMBER** *(include area code)*
U	U	U	UU	87	

Table of Contents

Introduction:

My breast cancer research program initially focused on the tumor suppressor BRCA1. In the past few years, we and others showed that BRCA1 plays critical roles in the maintenance of genomic stability. Loss of BRCA1 function leads to cell cycle checkpoint defects and contributes to the development of familial breast cancer. We have now expanded our research program beyond BRCA1 and DNA damage checkpoint control. We are studying several other signal transduction pathways, which are important for the maintenance of genomic stability and cell proliferation. These include Chfr and mitotic checkpoint regulation, and more recently DBC1 and its role in the regulation of SIRT1. We hope that the in-depth studies of these pathways and our attempt to develop new biomarkers and targets for therapeutic interventions will help eradicate breast cancer in the future.

Body:

The ultimate goal of our current research is to expand our knowledge of breast cancer development, improve methods for early detection, identify new targets and develop novel therapies for breast cancer treatment of patients. The specific projects are:

Specific Aim 1: Develop biomarkers for the identification of patients with benign breast disease who are likely to develop malignant tumors.

We are interested in identifying genetic alternations that would contribute to the development of malignant breast cancers. The overall idea is to develop a series of biomarkers and test whether any of them would be informative for risk assessment in women with benign breast disease and/or ductal carcinoma in situ.

It has been established that DNA damage checkpoint and cellular senescence are essential for the prevention of cancer initiation (Mallette and Ferbeyre, 2007; Yaswen and Campisi, 2007; Zhang, 2007). This is certainly the case for breast cancer development, since many genes involved in DNA damage response including BRCA1, BRCA2, p53, Chk2 and ATM are mutated in familial and sporadic breast cancer patients. In the last fiscal year, we have established IHC assays for the detection of the activation of DNA damage responsive pathways. We have also generated monoclonal antibodies specifically recognizing key mitotic kinases Aurora A and Plk1. These reagents worked well for immunostaining of cultured cells (data not shown). We are now establishing IHC protocols for the use of these reagents in frozen and/or paraffin-embedded tumor samples.

We have further explored the regulation of DNA damage checkpoint response, especially the regulation of BRCA1 following DNA damage. Using a tandem affinity purification approach, we have identified two upstream regulators of BRCA1 as RAP80 and CCDC98 (Kim et al., 2007a; Kim et al., 2007b). These two proteins form a stable complex and are specifically involved in the recruitment of BRCA1 following DNA damage (Kim et al., 2007a; Kim et al., 2007b). While BRCA1 is frequently mutated in familial breast cancer cases, mutation of BRCA1 is rare in sporadic breast cancer,

raising the possibility that other components in the DNA damage pathways may be targets of mutations in sporadic breast cancers. We would like to determine whether RAP80 or CCDC98 are mutated in sporadic breast cancers and contribute to breast cancer development. We have initiated collaboration with Dr. Nazneen Rahman at United Kingdom to explore this possibility.

Based on our recent discoveries, we now know that BRCA1 localizes to DNA damage sites via its interaction with the CCDC98/RAP80 complex. However, how RAP80 itself is recruited to the sites of DNA breaks remains a mystery. One clue that we had is that the ubiquitin-interacting motifs (UIMs) at the N-terminus of RAP80 are important for its focus localization. Based on *in vitro* studies, RAP80 UIMs interacts with Lys-63 linked, but not Lys-48 linked, polyubiquitination chains (Kim et al., 2007a). Therefore we were looking for an E3 ubiquitin ligase that would promote Lys-63 polyubiquitination and act upstream of RAP80/BRCA1. Interestingly, the answer finally came from a different project ongoing in the lab.

As I mentioned in our original application, we also studied a protein named Chfr (checkpoint protein with FHA and Ring domains) in the regulation of mitotic progression and breast cancer development. In order to determine the specificities of Chfr's FHA and RING domains, we isolated Ring domain nuclear factor 8 (RNF8) as a control, which represents the only other known mammalian protein that shares a similar domain organization (e.g. containing both FHA and RING domain). Interestingly and surprisingly, we found that RNF8, but not Chfr, can localize to DNA damage-induced foci. The Era of Hope award allowed us to further explore the role of RNF8 in DNA damage response. Our ongoing studies demonstrated that RNF8 and its RING domain E3 ligase activity are required for RAP80 and BRCA1's localization to DNA damage sites. These observations led to a hypothesis that RNF8 ubiquitinates one or several substrates at the sites of DNA damage. RAP80 then binds to these polyubiquitinated proteins and thus be recruited to the sites of DNA breaks. This unexpected discovery advanced our understanding of DNA damage response in humans. A manuscript summarizing these findings was just accepted for publication by Cell (Huen et al., 2007).

Besides the activation of DNA damage checkpoint pathways, senescence has also been implicated to be a barrier for cancer development. It remains elusive how senescence or aging process are normally regulated in humans and whether or not dysregulation of this pathway would contribute to breast cancer development. We decided to focus our attention on protein deacetylase SIRT1, since this protein has been shown to be required for aging or longevity regulation from yeast to mice. Using a tandem affinity purification approach we recently established in the lab, we purified SIRT1-containing complexes from human cells and identified DBC1 (deleted in breast cancer 1) as a major SIRT1-associated protein. Our subsequent biochemical studies suggest that DBC1 is a negative regulator of SIRT1 **(Figure 1)**. Moreover, DBC1 is involved in SIRT1-dependent stress response pathway (**Figure 2**). Together, this study established DBC1 as a major inhibitor of SIRT1 *in vivo* (**3rd revision under**

consideration by Nature). It also suggests that upregulation of SIRT1 activity (in the absence of DBC1) may allow cells to bypass senescence and promote malignant transformation, a hypothesis we are testing right now.

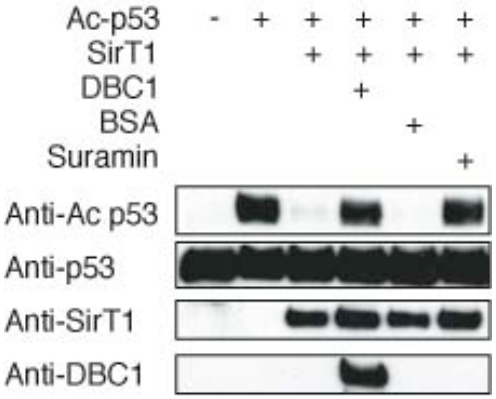

Figure 1. DBC1 inhibits SirT1 deacetylase activity. Acetylated p53 was incubated with either SirT1 or the SirT1-DBC1 complex in the presence of NAD as indicated. p53 acetylation was then assessed by immunoblotting with anti-acetyl-p53 antibody. Suramin, a small molecule inhibitor of SirT1 inhibitor, was included as a control in these experiments.

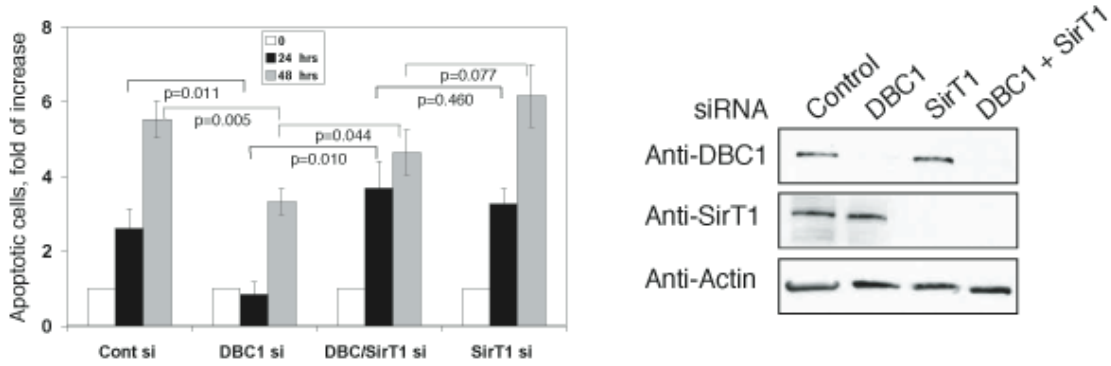

Figure 2. DBC1 regulates SirT1 function following stress stimuli. A549 cells were transfected with control, DBC1, SirT1 or DBC1 and SirT1 siRNAs. 72 hours later, transfected cells were treated with etoposide (20 μM, 24, 48 hours). The apoptotic cells were determined by Annexin V staining. The Y-axis represents fold of increase of apoptotic cells compared to mock-treated sample. The number represents the average of three different experiments and error bars represent the s.e.m.; *P* value was determined by Student's *t*-test. Cell lysates were blotted with anti-DBC1 or anti-SirT1 antibodies to confirm the downregulation of DBC1 or SirT1.

We would like to expand our understanding of genetic alternations that contribute to breast cancer development. Using bioinformatic approach, Dr. LaBaer has put together a nice collection of 1000 genes that have been implicated in breast cancer development (Witt et al., 2006). We would like to use these 1000 genes as our base to understand the interactive pathways involved in breast cancer development. The approach we are going to take is to purify all complexes containing these breast cancer related proteins. As mentioned above, we have recently adopted a tandem affinity protocol for the identification of protein complexes. We constructed a vector for the expression of SBP-Flag-S-protein tagged-protein in mammalian cells. SBP is a small peptide that binds effectively to streptavidin beads, which can be easily eluted with a solution containing biotin because of the higher affinity of the biotin/streptavidin

interaction. Flag-epitope tags have been used successfully for anti-Flag mAb-based affinity purification of protein complexes in mammalian cells. S peptide is another small peptide that binds efficiently with S protein beads and can also be used for affinity purification. All three affinity-purification methods worked very well and at least two sequential steps are necessary to obtain highly purified protein complexes in mammalian cells. To facilitate the transition to large-scale studies, we have now generated a Gateway compatible SBP-Flag-S-tagged mammalian expression construct, which allows us to transfer cDNAs into this vector via recombination-based HTS method. We have used this method and successfully identified the RAP80/Ccdc98 complex as BRCA1-associated proteins (Kim et al., 2007a; Kim et al., 2007b). We also used the same methodology and identified DBC1 as a major SIRT1 associated protein in mammalian cells. These testify the success of this method. Because of our expertise on DNA damage response and cell cycle regulation, we selected 96 genes from the BC1000 collection that are involved in these processes as the first step of this project. We are now generating stable cell lines expressing respectively these DNA damage and cell cycle proteins (**Figure 3**). We will purify protein complexes before and after DNA damage and at different cell cycle phases. The identities of these associated proteins will be revealed by mass spectrometry analysis. We hope that this large-scale study of protein complexes involved in breast cancer development will shed light on the complexity of signal transduction networks involved in breast cancer development. It may also provide some new biomarkers or targets for therapeutic intervention.

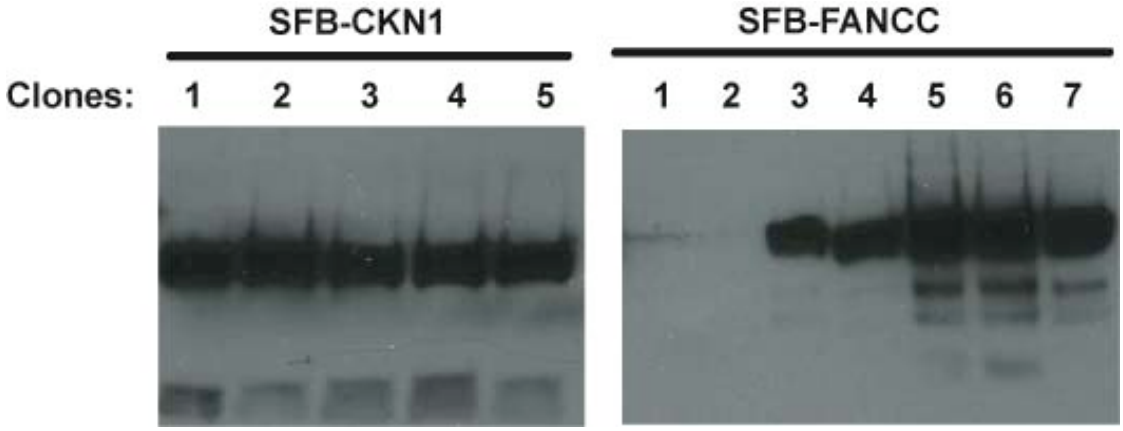

Figure 3. Generate cell lines stably expressing triple tagged breast cancer related proteins. 293T cells were transfected respectively with constructs encoding triple tagged (SFB-tagged) Cockayne syndrome protein 1 (CKN1) or Fanconi anemia complementation group C protein (FANCC). Stable clones were selected in medium containing puromycin. The expression of tagged proteins in these cell lines was analyzed by Western blots using anti-Flag antibody.

Specific Aim 2: Explore Chfr/Aurora pathway for breast cancer treatment.

As stated in our application, we studied the role of a new mitotic regulator Chfr in tumorigenesis. We have shown that Chfr directly regulates Aurora A expression. Increased Aurora A expression leads to genomic instability and probably explains the enhanced tumorigenesis in the absence of Chfr (Yu et al., 2005). Since Chfr is frequently downregulated in breast cancer while Aurora A is commonly upregulated in breast cancer, we hypothesize that the Chfr/Aurora pathway is important for breast cancer development. Tumors with Chfr deficiency are likely to depend heavily on Aurora A overexpression for cell proliferation. We originally proposed to test whether Aurora kinase inhibitor VX680 (Doggrell, 2004; Harrington et al., 2004) would be particularly effective in treating tumors with Chfr deficiency. For this purpose, we first generated a HeLa derivative cell line that stably expresses Chfr. Since HeLa cells normally do not express Chfr, we reason that we can use this pair of cell lines to study drug sensitivity in the presence or absence of Chfr. To specifically examine the correlation between Chfr expression and drug sensitivity in breast cancer, we now generated two pairs of breast cancer cell lines (MCF7 and MCF7+shRNA-Chfr, T47D and T47D+shRNA-Chfr) with or without Chfr expression (**Figure 4**). While we were just about to start this study, our recent finding using Aurora A-deficient mice raised the question about the potential side effects of using Aurora A inhibitors.

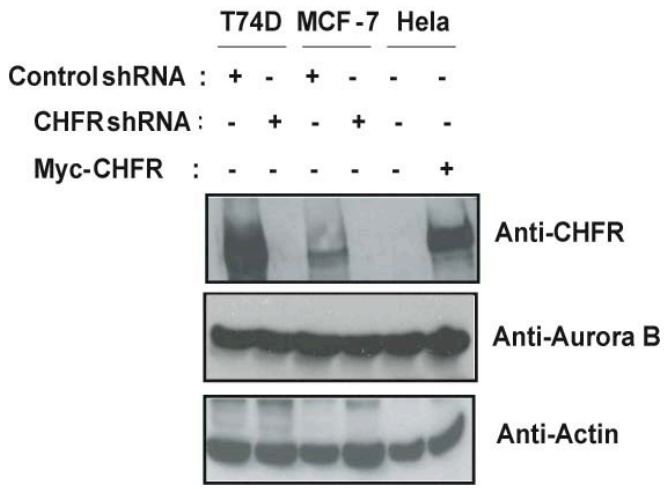

Figure 4. Establish breast cancer derivative cell lines with or without Chfr expression. Briefly, MCF7 and T47D cells were transfected with Chfr shRNA constructs. Stable clones were selected and Chfr expression was analyzed by Western blots (data not shown). We have successfully generated both MCF7 and T47D derivative cell lines with undetectable Chfr expression. Cell lysates were prepared from these cell lines and HeLa or HeLa cells stably transfected with Chfr. Western blot with Chfr antibody was performed to confirm the expression of Chfr in these cells. Anti-Aurora B and anti-actin immunoblots were included as loading controls.

In a project supported by NIH, we generated Aurora A knockout mice. Complete ablation of Aurora A leads to early embryonic lethality (data not shown), support a critical role of Aurora A in mitotic regulation. Surprisingly we found that Aurora A+/- mice developed tumors at a higher frequency than wild-type littermates (**Figure 5**), suggesting that an incomplete downregulation of Aurora A activity may also affect mitotic progression and lead to tumorigenesis. We are still determining whether this is indeed the case. This observation may not be directly applied to the development of VX680 or other Aurora inhibitors, since these small molecules inhibit not only Aurora A but also Aurora B and probably other kinases. Nevertheless, we are concerned about the potential side effects of specific Aurora A-based therapy for cancer treatment.

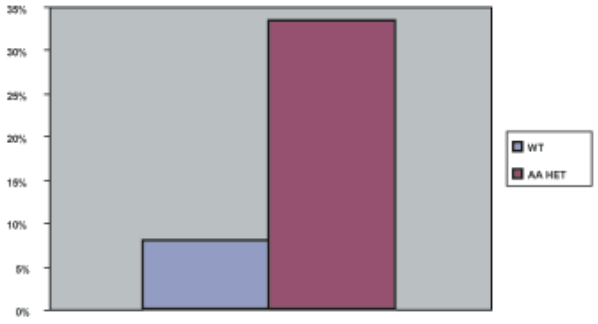

Organ	WT	HET
	(n=25)	(n=51)
	56 weeks	57 weeks
Lung	1	12
Intestine		1
Spleen		3
Liver	1	

Figure 5. Increase tumor incidence observed in Aurora A+/- mice. Wild-type and Aurora A+/- mice were all generated from the crossing of Aurora A+/- males and females. While we never obtained any viable Aurora A-/- mice, wild-type and Aurora A+/- mice appear to be normal. We sacrificed these animals when they were approximately one-year old and determined tumor incidence in all major organs. The percentages of tumor incidence are shown in the left panel. The right panel indicates the organ site affected by tumors in wild-type and Aurora A+/- mice.

While I was debating whether we should test Aurora inhibitors using Chfr-deficient cells, a recent publication by Dr. Petty's group further confirmed the frequent downregulation of Chfr in breast cancer (Privette et al., 2007), which supports our initial hypothesis that we may be able to take advantage of Chfr downregulation for the development of specific anti-cancer agents. We reason that these agents would have fewer side effects since Chfr is expressed in normal tissues, but specifically downregulated in tumors. We decided to initiate an unbiased screening for chemicals that are selectively toxic to Chfr-deficient cells. We just initiated this study, which is performed in collaboration with Dr. Taosheng Chen, who runs a High Throughput Screening Facility at St. Jude's children's hospital. We are performing an initial screen on a small library (400 compounds) using the T47D pair of cell lines. Any positives from this initial screen will be retested in the two other pairs of cell lines (MCF7 and MCF7+shRNA-Chfr, HeLa and HeLa+Chfr). We hope to use this first round of screening as proof-of-principle and determine which cell line pair is better for a larger scale screen, which we are planning to do using a collection of 6000 bioactive compounds. We hope that this study will produce some leading compounds that are specifically toxic to Chfr-deficient tumor cells.

Specific Aim 3: Develop novel adjuvant chemotherapeutic agents.

The ultimate goal of this project is to develop new therapeutic agents for breast cancer treatment. Since BRCA1-deficient cells are also known to be more sensitive to DNA damaging agents, we might be able to develop BRCA1 inhibitors that would sensitize sporadic breast cancer cells to radiation and/or standard chemotherapeutic drugs.

As we reported last year, we collaborated with Dr. Wei Wang at University of New Mexico to design small molecules that would specifically disrupt BRCA1 BRCT domain and phospho-protein interaction. Using *in silico* docking approach and initial screening of 74 compounds, we identified two compounds that could disrupt BRCA1 and phospho-BACH1 peptide interaction *in vitro*. Unfortunately the subsequent first eight (based on the first compound) and then 20 (based on the second compound) modified compounds do not improve the potency of the two compounds. Moreover, none of them showed any efficacy in sensitizing tumor cells *in vivo* (data not shown).

As reported last time, we also worked with Dr. Amar Natarajan at University of Texas Medical Branch, Galveston, TX, who developed a high-throughput assay for the identification of BRCA1 inhibitors (Lokesh et al., 2006). As we tested previously, their initial compound BI-94 worked well *in vitro*. Unfortunately, the BI-94 derivatives did not show any increased affinity or specificity (data not shown). Because of this, Dr. Natarajan went on and screened ~75K compounds and identified 57 hits. We are now testing these hits in our *in vivo* assays.

We can increase our success rate if we are able to identify additional drugable targets for anti-cancer treatment. So far the best targets for drug development are still protein kinases since the assays for HTS are well established. As a basic science laboratory, we are interested in establishing assays and collaborate with others for the development of kinase inhibitors. One of the major problems in the screening of small molecules for kinase inhibitors is the lack of specificity. Since only limited purified kinases are commercially available, it is difficult to know how specific any inhibitors are before conducting extensive *in vivo* studies. Because of this limitation, we decided to establish a large panel of tagged protein kinases for both *in vivo* and *in vitro* studies. Again, we are taking advantage of the triple-tagged Gateway compatible vectors we mentioned above in Aim 1. We have now cloned 255 kinases in these vectors. As a starting point, we have established cell lines stably expressing ~30 different kinases, respectively. There are several advantages of using human cell lines for the expression of these kinases. First, because these kinases are expressed in native environment, they are likely to be properly modified (since many kinases need to be activated by post-translational modification). Second, many kinases only become active when they are associated with their regulatory subunits (for example cyclin-dependent kinases). The kinases (or kinase complexes) purified from human cells are already in complex with their corresponding regulatory subunits. This gives us another advantage, since in principle we will not only be able to screen for inhibitors that block the activities of the kinase domains, but also screen for agents that would disrupt the interaction between kinases and their regulatory subunits. We are now testing whether these purified kinases are active *in vitro*. Interestingly, some kinases have very low autophosphorylation activities, but show strong kinase activities toward their physiological substrates (see **Figure 6**).

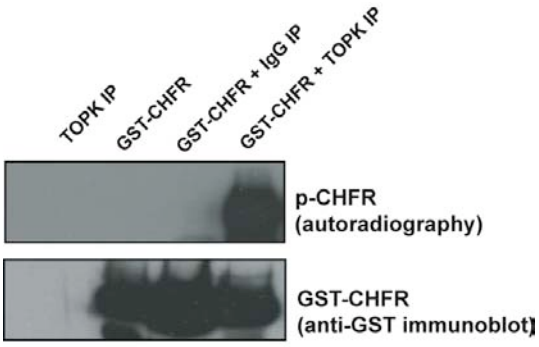

Figure 6. **Confirm TOPK kinase activity *in vitro*.** We generated a cell line stably expressing tagged TOPK kinase. Using this cell line, we were able to purify TOPK kinase and its associated proteins. One of them turned out to be Chfr (data not shown). Chfr is likely to be a substrate of TOPK, since TOPK has very low autophosphorylation activity but can robustly phosphorylate GST-Chfr *in vitro* (autoradiography shown in the upper panel). Equal amounts of GST-Chfr were included in IP/Kinase reactions as shown by anti-GST immunoblot (lower panel).

Therefore, we believe that the establishment of these panel of cell lines, each stably expressing a tagged kinase, will be abundantly useful in our future basic and translational studies. First, we will use these cell lines to identify all kinase-associated proteins by mass spectrometry analyses. This will help us identify not only regulatory subunits but also potential *in vivo* substrates of various kinases. Second, we can use them to define the consensus phosphorylation sites by different kinases. This part of the work will be done in collaboration with Dr. Ben Turk at Yale University, since Dr. Turk has established a HTS for the determination of consensus kinase phosphorylation sites (Hutti et al., 2004). We hope that the identification of regulatory subunits and physiological substrates of these kinases will help us further develop any kinase inhibitors, since we can use these substrates for establishing *in vitro* screening methods and also as *in vivo* surrogate markers for testing the potency and specificity of any potential kinase inhibitors.

Training potential for the PI:

The reviewer of our first annual report suggested us to provide a brief summary of how this training award is preparing the PI for an independent career in breast cancer. I appreciate this suggestion and would like to elaborate here what I have learned from my experience in carrying out these projects in the last two years.

The most important thing I learned is that our basic research needs to focus on solving clinical questions. Because of this training award, I have the opportunity to interact with many clinicians first at Mayo Clinic and now at Yale University. I am a member of breast cancer interest group and attend monthly meeting presented by both clinicians and basic scientists. From these interactions, I become more aware of the complexity of the clinical questions that I overlooked in my own research. I now realize that a comprehensive understanding of the biological system is the key for developing any useful agents that would have clinical impacts. Because of this realization, we expanded our research from the studies of individual proteins to intermediate-to-large scale studies, attempting to understand the interplays among different cellular pathways. While we will still conduct mechanistic-based studies of individual proteins and pathways, we hope

that these larger scale studies we initiated will provide useful information, reagents and foundation for our understanding of the biological system that leads to the development of breast cancer.

The other valuable lesson I learned is that it takes efforts from scientists from many disciplines to accomplish this goal of eradicating breast cancer. From my own research, I now appreciate the amount of work and expertise it requires to develop any reagents, assays or treatments that can have clinical applications. While it is important to accomplish one's particular goals in individual laboratories, it takes a lot more of organization and coordination skills to translate basic findings into clinical practice. This training award not only allows me the flexibility to start to answer some translational questions, but it also gives me an opportunity to establish myself as a leader in the basic and translational breast cancer research in the near future. I am now intimately involved in the organization of Yale breast cancer SPORE program. I hope by participating in this important process, I will learn how to integrate many research principles for the common goal of finding cures for breast cancer patients.

Key Research Accomplishments:

- We have identified two new BRCA1 associated proteins RAP80 and CCDC98 and demonstrated that these proteins act upstream of BRCA1 and participate in the regulation of BRCA1 following DNA damage. In addition, we have discovered a new E3 ubiquitin ligase RNF8, which plays a role early in DNA damage response.

- We have initiated a study of SIRT1 in an attempt to understand the role of senescence in tumorigenesis and aging. We are exciting to report that we have found the first SIRT1 regulator, DBC1, in the cell. Since DBC1 was originally cloned as a gene deleted in breast cancer, we will further explore whether DBC1/SIRT1 interaction would be altered in breast cancer and contribute to breast cancer development.

-We have started a large-scale study trying to understand the multiplicity of various signaling pathways involved in breast cancer development. This will be achieved by the identification of all breast cancer-related protein complexes. In the first phase of these experiments, we will purify 96 protein complexes under a variety of physiological conditions. We have already established twenty stable cell lines, each expressing a different protein that is known to be involved in breast cancer tumorigenesis.

-We have generated two paired breast cancer derivative cell lines with or without Chfr expression. An unbiased screening for cytotoxic agents that have specificity for Chfr-deficient tumor cells is in progress.

- We are continuing our collaboration with Dr. Amar Natarajan for the screening of compounds that would disrupt BRCA1 BRCT domain-phospho-peptide interaction. We were unable to improve the initial leading compound BI-94. A larger screening was conducted and we are now testing the compounds obtained from the second screen.

-We want to develop a panel of cell lines that would allow us to reliably produce all protein kinases for future screening of protein kinase inhibitors. We now have 255 kinases and have already generated ~30 stable cell lines, each expressing a tagged protein kinase in human cells.

Reportable Outcomes:

Kim, H., Chen, J., and Yu, X. (2007a). Ubiquitin-binding protein RAP80 mediates BRCA1-dependent DNA damage response. Science *316*, 1202-1205.

Kim, H., Huang, J., and Chen, J. (2007b). CCDC98 is a BRCA1-BRCT domain-binding protein involved in the DNA damage response. Nat Struct Mol Biol *14*, 710-715.

Huen, M.S.Y., Grant, R. Manke, I., Minn, K., Yu, X., Yaffe, M.B., and Chen, J. (2007) RNF8 transduces the DNA damage signal via histone ubiquitylation and checkpoint protein assembly. Cell, in press (expected publication date is Nov. 30, 2007).

Conclusions:

We have initiated all of the studies proposed in our application. We are accumulating reagents and establishing model systems for these studies. This groundwork will allow us to test our hypotheses in clinical settings in the near future.

References:

Doggrell, S. A. (2004). Dawn of Aurora kinase inhibitors as anticancer drugs. Expert Opin Investig Drugs *13*, 1199-1201.

Harrington, E. A., Bebbington, D., Moore, J., Rasmussen, R. K., Ajose-Adeogun, A. O., Nakayama, T., Graham, J. A., Demur, C., Hercend, T., Diu-Hercend, A.*, et al.* (2004). VX-680, a potent and selective small-molecule inhibitor of the Aurora kinases, suppresses tumor growth in vivo. Nat Med *10*, 262-267.

Huen, M.S.Y., Grant, R. Manke, I., Minn, K., Yu, X., Yaffe, M.B., and Chen, J. (2007) RNF8 transduces the DNA damage signal via histone ubiquitylation and checkpoint protein assembly. Cell, in press.

Hutti, J. E., Jarrell, E. T., Chang, J. D., Abbott, D. W., Storz, P., Toker, A., Cantley, L. C., and Turk, B. E. (2004). A rapid method for determining protein kinase phosphorylation specificity. Nat Methods *1*, 27-29.

Kim, H., Chen, J., and Yu, X. (2007a). Ubiquitin-binding protein RAP80 mediates BRCA1-dependent DNA damage response. Science *316*, 1202-1205.

Kim, H., Huang, J., and Chen, J. (2007b). CCDC98 is a BRCA1-BRCT domain-binding protein involved in the DNA damage response. Nat Struct Mol Biol *14*, 710-715.

Lokesh, G. L., Rachamallu, A., Kumar, G. D., and Natarajan, A. (2006). High-throughput fluorescence polarization assay to identify small molecule inhibitors of BRCT domains of breast cancer gene 1. Anal Biochem *352*, 135-141.

Mallette, F. A., and Ferbeyre, G. (2007). The DNA damage signaling pathway connects oncogenic stress to cellular senescence. Cell Cycle *6*, 1831-1836.
Privette, L. M., Gonzalez, M. E., Ding, L., Kleer, C. G., and Petty, E. M. (2007).

Altered expression of the early mitotic checkpoint protein, CHFR, in breast cancers: implications for tumor suppression. Cancer Res *67*, 6064-6074.

Witt, A. E., Hines, L. M., Collins, N. L., Hu, Y., Gunawardane, R. N., Moreira, D., Raphael, J., Jepson, D., Koundinya, M., Rolfs, A*., et al.* (2006). Functional proteomics approach to investigate the biological activities of cDNAs implicated in breast cancer. J Proteome Res *5*, 599-610.

Yaswen, P., and Campisi, J. (2007). Oncogene-induced senescence pathways weave an intricate tapestry. Cell *128*, 233-234.

Yu, X., Minter-Dykhouse, K., Malureanu, L., Zhao, W. M., Zhang, D., Merkle, C. J., Ward, I. M., Saya, H., Fang, G., van Deursen, J., and Chen, J. (2005). Chfr is required for tumor suppression and Aurora A regulation. Nat Genet *37*, 401-406.

Zhang, H. (2007). Molecular signaling and genetic pathways of senescence: Its role in tumorigenesis and aging. J Cell Physiol *210*, 567-574.

Appendices:

Manuscript 1:

Kim, H., Chen, J., and Yu, X. (2007a). Ubiquitin-binding protein RAP80 mediates BRCA1-dependent DNA damage response. Science *316*, 1202-1205.

Manuscript 2:

Kim, H., Huang, J., and Chen, J. (2007b). CCDC98 is a BRCA1-BRCT domain-binding protein involved in the DNA damage response. Nat Struct Mol Biol *14*, 710-715.

Manuscript 3:

Huen, M.S.Y., Grant, R. Manke, I., Minn, K., Yu, X., Yaffe, M.B., and Chen, J. (2007) RNF8 transduces the DNA damage signal via histone ubiquitylation and checkpoint protein assembly. Cell, in press.

Ubiquitin-Binding Protein RAP80 Mediates BRCA1-Dependent DNA Damage Response

Hongtae Kim, *et al.*

Science **316**, 1202 (2007);
DOI: 10.1126/science.1139621

Science (print ISSN 0036-8075; online ISSN 1095-9203) is published weekly, except the last week in December, by the American Association for the Advancement of Science, 1200 New York Avenue NW, Washington, DC 20005.

class of DNA repair proteins that uses tandem UIM domains as part of its recruitment to DSBs. In contrast to IRIF formation, incomplete BRCA1 localization at laser-induced DSBs still occurs in the absence of γH2AX (*22*), MDC1 (*17*), or RAP80 (Fig. 3, E and F). These findings may reflect the fact that BRCA1/BARD1 heterodimers are components of multiple distinct complexes (*9*) and that each may access DSBs by different mechanisms. Taken together, these findings strongly suggest an essential role for ubiquitin recognition by a specific BRCA1 complex in the response to DSB formation. In addition, the synthesis and turnover of certain polyubiquitinated structures by BRCA1 E3 and BRCC36 DUB activities, respectively, may contribute to BRCA1-dependent DSB repair.

References

1. C. H. Bassing *et al.*, *Cell* **114**, 359 (2003).
2. A. Celeste *et al.*, *Cell* **114**, 371 (2003).
3. Y. Wang *et al.*, *Nat. Genet.* **37**, 750 (2005).
4. G. S. Stewart, B. Wang, C. R. Bignell, A. M. Taylor, S. J. Elledge, *Nature* **421**, 961 (2003).
5. M. Stucki *et al.*, *Cell* **123**, 1213 (2005).
6. E. P. Rogakou, C. Boon, C. Redon, W. M. Bonner, *J. Cell Biol.* **146**, 905 (1999).
7. A. Celeste *et al.*, *Science* **296**, 922 (2002); published online 4 April 2002 (10.1126/science.1069398).
8. C. H. Bassing *et al.*, *Proc. Natl. Acad. Sci. U.S.A.* **99**, 8173 (2002).
9. R. A. Greenberg *et al.*, *Genes Dev.* **20**, 34 (2006).
10. S. B. Cantor *et al.*, *Cell* **105**, 149 (2001).
11. X. Yu, L. C. Wu, A. M. Bowcock, A. Aronheim, R. Baer, *J. Biol. Chem.* **273**, 25388 (1998).
12. Y. Shiloh, *Nat. Rev. Cancer* **3**, 155 (2003).
13. J. Peng *et al.*, *Nat. Biotechnol.* **21**, 921 (2003).
14. F. Wu-Baer, K. Lagrazon, W. Yuan, R. Baer, *J. Biol. Chem.* **278**, 34743 (2003).
15. J. R. Morris, E. Solomon, *Hum. Mol. Genet.* **13**, 807 (2004).
16. J. Polanowska, J. S. Martin, T. Garcia-Muse, M. I. Petalcorin, S. J. Boulton, *EMBO J.* **25**, 2178 (2006).
17. S. Bekker-Jensen *et al.*, *J. Cell Biol.* **173**, 195 (2006).
18. Y. Dong *et al.*, *Mol. Cell* **12**, 1087 (2003).
19. X. Chen, C. A. Arciero, C. Wang, D. Broccoli, A. K. Godwin, *Cancer Res.* **66**, 5039 (2006).
20. X. Yu, S. Fu, M. Lai, R. Baer, J. Chen, *Genes Dev.* **20**, 1721 (2006).
21. X. I. Ambroggio, D. C. Rees, R. J. Deshaies, *PLoS Biol.* **2**, E2 (2004).
22. A. Celeste *et al.*, *Nat. Cell Biol.* **5**, 675 (2003).

Supporting Online Material

www.sciencemag.org/cgi/content/full/316/5828/1198/DC1
Materials and Methods
Figs. S1 to S4
References and Notes

4 January 2007; accepted 10 April 2007
10.1126/science.1139516

Ubiquitin-Binding Protein RAP80 Mediates BRCA1-Dependent DNA Damage Response

Hongtae Kim,[1] Junjie Chen,[1]* Xiaochun Yu[2]*

Mutations in the breast cancer susceptibility gene 1 (*BRCA1*) are associated with an increased risk of breast and ovarian cancers. BRCA1 participates in the cellular DNA damage response. We report the identification of receptor-associated protein 80 (RAP80) as a BRCA1-interacting protein in humans. RAP80 contains a tandem ubiquitin-interacting motif domain, which is required for its binding with ubiquitin in vitro and its damage-induced foci formation in vivo. Moreover, RAP80 specifically recruits BRCA1 to DNA damage sites and functions with BRCA1 in G_2/M checkpoint control. Together, these results suggest the existence of a ubiquitination-dependent signaling pathway involved in the DNA damage response.

Despite developing various DNA lesions generated during DNA replication or after exposure to environmental agents, cells normally maintain their genomic integrity and prevent neoplastic transformation because of the existence of several cell cycle checkpoints and DNA repair systems (*1*–*3*). Many proteins [including the protein kinase ataxia-telangiectasia mutated (ATM), γ-H2AX, mediator of DNA damage checkpoint protein 1 (MDC1), Nijmegen breakage syndrome 1 (NBS1), BRCA1, and checkpoint kinases 1 and 2 (Chk1 and Chk2)] are involved in the ionizing radiation (IR)–induced DNA damage response pathway (*4*). ATM is recruited to and activated at the sites of DNA breaks. Activated ATM transduces DNA damage signals to downstream proteins, including BRCA1. *BRCA1* encodes a tumor suppressor gene that is mutated in ~50% of hereditary breast and ovarian cancer patients (*5*, *6*). The human BRCA1 protein contains an N-terminal RING finger domain that has intrinsic E3 ubiquitin ligase activity and tandem BRCA1 C-terminal (BRCT) domains at its C terminus, which are phosphoserine- or phosphothreonine-binding motifs (*7*–*9*). Many disease-causing mutations are detected within these two regions of BRCA1.

Although BRCA1 is recruited to the sites of DNA breaks and participates in cell cycle checkpoint control, it remains obscure how the recruitment of BRCA1 is controlled in the cell. We purified BRCA1-BRCT domains from human leukemia K562 cells stably expressing this protein with N-terminal S-tag, Flag epitope, and streptavidin-binding peptide (SFB) triple tags (SFB-BRCA1-BRCT). We detected three specific bands that eluted with the SFB-BRCA1-BRCT domain but not with the SFB-BARD1-BRCT domain (Fig. 1A), where BARD1 signifies the BRCA1-associated RING domain protein 1. Mass spectrometry analysis revealed that these three proteins (respectively) are BRCA1-associated C-terminal helicase (BACH1), C-terminal binding protein–interacting protein (CtIP), and RAP80. BACH1 and CtIP are two known BRCA1 BRCT domain-binding proteins (*9*, *10*). RAP80 was originally identified as a retinoid-related testis-associated protein (*11*). The physiological function of RAP80 is unknown. We first confirmed the association between RAP80 and BRCA1 both in vitro and in vivo (Fig. 1B and fig. S1) (*12*). The interaction between BRCA1 and RAP80 remained the same before or after DNA damage (Fig. 1C).

BRCA1 relocalizes to sites of DNA breaks in cells exposed to IR. Immunostaining showed RAP80 to be evenly distributed in the nucleoplasm in normal cells (Fig. 2A). However, after exposure of cells to IR, RAP80 relocalized to foci that colocalized with γ-H2AX and BRCA1 (Fig. 2, A and B). RAP80 also associated with chromatin only in cells exposed to IR (Fig. 2C). Together, these data indicate that the localization of RAP80, like that of BRCA1, is regulated in response to DNA damage.

RAP80 isolated from irradiated cells migrated more slowly during SDS–polyacrylamide gel electrophoresis (SDS-PAGE) than did RAP80 isolated from unirradiated cells. Moreover, phosphatase treatment reversed the slow mobility of RAP80 prepared from irradiated cells (Fig. 2D), indicating that RAP80 may be phosphorylated in cells exposed to IR. We confirmed this using a phosphospecific antibody raised against a phosphorylation site that we identified (Ser^{101}; fig. S2). The ATM protein kinase is activated in response to DNA damage and phosphorylates many proteins involved in the DNA damage response. Treatment of cells with two different ATM kinase inhibitors, wortmannin and caffeine, abolished the IR-induced mobility shift of RAP80 (fig. S3A). The mobility shift of RAP80 was only observed in cells expressing wild-type (WT) ATM but not in ATM-deficient cells (Fig. 2E). These data suggest that ATM is required for damage-induced phosphorylation of RAP80.

The accumulation of RAP80 to the sites of DNA breaks depended on MDC1 and H2AX (Fig. 2, F and G) but not on NBS1, p53 binding

[1]Department of Therapeutic Radiology, Yale University School of Medicine, Post Office Box 208040, New Haven, CT 06520, USA. [2]Division of Molecular Medicine and Genetics, Department of Internal Medicine, University of Michigan Medical School, 109 Zina Pitcher Place, 1520 Biomedical Science Research Building, Ann Arbor, MI 48109, USA.

*To whom correspondence should be addressed. E-mail: Junjie.chen@yale.edu (J.C.); xiayu@med.umich.edu (X.Y.)

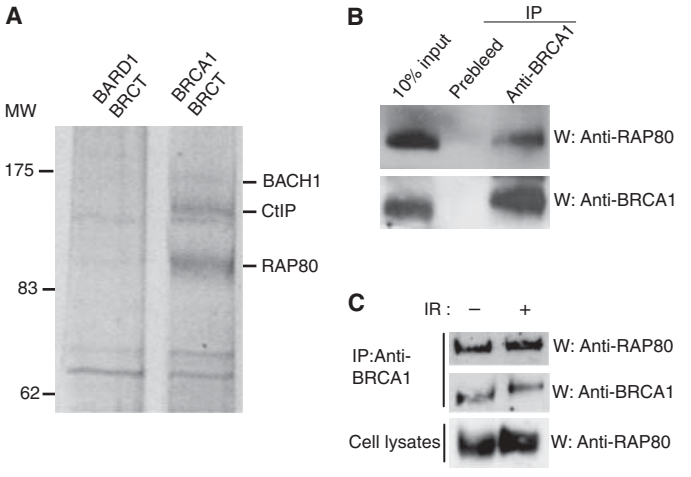

Fig. 1. Identification of RAP80 as a BRCA1-binding protein. (**A**) Silver staining of affinity-purified BRCA1-BRCT complexes. The cell extracts prepared from K562 cells stably expressing SFB-BRCA1-BRCT or SFB-BARD1-BRCT were subjected to two rounds of affinity purification. Final elutes were analyzed by SDS-PAGE and visualized by silver staining. The specific bands were excised from the silver-stained gel, and the peptides were identified by matrix-assisted laser desorption/ionization–time-of-flight mass spectrometry. Lines indicate protein bands corresponding to BACH1, CtIP, and RAP80. (**B**) The interaction between endogenous BRCA1 and RAP80. We performed immunoprecipitation (IP) reactions using preimmune serum or antibody to BRCA1. The immunoprecipitates were subjected to immunoblotting analyses with antibodies to BRCA1 or RAP80. (**C**) The interaction between BRCA1 and RAP80 before and after exposure of cells to IR. Lysates prepared from mock-treated or irradiated 293T cells were immunoprecipitated with antibody to BRCA1. The immunoprecipitates were separated by SDS-PAGE and immunoblotted with the indicated antibodies (top two lanes). The amount of endogenous RAP80 in cells before and after radiation was shown in the bottom lane.

protein 1 (53BP1), or BRCA1 (fig. S3, B to D). When we reduced endogenous RAP80 expression using RAP80 small interfering RNAs (siRNAs), we still detected damage-induced foci formation of MDC1, γ-H2AX, and 53BP1. However, no BRCA1 foci were present in these RAP80-depleted cells (Fig. 2H), suggesting that RAP80 acts upstream of BRCA1 and is required for the accumulation of BRCA1 to sites of DNA breaks.

We also determined which regions of RAP80 are important for its focus localization. Full-length and several internal deletion mutants of RAP80 localized to nuclear foci in cells with DNA damage, whereas RAP80D1 and RAP80D2 did not (Fig. 3A and fig. S4A). Because RAP80D1 and RAP80D2 are the only two internal deletion mutants that lack the two putative ubiquitin-interacting motifs (UIMs) (*13*), these results imply that the region containing UIMs may be required for RAP80 localization to DNA damage foci. The putative UIMs in RAP80 largely match with the UIM consensus sequence (fig. S4B). To determine whether the tandem RAP80 UIMs indeed bind to ubiquitin, we used a ubiquitin–

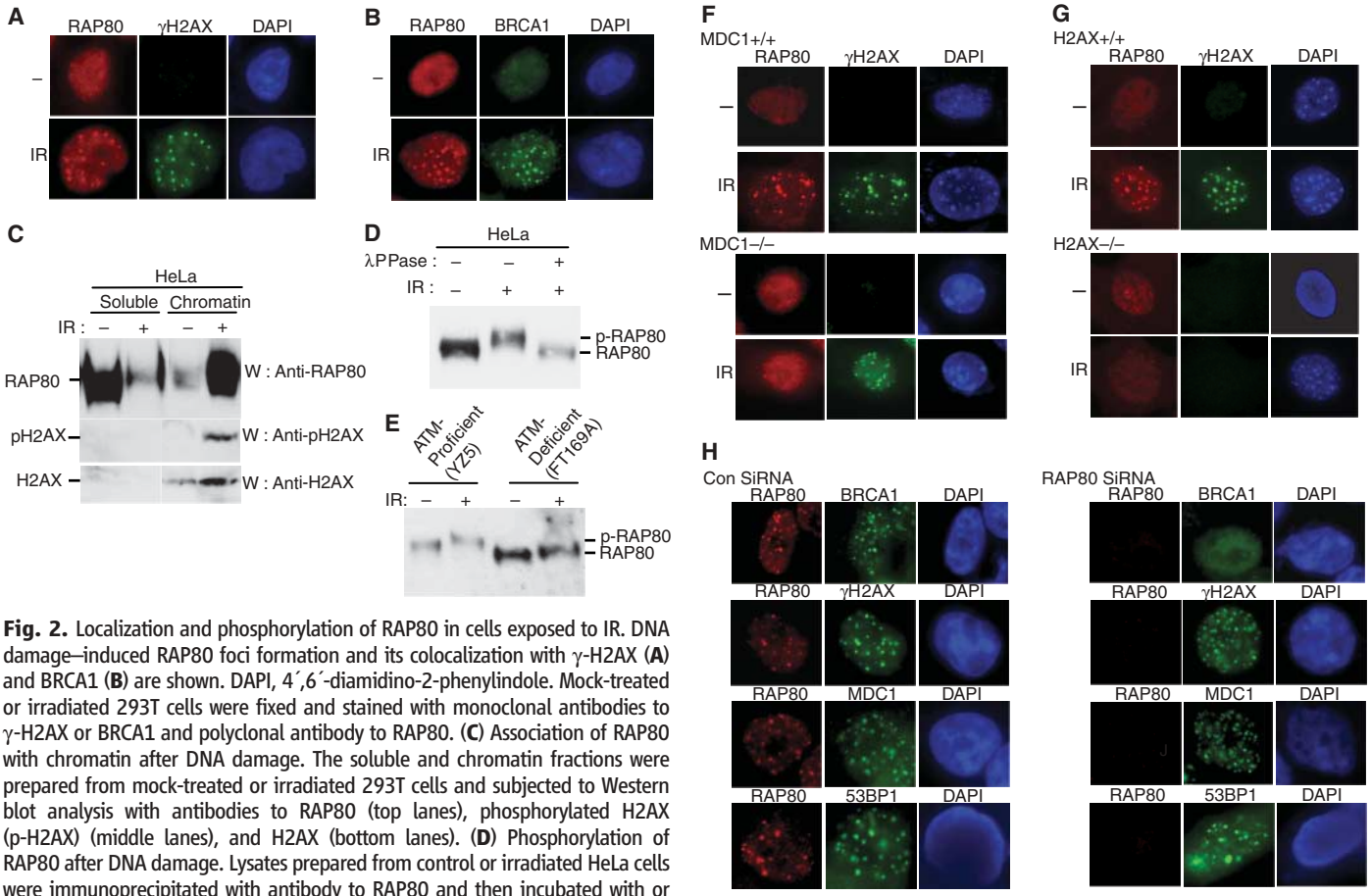

Fig. 2. Localization and phosphorylation of RAP80 in cells exposed to IR. DNA damage–induced RAP80 foci formation and its colocalization with γ-H2AX (**A**) and BRCA1 (**B**) are shown. DAPI, 4′,6′-diamidino-2-phenylindole. Mock-treated or irradiated 293T cells were fixed and stained with monoclonal antibodies to γ-H2AX or BRCA1 and polyclonal antibody to RAP80. (**C**) Association of RAP80 with chromatin after DNA damage. The soluble and chromatin fractions were prepared from mock-treated or irradiated 293T cells and subjected to Western blot analysis with antibodies to RAP80 (top lanes), phosphorylated H2AX (p-H2AX) (middle lanes), and H2AX (bottom lanes). (**D**) Phosphorylation of RAP80 after DNA damage. Lysates prepared from control or irradiated HeLa cells were immunoprecipitated with antibody to RAP80 and then incubated with or without λ phosphatase for 1 hour at 30°C. λPPase, λ protein phosphatase. The samples were subjected to immunoblotting with antibody to RAP80. (**E**) Requirement of ATM for IR-induced phosphorylation of RAP80. ATM-deficient FT169A cells and cells reconstituted with WT ATM (YZ5) were exposed to IR. Immunoprecipitation and immunoblotting were performed as described in (D). (**F** and **G**) Dependence of DNA damage–induced RAP80 foci formation. MDC1$^{+/+}$ and MDC1$^{-/-}$ mouse embryo fibroblasts (MEFs) (F) and H2AX$^{+/+}$ and H2AX$^{-/-}$ MEFs (G) were exposed to IR. The immunostaining experiments were performed as described in (A). (**H**) Requirement of RAP80 for damage-induced BRCA1 foci formation. Control (con) or RAP80 siRNA-transfected 293T cells were exposed to IR. Immunostaining was conducted with monoclonal antibodies to BRCA1, MDC1, 53BP1, or γ-H2AX and polyclonal antibody to RAP80.

glutathione *S*-transferase fusion protein (Ubi-GST). Ubi-GST specifically bound to the WT RAP80 but not to RAP80 lacking the two putative UIMs (RAP80D1; Fig. 3B). We also tested the binding of WT or mutant RAP80 UIMs [mutation of Ala^{88}→Gly^{88} (A88G) (*14*) and S92A in the first UIM and A113G and S117A in the second UIM] with Ubi-GST. The Ubi-GST specifically interacted with RAP80 UIM but not with the UIMs containing point mutations (Fig. 3B). We further checked whether point mutants within RAP80 UIMs would disrupt RAP80 foci formation in vivo. WT RAP80 and the RAP80P4 mutant (mutation of the linker region between two UIMs) formed detectable damage-induced nuclear foci, whereas the RAP80P1, RAP80P2, and RAP80P3 point mutants did not (Fig. 3C and fig. S4A). RAP80P1, RAP80P2, and RAP80P3 contain mutations within the first UIM (A88G and S92A), the second UIM (A113G and S117A), or both UIMs (A88G, S92A, A113G, and S117A), respectively. Therefore, the ubiquitin-binding activity of RAP80 correlates with its ability to localize to damage-induced foci in vivo. Like RAP80, the *Homo sapiens* DnaJ1A (HSJ1A) protein localizes to nuclei and also contains two UIMs. However, full-length HSJ1A or a construct containing the HSJ1A UIM region did not form nuclear foci in cells with DNA damage (fig. S4C). Thus, the ability to form nuclear foci is specific for the RAP80 UIM region. Notably, RAP80 UIMs bind specifically to Lys^{63}-linked but not to Lys^{48}-linked polyubiquitin chains in vitro (fig. S5).

Cells carrying BRCA1 mutants display increased sensitivity to IR and defective G_2/M checkpoint control (*15*). We examined whether the loss of the RAP80 would result in similar defects in the DNA damage response. Both RAP80 siRNAs that we synthesized efficiently decreased RAP80 expression in cells (Fig. 4A). Using a previously established G_2/M checkpoint assay (*16*), we showed defective G_2/M checkpoint control in RAP80-depleted cells (Fig. 4B). Similar G_2/M checkpoint defects were also observed in BRCA1- or CtIP-depleted cells (fig. S6). The protein kinase Chk1 is required for the G_2/M checkpoint control (*17*, *18*) and acts downstream of BRCA1 in response to IR (*19*, *20*). If RAP80 functions upstream of BRCA1, we would expect a defective Chk1 activation in RAP80-depleted cells. This is indeed the case (Fig. 4C). RAP80-depleted cells were also more sensitive to radiation than control cells (Fig. 4D). These data together indicate that RAP80 acts upstream of BRCA1 and specifically regulates BRCA1 functions after DNA damage.

Exactly how RAP80 is recruited to DNA damage sites is still unknown. Because RAP80 UIMs bind directly to ubiquitin in vitro, we reason that one or several ubiquitinated proteins might bind RAP80 and recruit RAP80 to the DNA damage sites. There are several proteins known to be ubiquitinated and localized to the sites of DNA damage (*21*–*23*). One of them is Fanconi anemia complementation group D2 (FANCD2). However, RAP80 foci still form normally after irradiation in FANCD2-deficient cells (fig. S7), suggesting that there may be other as-yet-unidentified ubiquitinated proteins that act

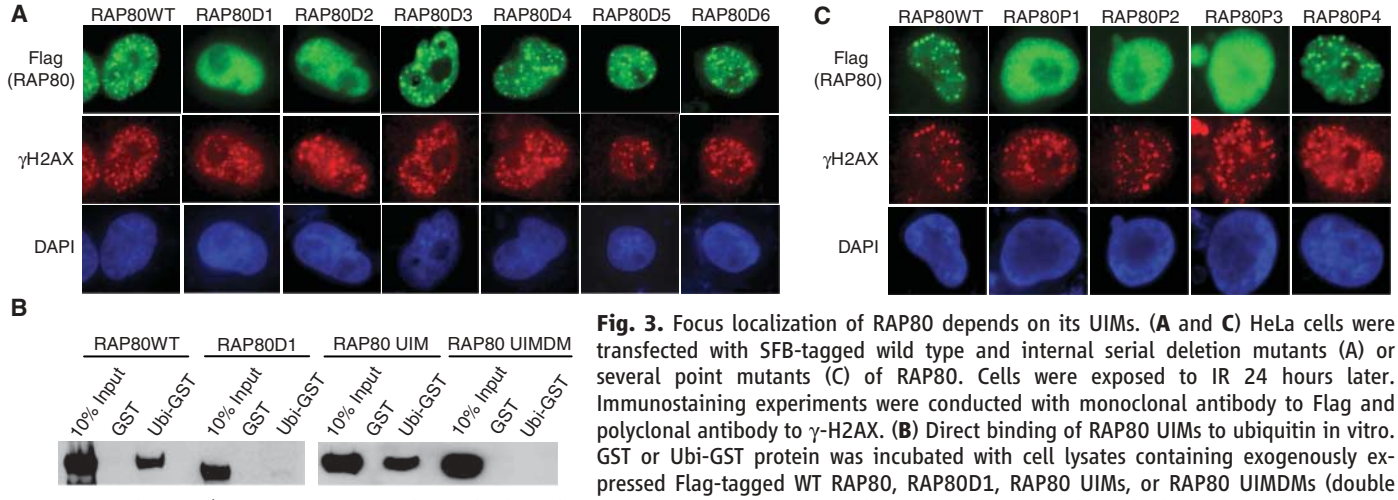

Fig. 3. Focus localization of RAP80 depends on its UIMs. (**A** and **C**) HeLa cells were transfected with SFB-tagged wild type and internal serial deletion mutants (A) or several point mutants (C) of RAP80. Cells were exposed to IR 24 hours later. Immunostaining experiments were conducted with monoclonal antibody to Flag and polyclonal antibody to γ-H2AX. (**B**) Direct binding of RAP80 UIMs to ubiquitin in vitro. GST or Ubi-GST protein was incubated with cell lysates containing exogenously expressed Flag-tagged WT RAP80, RAP80D1, RAP80 UIMs, or RAP80 UIMDMs (double mutations in the UIMs). After extensive washing, the bound RAP80 proteins were analyzed by immunoblotting with antibody to Flag.

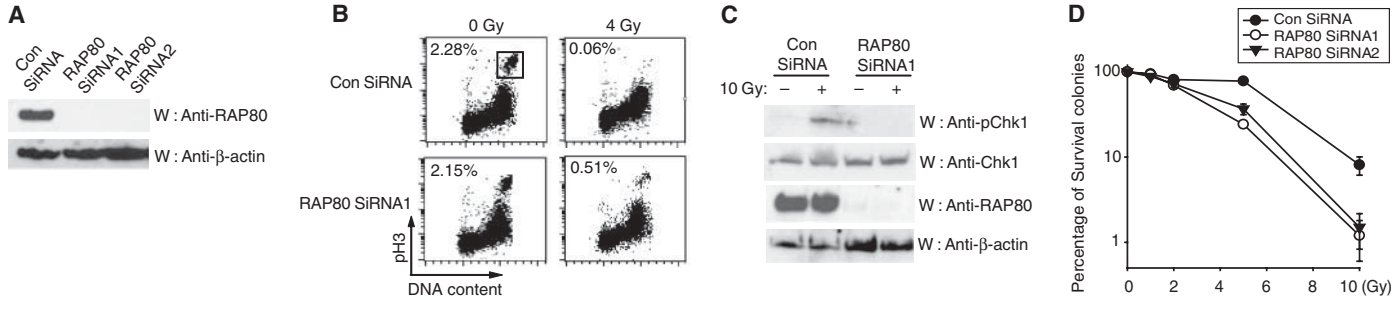

Fig. 4. Requirement of RAP80 for the IR-induced G_2/M checkpoint. (**A**) Western blot analysis for RAP80 expression level. RAP80 protein levels were analyzed by immunoblotting with antibodies to RAP80 with the use of control or RAP80 siRNA-transfected cell lysates. (**B**) G_2/M checkpoint in RAP80-depleted cells. HeLa cells transfected with control or RAP80 siRNAs were exposed to 0 or 4 grays (Gy) of IR. Cells were incubated for 1 hour before fixation and subjected to staining with antibody to phosphorylated histone H3 (pH3) and propidium iodide. The percentages of mitotic cells were determined by fluorescence-activated cell sorting analysis. The boxed area in the top left panel indicates mitotic cells. (**C**) Requirement of RAP80 for Chk1 phosphorylation after DNA damage. Control or RAP80 siRNA-transfected HeLa cells were exposed to IR. Cells were harvested 2 hours later, and lysates were immunoblotted with indicated antibodies. (**D**) Radiation sensitivity of cells lacking RAP80. HeLa cells were transfected with control or RAP80 siRNAs. Cells were counted and irradiated with various doses of IR. Percentages of surviving colonies were determined 11 days later. These experiments were performed in triplicate, and the results represent the average of two or three independent experiments. Error bars indicate SD for different doses of irradiation.

early in DNA damage response and regulate RAP80 localization.

Many cell cycle checkpoint proteins, including ATM, Chk2, BRCA1, and p53, play critical roles in the maintenance of genomic stability. Their mutation often results in increased tumor incidence, highlighting the importance of the integrity of DNA damage pathways in tumor suppression. As a BRCA1-associated protein involved in DNA damage checkpoint control, RAP80 may also function as a tumor suppressor and be dysregulated or mutated in human patients. Future genetic studies will allow us to test this possibility.

References and Notes

1. B. B. Zhou, S. J. Elledge, *Nature* **408**, 433 (2000).
2. J. Rouse, S. P. Jackson, *Science* **297**, 547 (2002).
3. W. C. Hahn, R. A. Weinberg, *N. Engl. J. Med.* **347**, 1593 (2002).
4. T. T. Su, *Annu. Rev. Genet.* **40**, 187 (2006).
5. F. J. Couch *et al.*, *N. Engl. J. Med.* **336**, 1409 (1997).
6. D. Ford *et al.*, *Am. J. Hum. Genet.* **62**, 676 (1998).
7. R. Hashizume *et al.*, *J. Biol. Chem.* **276**, 14537 (2001).
8. A. Chen, F. E. Kleiman, J. L. Manley, T. Ouchi, Z. Q. Pan, *J. Biol. Chem.* **277**, 22085 (2002).
9. X. Yu, J. Chen, *Mol. Cell. Biol.* **24**, 9478 (2004).
10. S. B. Cantor *et al.*, *Cell* **105**, 149 (2001).
11. Z. Yan, Y. S. Kim, A. M. Jetten, *J. Biol. Chem.* **277**, 32379 (2002).
12. Materials and methods are available as supporting material on *Science* Online.
13. S. Hirano *et al.*, *Nat. Struct. Mol. Biol.* **13**, 272 (2006).
14. Single-letter abbreviations for the amino acid residues are as follows: A, Ala; C, Cys; D, Asp; E, Glu; F, Phe; G, Gly; H, His; I, Ile; K, Lys; L, Leu; M, Met; N, Asn; P, Pro; Q, Gln; R, Arg; S, Ser; T, Thr; V, Val; W, Trp; and Y, Tyr.
15. C. X. Deng, S. G. Brodie, *Bioessays* **22**, 728 (2000).
16. B. Xu, S. Kim, M. B. Kastan, *Mol. Cell. Biol.* **21**, 3445 (2001).
17. Q. Liu *et al.*, *Genes Dev.* **14**, 1448 (2000).
18. H. Takai *et al.*, *Genes Dev.* **14**, 1439 (2000).
19. R. I. Yarden, S. Pardo-Reoyo, M. Sgagias, K. H. Cowan, L. C. Brody, *Nat. Genet.* **30**, 285 (2002).
20. P. B. Deming *et al.*, *Proc. Natl. Acad. Sci. U.S.A.* **98**, 12044 (2001).
21. X. Yu, S. Fu, M. Lai, R. Baer, J. Chen, *Genes Dev.* **20**, 1721 (2006).
22. X. Wang, P. R. Andreassen, A. D. D'Andrea, *Mol. Cell. Biol.* **24**, 5850 (2004).
23. R. Montes de Oca *et al.*, *Blood* **105**, 1003 (2005).

24. We thank J. Wood for proofreading the manuscript; J. Hohfeld and B. Horazdovsky for providing constructs encoding HSJ1A and Ubi-GST, respectively; and A. D'Andrea for providing FANCD2-deficient and FANCD2-reconstituted cells. This work was supported by grants from NIH (grant number RO1CA089239 to J.C.), the Ovarian Cancer Research Fund (X.Y.), the University of Michigan Cancer Center Developmental Fund (X.Y.), the U.S. Department of Defense (DOD) Era of Hope Scholars Award (J.C.), and the DOD Breast Cancer Research Program Idea Award (X.Y.).

Supporting Online Material

www.sciencemag.org/cgi/content/full/316/5828/1202/DC1
Materials and Methods
Figs. S1 to S9
References

5 January 2007; accepted 10 April 2007
10.1126/science.1139621

How Synaptotagmin Promotes Membrane Fusion

Sascha Martens,[1] Michael M. Kozlov,[2] Harvey T. McMahon[1]*

Synaptic vesicles loaded with neurotransmitters are exocytosed in a soluble *N*-ethylmaleimide–sensitive factor attachment protein receptor (SNARE)–dependent manner after presynaptic depolarization induces calcium ion (Ca^{2+}) influx. The Ca^{2+} sensor required for fast fusion is synaptotagmin-1. The activation energy of bilayer-bilayer fusion is very high (≈40 k_BT). We found that, in response to Ca^{2+} binding, synaptotagmin-1 could promote SNARE-mediated fusion by lowering this activation barrier by inducing high positive curvature in target membranes on C2-domain membrane insertion. Thus, synaptotagmin-1 triggers the fusion of docked vesicles by local Ca^{2+}-dependent buckling of the plasma membrane together with the zippering of SNAREs. This mechanism may be widely used in membrane fusion.

At the synapse, neurotransmitter release is mediated by the Ca^{2+}-induced fusion of transmitter-loaded synaptic vesicles with the presynaptic plasma membrane. The plasma membrane–localized target (t)-SNAREs ([soluble *N*-ethylmaleimide–sensitive factor attachment protein 25 (SNAP-25) and syntaxin-1)] and the vesicle (v)–localized v-SNARE (synaptobrevin) and synaptotagmin-1 (syt1) are involved in the Ca^{2+}-triggered fusion of synaptic vesicles with the plasma membrane (*1*). The three SNAREs are believed to bring the two membranes destined for fusion into close apposition. Syt1 has been shown to be the Ca^{2+} sensor responsible for Ca^{2+}-triggered fusion (*2*), but the molecular mechanism by which syt1 accomplishes this is not fully understood. Syt1 is a vesicle-localized transmembrane protein with two cytoplasmic C2 domains, C2A and C2B (Fig. 1A). The C2A and the C2B domains each bind Ca^{2+}, which enables them to interact with membranes (*3*, *4*). This activity is implicated in the triggering of membrane fusion (*5*, *6*). In addition, Ca^{2+}-dependent and -independent interactions between syt1 with SNAREs have been shown (*7*).

The fusion of two membranes is now widely believed to occur through a hemifusion intermediate (*8*). For hemifusion to occur, high energy barriers must be overcome, which are thought to be related to the curvature deformations generated within the membranes during stalk formation and subsequent stages of membrane merging (*8*, *9*). Syt1 has been shown to trigger Ca^{2+}-induced fusion and bind to membranes in a Ca^{2+}-dependent manner, and thus we investigated whether it could promote membrane fusion and, consequently, exocytosis, by affecting local membrane curvature.

Ca^{2+} binding by syt1 is mediated by a series of conserved aspartate residues that line pockets on one end of each of the C2A and C2B domains (*3*, *10*) (Fig. 1A). We used a syt1 construct lacking the transmembrane domain but having the double C2 domain module (C2AB) (*11*). Ca^{2+} binding allows the C2A and C2B domains to interact with negatively charged phospholipids such as phosphatidylserine (PtdSer) and phosphatidylinositol-4,5-bisphosphate [PtdIns(4,5)P_2] (*12*, *13*) (fig. S1). This interaction results in the insertion of four loops (two from each of the C2 domains) into the lipid bilayer (*14*, *15*). M173, F234, V304, and I367 (*16*) located on the tips of the membrane-binding loops (Fig. 1A) penetrate to a third of the lipid monolayer depth (*15*). This kind of hydrophobic-loop insertion should generate a tendency for the monolayer to bend to relieve the tension created by the insertion. If syt1 contributes to spontaneous membrane curvature (*8*), the closer the membrane curvature is to that preferentially produced by syt1, the stronger the syt1 affinity for membrane binding should be. Conversely, addition of syt1 to initially flat membranes should induce a positive curvature.

We incubated liposomes of different sizes, and, consequently, of different curvatures, with syt1 C2AB domains in the presence and absence of 1 mM Ca^{2+}. The binding of syt1 to membranes was monitored by a cosedimentation assay (Fig. 1B). Syt1 showed a clear preference for binding smaller liposomes (Fig. 1, Bii and C). This effect was observed only in the presence of Ca^{2+}, whereas the Ca^{2+}-independent interaction of syt1 with liposomes was size independent (Fig. 1Bi). This positive-curvature preference was largely lost when we increased the strength of interaction of syt1 with the membrane by elevating the PtdSer content in the liposomes from 15 to 25% (Fig. 1D). Likewise, the binding to Folch liposomes, which are rich in PtdSer, was largely curvature independent. The syt1 C2AB domain

[1]Medical Research Council–Laboratory of Molecular Biology, Hills Road, CB2 0QH Cambridge, UK. [2]Department of Physiology and Pharmacology, Sackler Faculty of Medicine, Tel Aviv University, 69978 Tel Aviv, Israel.

*To whom correspondence should be addressed. E-mail: hmm@mrc-lmb.cam.ac.uk

nature structural & molecular biology

CCDC98 is a BRCA1-BRCT domain–binding protein involved in the DNA damage response

Hongtae Kim[1,2], Jun Huang[1,2] & Junjie Chen[1]

The product of the breast cancer-1 gene, *BRCA1*, plays a crucial part in the DNA damage response through its interactions with many proteins, including BACH1, CtIP and RAP80. Here we identify a coiled-coil domain–containing protein, CCDC98, as a BRCA1-interacting protein. CCDC98 colocalizes with BRCA1 and is required for the formation of BRCA1 foci in response to ionizing radiation. Moreover, like BRCA1, CCDC98 has a role in radiation sensitivity and damage-induced G2/M checkpoint control. Together, these results suggest that CCDC98 is a mediator of BRCA1 function involved in the mammalian DNA damage response.

To survive and maintain their genomic integrity, cells are equipped with the ability to sense and respond to DNA damage[1,2]. The importance of this surveillance system has been demonstrated by the finding that inactivation of the DNA damage response can lead to cancer-susceptibility syndromes and neoplastic transformation. Many proteins, including the protein kinase ataxia-telangiectasia mutated (ATM), phosphorylated histone H2AX (γH2AX) and mediator of DNA damage checkpoint-1 (MDC1), are involved in sensing, transducing and responding to DNA damage signals[3]. The product of *BRCA1* is also a checkpoint mediator, and its BRCT domains function in this process by interacting with phosphoserine or phosphothreonine motifs[4–6]. Previous studies have shown that the BRCA1-BRCT domains are important for BRCA1's functions in tumor suppression[7] and the DNA damage response[8–10]. In the presence of DNA lesions, BRCA1 participates in many DNA damage response pathways, including cell-cycle checkpoints during S phase and at the G2/M transition, and DNA repair via homologous recombination[8–11]. Defects in these checkpoints and DNA repair may underlie the increased tumorigenesis observed in patients with *BRCA1* mutations.

Although BRCA1 is known to be recruited to DNA breaks and to participate in checkpoint regulation, it is not yet clear how the recruitment of BRCA1 is controlled in the cell. To gain further insights into the regulation of BRCA1 upon DNA damage, we sought to identify previously unknown BRCA1-BRCT domain–binding proteins using a tandem affinity-purification approach. Here we report that human CCDC98 protein associates with BRCA1 and demonstrate that CCDC98 acts upstream of BRCA1 and regulates the BRCA1-dependent DNA damage signaling pathway.

RESULTS

CCDC98 is a BRCA1-associated protein

To identify additional BRCA1-associated proteins, we purified BRCA1-BRCT domain–containing complexes from human embryonic kidney 293T cells stably expressing a BRCA1-BRCT domain with an N-terminal triple tag comprising an S tag, a Flag epitope and a streptavidin-binding peptide (SFB–BRCA1-BRCT). Mass spectrometry revealed a number of known BRCA1-associated proteins, including BRCA1-associated C-terminal helicase (BACH1), CtBP-interacting protein (CtIP) and receptor associated protein-80 (RAP80)[6,12–15]. In the same experiment, we also identified several putative BRCA1-associated proteins (**Supplementary Table 1** online). Among these, we paid special attention to a coiled-coil domain–containing protein, CCDC98. This protein contains an SPTF motif at its extreme C terminus; an identical sequence in BACH1 is required for interaction of BACH1 with BRCA1-BRCT domains[6]. The physiological function of CCDC98 is unknown. Notably, we also identified CCDC98 as a RAP80-associated protein in a tandem affinity purification of RAP80-containing complexes (**Supplementary Table 2** online), confirming that CCDC98 and RAP80 interact. As both CCDC98 and RAP80 exist in BRCA1-containing complexes (**Supplementary Tables 1** and **2**), we speculated that these three proteins might form a complex.

BRCA1 specifically binds the SPTF motif of CCDC98

We confirmed the association of CCDC98 with BRCA1 and RAP80 using coimmunoprecipitation experiments (**Fig. 1a**). In addition, bacterially expressed glutathione *S*-transferase (GST)-tagged BRCA1-BRCT domain and GST-RAP80 pulled down CCDC98 from cell extracts (**Fig. 1b**), again confirming that CCDC98 interacts with both BRCA1 and RAP80. Notably, although CCDC98 interacted with the BRCA1-BRCT domain in a phosphorylation-dependent manner, its association with RAP80 was phosphorylation independent (**Fig. 1b**).

Prompted by this phosphorylation-dependent interaction between BRCA1-BRCT and CCDC98, we examined whether the C-terminal SPTF motif of CCDC98 is required for its interaction with BRCA1-BRCT. GST–BRCA1-BRCT specifically bound wild-type CCDC98 and

[1]Department of Therapeutic Radiology, Yale University School of Medicine, P.O. Box 208040, New Haven, Connecticut 06520, USA. [2]These authors contributed equally to this work. Correspondence should be addressed to J.C. (junjie.chen@yale.edu).

Received 23 April; accepted 26 June; published online 22 July 2007; doi:10.1038/nsmb1277

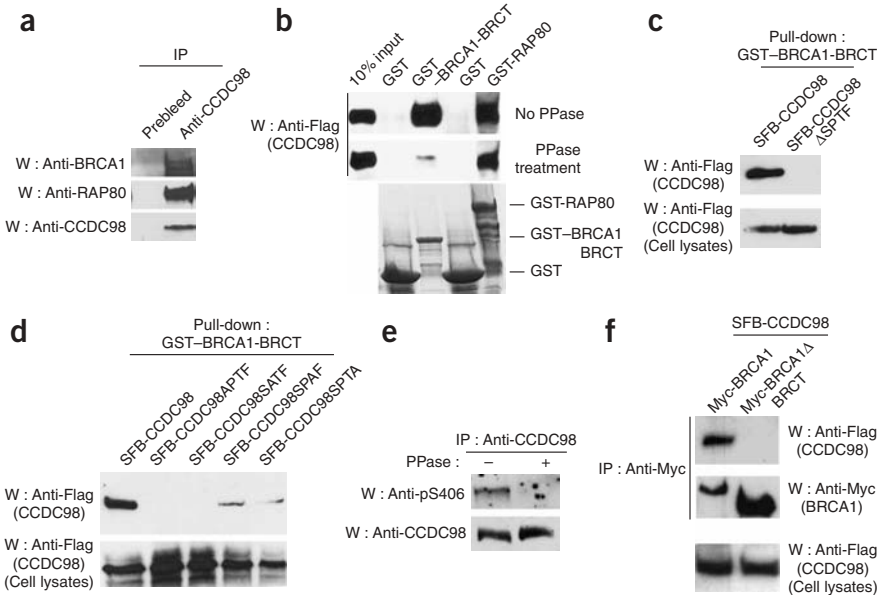

Figure 1 Identification of CCDC98 as a BRCA1-binding protein. (**a**) The interaction between endogenous CCDC98 and BRCA1 or RAP80. Immunoprecipitation (IP) reactions were done using preimmune serum (prebleed) or anti-CCDC98. Western blotting analyses (W) were done with indicated antibodies. (**b**) Phosphorylation-dependent interaction between BRCA1-BRCT and CCDC98. GST, GST–BRCA1-BRCT or GST-RAP80 was incubated with cell lysates containing exogenously expressed Flag-tagged wild-type CCDC98, with or without phosphatase. Bound CCDC98 was analyzed by anti-Flag immunoblotting. Lower gel shows amounts of proteins used in these experiments. (**c**,**d**) Beads with GST–BRCA1-BRCT were incubated with cell lysates containing exogenously expressed SFB-tagged wild-type CCDC98, CCDC98ΔSPTF or SPTF point mutants with the C-terminal sequences indicated in their names (CCDC98APTF, CCDC98SATF, CCDC98SPAF and CCDC98SPTA). Bound CCDC98 proteins were analyzed by anti-Flag immunoblotting. (**e**) CCDC98 is phosphorylated at Ser406. IP reactions using anti-CCDC98 were followed by mock or phosphatase treatment. Western blotting was done with indicated antibodies. (**f**) 293T cells were transfected with plasmid encoding Myc-BRCA1 or Myc-BRCA1ΔBRCT and with plasmid encoding SFB-CCDC98. Cell lysates were subjected to immunoprecipitation and immunoblotting with indicated antibodies (upper blots). Lower blot shows amounts of SFB-tagged CCDC98 in lysates.

did not bind CCDC98 lacking the C-terminal SPTF sequence (CCDC 98ΔSPTF; **Fig. 1c**). We also generated several point mutations in the SPTF motif of CCDC98. Whereas GST–BRCA1-BRCT specifically pulled down wild-type CCDC98, its affinities for the CCDC98 point mutants were greatly diminished (**Fig. 1d**). Using a phosphospecific antibody against the Ser406 residue in the SPTF motif, we confirmed that this serine residue is indeed phosphorylated *in vivo* (**Fig. 1e**). This phosphorylation and the BRCA1-CCDC98 interaction did not change after DNA damage (data not shown). Only wild-type BRCA1, and not a BRCA1 variant lacking the BRCT regions (BRCA1ΔBRCT), associated with CCDC98 *in vivo* (**Fig. 1f**). Together, these data suggest that CCDC98 binds BRCA1 in a phosphorylation-dependent manner through an interaction between BRCA1-BRCT and the C-terminal SPTF motif of CCDC98.

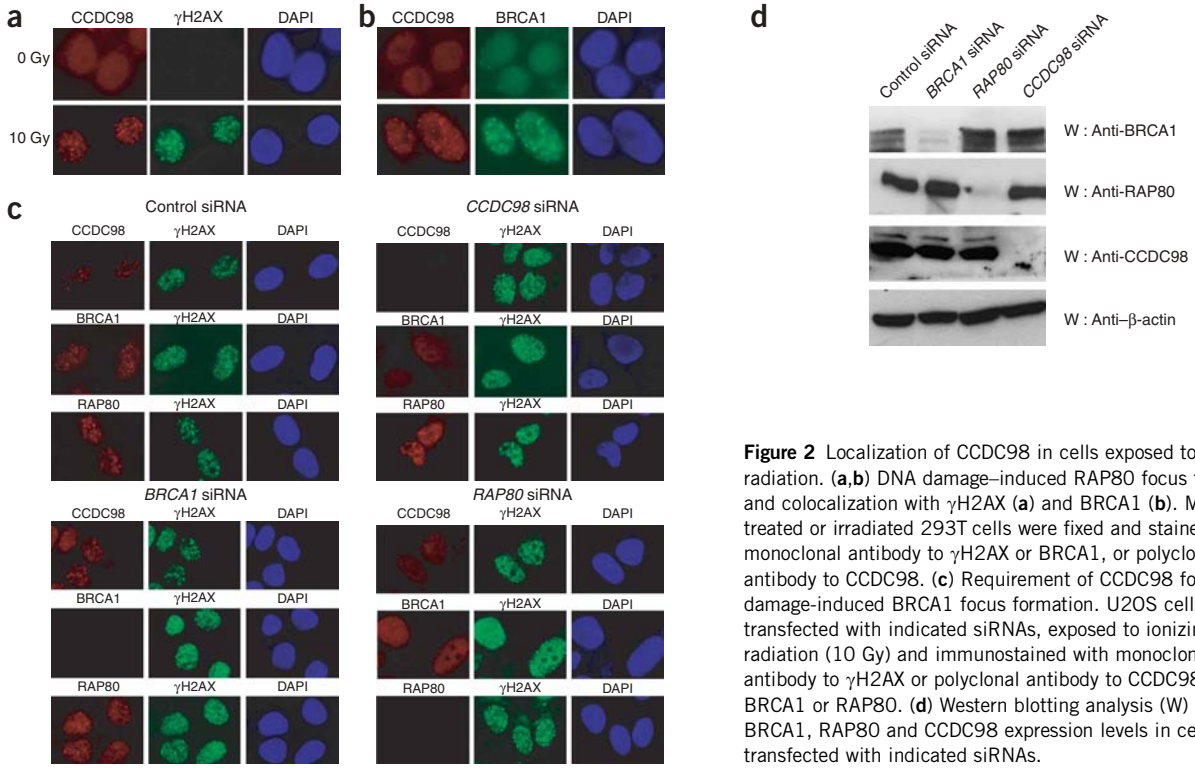

Figure 2 Localization of CCDC98 in cells exposed to ionizing radiation. (**a**,**b**) DNA damage–induced RAP80 focus formation and colocalization with γH2AX (**a**) and BRCA1 (**b**). Mock-treated or irradiated 293T cells were fixed and stained with monoclonal antibody to γH2AX or BRCA1, or polyclonal antibody to CCDC98. (**c**) Requirement of CCDC98 for damage-induced BRCA1 focus formation. U2OS cells were transfected with indicated siRNAs, exposed to ionizing radiation (10 Gy) and immunostained with monoclonal antibody to γH2AX or polyclonal antibody to CCDC98, BRCA1 or RAP80. (**d**) Western blotting analysis (W) of BRCA1, RAP80 and CCDC98 expression levels in cells transfected with indicated siRNAs.

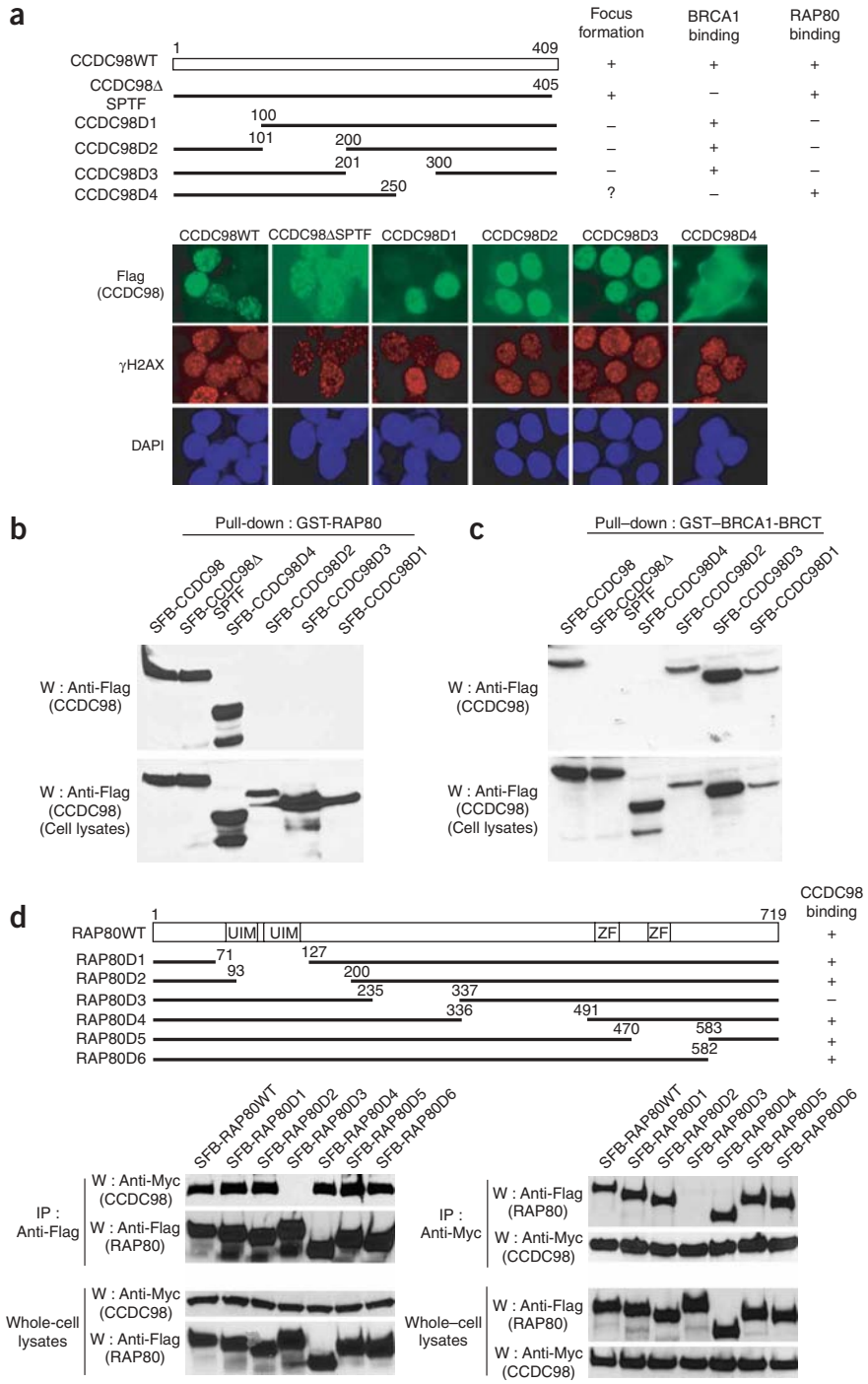

Figure 3 Focus localization of CCDC98 depends on its N-terminal RAP80-binding region. (**a**) 293T cells were transfected with SFB-tagged wild-type (WT) CCDC98 or deletion mutants shown in diagram. After 24 h, cells were exposed to 10 Gy of ionizing radiation. Eight hours after irradiation, cells were fixed and stained with monoclonal anti-Flag or polyclonal anti-γH2AX. (**b**,**c**) Mapping of the RAP80- and BRCA1-interacting domains in CCDC98. Beads coated with GST-RAP80 (**b**) or GST–BRCA1-BRCT (**c**) were incubated with cell lysates containing exogenously expressed SFB-tagged WT CCDC98 or deletion mutants. After extensive washing, bound RAP80 was analyzed by western blotting (W) with anti-Flag. (**d**) SFB-tagged WT RAP80 and its internal deletion mutants were used to map the CCDC98-interacting domain in RAP80. 293T cells were transfected with plasmids encoding Myc-CCDC98 and the indicated SFB-RAP80 proteins. Cell lysates were subjected to immunoprecipitation (IP) and immunoblotting with indicated antibodies (top blots). Bottom blots show amounts of SFB-RAP80 and Myc-CCDC98 in these lysates.

CCDC98 and BRCA1 form foci after DNA damage

As BRCA1 localizes to sites of DNA breaks in cells exposed to ionizing radiation, we checked the localization of CCDC98 before and after DNA damage. Using an antibody to CCDC98, we found the protein to be evenly distributed in the nucleoplasm of normal cells (**Fig. 2a**). After cells were exposed to ionizing radiation, CCDC98 localized to DNA damage–induced foci and colocalized with γH2AX (a marker of DNA damage) and BRCA1 (**Fig. 2a**,**b**). This indicates that the localization of CCDC98, like that of BRCA1, is regulated in response to DNA damage. Notably, we discovered that BRCA1 did not accumulate at DNA breaks in cells where *CCDC98* messenger RNA was depleted using short interfering RNA (siRNA); however, the localization of RAP80 to damage sites was normal in these cells (**Fig. 2c**). Moreover, formation of both BRCA1 and CCDC98 foci was abolished in *RAP80*-depleted cells, but formation of CCDC98 and RAP80 foci was normal in *BRCA1*-depleted cells (**Fig. 2c**). As a control, we showed that the expression level of BRCA1 is the same with or without *CCDC98* knockdown (**Fig. 2d**). In addition, *RAP80* knockdown also does not change the expression of CCDC98 or BRCA1 (**Fig. 2d**). Collectively, these data suggest that CCDC98 acts downstream of RAP80 but upstream of BRCA1 in the DNA damage response pathway.

CCDC98 focus formation depends on its N terminus

Our results suggested that CCDC98 forms a complex with RAP80 and BRCA1 and localizes to sites of damaged DNA. Next, we attempted to determine which regions of CCDC98 are important for its localization to foci. Full-length CCDC98 and CCDC98ΔSPTF mutant localized normally to nuclear foci in cells with DNA damage, whereas all of the other CCDC98 deletion mutants we tested did not (**Fig. 3a**). All three N-terminal and internal deletion mutants of CCDC98 also did not bind RAP80 (**Fig. 3b**), whereas CCDC98ΔSPTF and a CCDC98 mutant with a large C-terminal deletion (CCDC98D4) were defective in BRCA1 binding (**Fig. 3c**). Because it localizes to the cytoplasm, it is difficult to interpret the results obtained with the CCDC98D4 mutant (two putative nuclear localization sequences, 358-Lys-Arg-Ser-Arg-361 and 368-Lys-Arg-Ser-Lys-371, are deleted in this mutant). Nevertheless, these data suggest that CCDC98 mediates the interaction between BRCA1 and RAP80

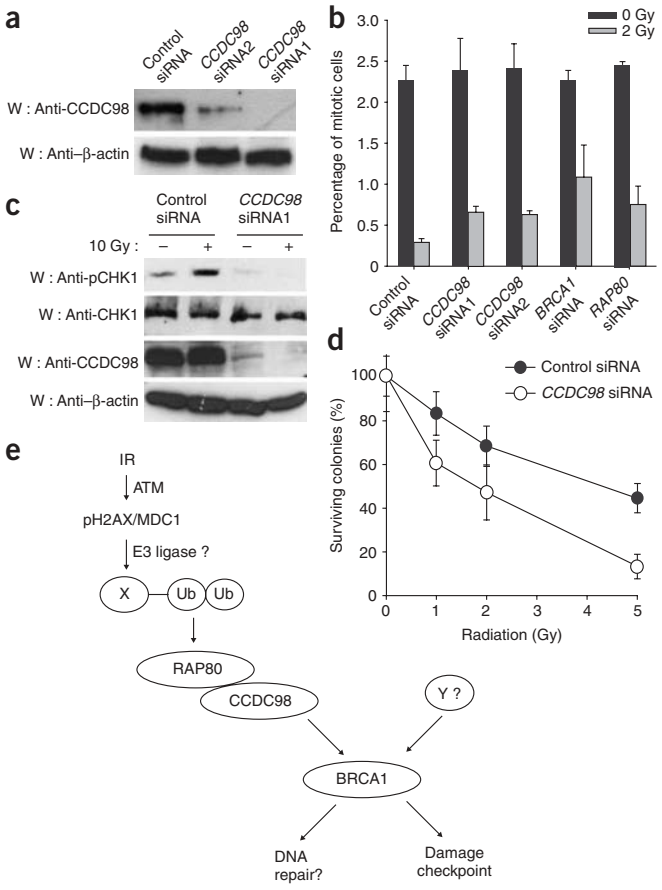

Figure 4 Requirement of CCDC98 for ionizing radiation–induced DNA damage response. (**a**) Western blotting analysis (W) of CCDC98 expression in cells transfected with indicated siRNAs. (**b**) G2/M checkpoint control in *CCDC98* knockdown cells. HeLa cells transfected with indicated siRNAs were exposed to 0 or 2 Gy of ionizing radiation. Cells were fixed and stained with histone-specific anti-pH3 (a mitotic marker) and propidium iodide. Percentages of mitotic cells were determined by FACS analysis. Data shown are averages of three independent experiments; error bars indicate s.d. (**c**) Requirement of CCDC98 for CHK1 phosphorylation after DNA damage. Control or *CCDC98* siRNA–transfected HeLa cells were exposed to 0 or 10 Gy of ionizing radiation, harvested 2 h later and immunoblotted with indicated antibodies. (**d**) Radiation sensitivity of cells lacking CCDC98. HeLa cells were transfected with control or *CCDC98* siRNAs. Cells were irradiated with indicated doses of ionizing radiation. Percentage of colonies surviving was determined 10–12 d later. Experiments were done in triplicate; results shown are averages of two or three independent experiments at each dose; error bars indicate s.d. (**e**) Model of the DNA damage response pathway that integrates CCDC98. Our data indicate that CCDC98 operates upstream of BRCA1 and specifically regulates BRCA1 localization and function after DNA damage.

and that the localization of CCDC98 to foci depends on its interaction with RAP80.

We confirmed a strong interaction between CCDC98 and RAP80 using a baculovirus-insect cell system (**Supplementary Fig. 1** online). Using a series of deletion mutants of RAP80, we identified a region (residues 235–337) on the C-terminal side of the ubiquitin-interacting motifs (UIMs) that is required for its interaction with CCDC98 (**Fig. 3d**). The same region of RAP80 is also important for its association with BRCA1 *in vivo* (**Supplementary Fig. 2** online), an observation which agrees with our proposal that CCDC98 bridges the interaction between RAP80 and BRCA1.

CCDC98 is required in the G2/M checkpoint

The loss of BRCA1 leads to defects in the DNA damage response—in particular, impaired cell-cycle checkpoints and increased sensitivity to DNA damaging agents[16,17]. We therefore examined whether the loss of CCDC98 results in similar defects in the DNA damage response. Both *CCDC98* siRNAs we synthesized efficiently decreased CCDC98 expression in cells (**Fig. 4a**). Cells treated with these siRNAs showed defective G2/M checkpoint control after DNA damage (**Fig. 4b** and **Supplementary Fig. 3** online). The protein kinase CHK1 acts downstream of BRCA1 and is required for this G2/M checkpoint control in response to ionizing radiation[18–21]. If CCDC98 functions upstream of BRCA1, a defect in CHK1 activation is expected in cells depleted of CCDC98. This is indeed the case (**Fig. 4c**). *CCDC98* knockdown cells were also more sensitive to radiation than cells transfected with control siRNA (**Fig. 4d**). These data indicate that CCDC98 is a key upstream regulator that influences BRCA1 function upon DNA damage (**Fig. 4e**).

DISCUSSION

In this study, we identified CCDC98 as a BRCA1-BRCT–binding protein. Like BRCA1, CCDC98 normally exists in the nucleoplasm but localizes to DNA breaks after exposure to ionizing radiation. CCDC98 also participates in the BRCA1-dependent G2/M checkpoint control, suggesting that CCDC98 functions together with BRCA1 in the DNA damage response.

Besides CCDC98, the ubiquitin-interacting protein RAP80 was also identified as a BRCA1-associated protein in our biochemical purification of BRCA1-containing complexes. Studies from several groups, including ours, have demonstrated that RAP80 acts upstream of BRCA1 and regulates BRCA1 localization and function after DNA damage[13–15]. Moreover, another group has also identified CCDC98 (called Abraxas in their study) as a BRCA1-interacting protein[15]. Similar to our current study, they also showed that CCDC98/Abraxas interacts with BRCA1 in a phosphorylation-dependent manner via its C-terminal SPTF motif[15]. Here, we have expanded on our initial observations and demonstrated a hierarchy in this DNA damage signal transduction pathway. We show that although RAP80 is required for formation of both CCDC98 and BRCA1 foci, CCDC98 is required for formation of only BRCA1 and not RAP80 foci. Moreover, abolishing BRCA1 does not affect either RAP80 or CCDC98 focus formation after DNA damage. Thus, we are able to delineate a signaling pathway from RAP80 to CCDC98 and then to BRCA1 (**Fig. 4e**).

Our study also permits a better understanding of CCDC98's activity as a mediator in this process. We show that the N terminus of CCDC98 is required for RAP80 binding, and its C-terminal phosphorylation motif is required for BRCA1 binding. In agreement with the notion that CCDC98 functions downstream of RAP80, only the N-terminal RAP80-binding domain of CCDC98 is important for its localization to foci after DNA damage. Putting all these studies together, we now have a better understanding of the mechanisms underlying the recruitment of BRCA1 to damaged DNA. RAP80 binds directly to the N terminus of CCDC98. This interaction is not phosphorylation dependent, but rather allows formation of a stable complex between RAP80 and CCDC98. After DNA damage, the RAP80–CCDC98 complex localizes to damage sites. RAP80's localization to foci depends on its UIM domain, which probably binds unidentified ubiquitinated proteins at DNA breaks. Through its C-terminal phosphorylation motif, CCDC98 then recruits BRCA1 to the DNA damage sites and regulates BRCA1-dependent checkpoint control.

The factors that act upstream of the RAP80–CCDC98 complex and recruit it to sites of DNA damage remain elusive. What we do know is that both γH2AX and MDC1 are upstream regulators and are required for the focus formation of many checkpoint proteins, including RAP80 and BRCA1. Because the localization of RAP80 seems to depend on the ability of its UIM domain to bind polyubiquitinated proteins, we speculate that there is at least one E3 ubiquitin ligase involved in this process. This unidentified E3 ligase may act after γH2AX and MDC1 to facilitate protein ubiquitination at sites of DNA damage, which would in turn serve as a signal to recruit RAP80–CCDC98 and BRCA1. The identification of this E3 ligase and its substrates at DNA breaks would provide further insight into the complex regulation of DNA damage response pathways.

Although RAP80 and CCDC98 seem to function upstream of BRCA1 in the DNA damage signal transduction pathway, it is noteworthy that checkpoint defects observed in *RAP80*- or *CCDC98*-deficient cells are not as severe as those observed in cells with a *BRCA1* deficiency. One likely explanation is that there are proteins other than RAP80 and CCDC98 that also participate in regulating BRCA1 function after DNA damage. We hope that future studies will identify this parallel pathway, revealing exactly how the tumor suppressor BRCA1 is regulated after DNA damage and contributes to the maintenance of genomic stability.

METHODS

Plasmids. Human *CCDC98* full-length complementary DNA was obtained using reverse-transcription PCR. Wild-type human CCDC98 and its point mutants and deletion mutants were generated by PCR and subcloned into a modified pIRES-EGFP mammalian expression vector to create constructs encoding SFB-tagged wild-type or mutant CCDC98. DNA fragments encoding BRCA1-BRCT domain and RAP80 were also generated by PCR and subcloned into pGEX-4T-1 vector (Pharmacia) to make constructs for expression of GST–BRCA1-BRCT and GST-RAP80, respectively. Myc-BRCA1, Myc-BRCA1ΔBRCT, and full-length human RAP80 and its deletion mutants were described[13].

Cell culture and treatment with ionizing radiation. HeLa, U2OS and 293T cells were purchased from the American Type Culture Collection and maintained in RPMI 1,640 medium supplemented with 10% (v/v) FBS at 37 °C in 5% CO_2. Cells were irradiated at the indicated doses using a JL Shepherd ^{137}Cs radiation source. The irradiated cells were then returned to the same culture conditions and maintained for the periods of time specified in the figure legends.

Short interfering RNA. All siRNA duplexes used in this study were purchased from Dharmacon. The sequences of *RAP80* siRNA, *CCDC98* siRNA 1, *CCDC98* siRNA 2, *BRCA1* siRNA and the control siRNA are 5′-GAAGGAUGUGGAAACUACCdTdT-3′, 5′-CAGGGUACCUUUAGUGGUUUU-3′, 5′-ACACAAGACAAACGAUCUAUU-3′ and 5′-UCACAGUGUCCUUUAUGUAdTdT-3′ and 5′-UUCAAUAAAUUCUUGAGGUUU-3′, respectively. siRNAs were transfected into the cells using Oligofectamine (Invitrogen) according to the manufacturer's instructions.

Antibodies, transfection and immunoprecipitation procedures. Rabbit antibodies to BRCA1, CCDC98 and RAP80 were raised by immunizing rabbits with GST-BRCA1 fragments, GST-CCDC98 and GST-RAP80 (residues 1–354) respectively. Phosphospecific antibody to Ser406 was generated by immunizing rabbits with KLH-conjugated GFGEYSR-pS-PTF peptide. The resulting rabbit polyclonal sera were affinity-purified using the SulfoLink or AminoLink Plus Immobilization and Purification Kit (Pierce). γH2AX antibodies were described[22]. Antibodies to Flag and β-actin were purchased from Sigma. Antibody to phosphorylated histone H3 (pH3) was purchased from Upstate Biotechnology. Transient transfection was done using Fugene 6 transfection reagent (Roche) according to the manufacturer's instructions. For immunoprecipitation, cells were washed with ice-cold PBS and then lysed in NETN buffer (0.5% (v/v) Nonidet P-40, 20 mM Tris (pH 8.0), 50 mM NaCl, 50 mM NaF, 100 μM Na_3VO_4, 1 mM DTT and 50 μg ml^{-1} PMSF) at 4 °C for 10 min. Crude lysates were cleared by centrifugation at 14,000 r.p.m. (Micro 240A, Scientific) and 4 °C for 5 min, and supernatants were incubated with protein A–agarose–conjugated primary antibodies. The immunocomplexes were washed three times with NETN buffer and then subjected to SDS-PAGE. Western blotting was done using the antibodies specified in the figures.

Cell lines and affinity purification of SFB-tagged protein complexes. To establish cell lines stably expressing various epitope-tagged proteins, 293T cells were transfected with plasmids encoding SFB-tagged proteins and pGK-Puro. Forty-eight hours after transfection, the cells were split at a 1:10 ratio and cultured in medium containing puromycin (10 μg ml^{-1}) for 3 weeks. The individual puromycin-resistant colonies were isolated and screened by western blotting. 293T cells stably expressing tagged proteins were lysed with 4 ml NETN buffer on ice for 10 min. Crude lysates were cleared by centrifugation at 14,000 r.p.m. (Micro 240A, Scientific) at 4 °C for 10 min, and supernatants were incubated with 300 μl streptavidin-conjugated beads (Amersham). The immunocomplexes were washed three times with NETN buffer and then bead-bound proteins were eluted with 500 μl NETN buffer containing 2 mg ml^{-1} biotin (Sigma). The eluted supernatant was incubated with 60 μl S protein beads (Novagen). The immunocomplexes were washed three times with NETN buffer and subjected to SDS-PAGE. Protein bands were visualized by silver staining, excised and digested, and the peptides were analyzed by mass spectrometry.

Glutathione *S*-transferase pull-down assay. GST fusion protein was expressed in *Escherichia coli* and purified as described[23]. GST fusion protein or GST alone (2 μg) was immobilized on glutathione-Sepharose 4B beads and incubated for 2 h at 4 °C with lysates prepared from cells transiently transfected with plasmids encoding the indicated proteins. After washing with NETN buffer, the samples were separated by SDS-PAGE and analyzed by western blotting.

Immunofluorescent staining. Cells grown on coverslips were fixed with 3% (w/v) paraformaldehyde at room temperature for 15 min and then permeabilized with PBS containing 0.5% (v/v) Triton X-100 at room temperature for 5 min. The coverslips were blocked with PBS containing 5% (v/v) goat serum at room temperature for 30 min before incubation with primary antibodies at room temperature for 20 min. After washing with PBS, cells were incubated with the secondary antibodies fluorescein isothiocyanate–conjugated goat anti-mouse IgG, rhodamine-conjugated goat anti-rabbit IgG or rhodamine-conjugated goat anti-mouse IgG (Jackson ImmunoResearch) at room temperature for 20 min. Nuclei were counterstained with 4,6-diamidino-2-phenylindole (DAPI). After a final wash with PBS, coverslips were mounted with glycerin containing *p*-phenylenediamine. All images were obtained with a Nikon ECLIPSE E800 fluorescence microscope.

G2/M cell-cycle checkpoint assay. HeLa cells in a 100-mm plate were transfected twice with control or *CCDC98* siRNAs at 24-h intervals. Forty-eight hours after the second transfection, transfected cells were mock-treated or irradiated at indicated doses using a JL Shepherd ^{137}Cs radiation source. One hour after irradiation, cells were fixed with 70% (v/v) ethanol at –20 °C for 24 h, then stained with rabbit antibody to pH3 and incubated with fluorescein isothiocyanate–conjugated goat secondary antibody to rabbit immunoglobulin. The stained cells were treated with RNase A, incubated with propidium iodide and then analyzed by flow cytometry.

Cell survival assays. HeLa cells in a 60-mm plate were transfected twice with control or *CCDC98* siRNAs at 24-h intervals. Forty-eight hours after the second transfection, transfected cells were irradiated at the indicated doses using a JL Shepherd ^{137}Cs radiation source. Ten to twelve days after irradiation, cells were washed with PBS, fixed and stained with 2% (w/v) methylene blue, and the colonies were counted.

Note: Supplementary information is available on the Nature Structural & Molecular Biology website.

ACKNOWLEDGMENTS

We thank members of the Chen laboratory for helpful discussions and technical support. This work was supported in part by grants from the US National

Institute of Health (RO1CA089239 to J.C.) and the US Department of Defense breast cancer Era of Hope Scholar Award (W81XWH-05-1-0470 to J.C.).

AUTHOR CONTRIBUTIONS

H.K., J.H. and J.C. designed experiments and interpreted the data; H.K. and J.H. performed all experiments; H.K. and J.C. prepared the manuscript.

COMPETING INTERESTS STATEMENT

The authors declare no competing financial interests.

Published online at http://www.nature.com/nsmb/
Reprints and permissions information is available online at http://npg.nature.com/reprintsandpermissions

1. Zhou, B.B. & Elledge, S.J. The DNA damage response: putting checkpoints in perspective. *Nature* **408**, 433–439 (2000).
2. Rouse, J. & Jackson, S.P. Interfaces between the detection, signaling, and repair of DNA damage. *Science* **297**, 547–551 (2002).
3. Su, T.T. Cellular responses to DNA damage: one signal, multiple choices. *Annu. Rev. Genet.* **40**, 187–208 (2006).
4. Manke, I.A., Lowery, D.M., Nguyen, A. & Yaffe, M.B. BRCT repeats as phosphopeptide-binding modules involved in protein targeting. *Science* **302**, 636–639 (2003).
5. Yu, X., Chini, C.C., He, M., Mer, G. & Chen, J. The BRCT domain is a phospho-protein binding domain. *Science* **302**, 639–642 (2003).
6. Yu, X. & Chen, J. DNA damage-induced cell cycle checkpoint control requires CtIP, a phosphorylation-dependent binding partner of BRCA1 C-terminal domains. *Mol. Cell. Biol.* **24**, 9478–9486 (2004).
7. Ludwig, T., Fisher, P., Ganesan, S. & Efstratiadis, A. Tumorigenesis in mice carrying a truncating Brca1 mutation. *Genes Dev.* **15**, 1188–1193 (2001).
8. Scully, R. & Livingston, D.M. In search of the tumour-suppressor functions of BRCA1 and BRCA2. *Nature* **408**, 429–432 (2000).
9. Deng, C.X. & Brodie, S.G. Roles of BRCA1 and its interacting proteins. *Bioessays* **22**, 728–737 (2000).
10. Venkitaraman, A.R. Cancer susceptibility and the functions of BRCA1 and BRCA2. *Cell* **108**, 171–182 (2002).
11. Deng, C.X. Roles of BRCA1 in centrosome duplication. *Oncogene* **21**, 6222–6227 (2002).
12. Cantor, S.B. *et al.* BACH1, a novel helicase-like protein, interacts directly with BRCA1 and contributes to its DNA repair function. *Cell* **105**, 149–160 (2001).
13. Kim, H., Chen, J. & Yu, X. Ubiquitin-binding protein RAP80 mediates BRCA1-dependent DNA damage response. *Science* **316**, 1202–1205 (2007).
14. Sobhian, B. *et al.* RAP80 targets BRCA1 to specific ubiquitin structures at DNA damage sites. *Science* **316**, 1198–1202 (2007).
15. Wang, B. *et al.* Abraxas and RAP80 form a BRCA1 protein complex required for the DNA damage response. *Science* **316**, 1194–1198 (2007).
16. Xu, B., Kim, S. & Kastan, M.B. Involvement of Brca1 in S-phase and G_2-phase checkpoints after ionizing irradiation. *Mol. Cell. Biol.* **21**, 3445–3450 (2001).
17. Cortez, D., Wang, Y., Qin, J. & Elledge, S.J. Requirement of ATM-dependent phosphorylation of brca1 in the DNA damage response to double-strand breaks. *Science* **286**, 1162–1166 (1999).
18. Liu, Q. *et al.* Chk1 is an essential kinase that is regulated by Atr and required for the G_2/M DNA damage checkpoint. *Genes Dev.* **14**, 1448–1459 (2000).
19. Takai, H. *et al.* Aberrant cell cycle checkpoint function and early embryonic death in Chk1(−/−) mice. *Genes Dev.* **14**, 1439–1447 (2000).
20. Yarden, R.I., Pardo-Reoyo, S., Sgagias, M., Cowan, K.H. & Brody, L.C. BRCA1 regulates the G2/M checkpoint by activating Chk1 kinase upon DNA damage. *Nat. Genet.* **30**, 285–289 (2002).
21. Deming, P.B. *et al.* The human decatenation checkpoint. *Proc. Natl. Acad. Sci. USA* **98**, 12044–12049 (2001).
22. Lou, Z. *et al.* MDC1 maintains genomic stability by participating in the amplification of ATM-dependent DNA damage signals. *Mol. Cell* **21**, 187–200 (2006).
23. Hofer, B., Backhaus, S. & Timmis, K.N. The biphenyl/polychlorinated biphenyl-degradation locus (bph) of Pseudomonas sp. LB400 encodes four additional metabolic enzymes. *Gene* **144**, 9–16 (1994).

RNF8 transduces the DNA damage signal via histone ubiquitylation and checkpoint protein assembly

Michael S.Y. Huen[1,*], Robert Grant[2,*], Isaac Manke[2], Kay Minn[3], Xiaochun Yu[4,#], Michael B Yaffe[2,#] , Junjie Chen[1,#]

[1]Department of Therapeutic Radiology, Yale University School of Medicine, New Haven, CT 06520, [2]Center for Cancer Research, Depts. of Biology and Biological Engineering, Massachusetts Institute of Technology, Cambridge, MA 021329**,** [3]Department of Oncology Research, Mayo Clinic College of Medicine, Rochester, MN 55905, USA, [4]Division of Molecular Medicine and Genetics, Department of Internal Medicine, University of Michigan Medical School, Ann Arbor, MI 48109, USA

*These authors contributed equally to this study.

[#]Co-corresponding authors

Summary

DNA damage signaling utilizes a multitude of post-translational modifiers as molecular switches to regulate cell cycle checkpoints, DNA repair, cellular senescence and apoptosis. Here we show that RNF8, a FHA/RING domain-containing protein, plays a critical role in the early DNA damage response. We have solved the X-ray crystal structure of the FHA domain structure at 1.35Å. We have shown that RNF8 facilitates the accumulation of checkpoint mediator proteins BRCA1 and 53BP1 to the damaged chromatin, on one hand through the phospho-dependent FHA domain-mediated binding of RNF8 to MDC1, on the other hand via its role in ubiquitylating H2AX and possibly other substrates at damage sites. Moreover, RNF8-depleted cells displayed a defective G2/M checkpoint and increased IR sensitivity. Together, our study implicates RNF8 as a novel DNA damage responsive protein that integrates protein phosphorylation and ubiquitylation signaling, and plays a critical role in the cellular response to genotoxic stress.

Introduction

Faithful duplication and segregation of DNA is essential to maintain genomic integrity during cell division. DNA lesions elicit a DNA damage response, which collectively includes DNA repair, activation of cell cycle checkpoints, chromatin remodeling, cellular senescence and apoptosis. Mutations in a variety of components involved in these cellular processes directly contribute to tumorigenesis (Bartkova et al., 2005; Gorgoulis et al., 2005), highlighting the importance of these damage-induced signaling cascades in tumor suppression. Accumulating evidence suggests that the ATM/ATR-dependent phosphorylation of histone variant H2AX to create γH2AX is the initial signal for subsequent accumulation of various mediators/repair proteins to DNA lesions (Bassing et al., 2003; Celeste et al., 2003). A positive feedback loop has been proposed in which ATM/ATR concentrates at γH2AX-containing double strand breaks via MDC1 to further phosphorylate adjacent H2AX molecules and amplify the DNA damage signal (Lou et al., 2006; Stucki et al., 2005). Through this signal amplification step, a number of mediator/repair proteins, including BRCA1 and 53BP1, concentrate to sites of DNA damage to facilitate downstream checkpoint activation.

We and others have previously demonstrated that tandem BRCT domains serve as phospho-peptide binding motifs that mediate protein-protein interactions (Manke et al., 2003; Yu et al., 2003). Specifically, a number of DNA damage response proteins, including BRCA1 and MDC1 (Fernandez-Capetillo et al., 2002; Goldberg et al., 2003; Lou et al., 2003a; Lou et al., 2003b; Stewart et al., 2003), harbor BRCT domains that mediate binding to their respective partners in a phosphorylation-dependent manner (Yu and Chen, 2004; Stucki et al., 2005). In addition to tandem BRCT domains, the FHA

domain constitutes a separate class of phospho-peptide binding modules (Durocher et al., 2000). Many FHA domain-containing proteins have been reported to play a role in DNA repair, cell cycle arrest, and pre-mRNA processing (Sun et al., 1998; Li et al., 2000). The reversibility and sequence selectivity of ligand binding afforded by these and other phospho-peptide binding domain-containing proteins allows individual protein-protein interactions that control downstream responses to be tightly regulated in a stimulus-dependent manner.

Recent studies have provided additional insight into the phosphorylation-dependent regulation of the DNA damage signaling network. However, the detailed mechanisms by which the initial γH2AX signal at DNA lesions becomes propagated, amplified, and modified to concentrate checkpoint mediator proteins to these sites remains obscure. Here we report our study of an FHA and Ring domain-containing protein, RNF8, which serves as the molecular linker for communication between the protein phosphorylation and protein ubiquitylation pathways that are crucial for the activation and maintenance of the DNA damage response.

Results

RNF8 is a DNA damage responsive protein

We have previously studied the role of the FHA domain and Ring domain-containing protein Chfr in mitosis (Yu et al., 2005). In the course of these studies we used a protein named RNF8 as a control because it is the only other known mammalian protein that shares a similar domain organization with Chfr (**Supplementary Figure 1A**). RNF8

was initially reported to interact with Class III human ubiquitin-conjugating enzymes (E2s) through its RING domain (Ito et al., 2001). RNF8 was later shown to bind to the Retinoid X Receptor and regulate its transcriptional activity (Takano et al., 2004). Because several FHA domain-containing proteins are known to play a role in DNA damage signaling, we investigated whether RNF8 or Chfr might participate in the DNA damage response. Cells stably expressing tagged-RNF8 or Chfr were irradiated. Interestingly and surprisingly, RNF8 foci can be readily observed after DNA damage, and these foci co-localized with the DNA damage marker γ-H2AX (**Figure 1A**). Despite the resemblance of RNF8 and Chfr (**Supplementary Figure 1A**), we did not observe any Chfr focus formation following DNA damage (**Figure 1A**), indicating that these two related proteins have distinct cellular functions.

To confirm the observed IR-induced focus localization of RNF8, we generated a polyclonal antibody specifically recognizing RNF8 (**Supplementary Figure 1B**). IR-induced foci (IRIF) of endogenous RNF8 can be readily visualized (**Figure 1B**). The fact that RNF8 foci overlap with those of γH2AX prompted us to speculate that RNF8 might function in the DNA damage response. We therefore examined the localization of RNF8 with several proteins known to be involved in this damage-induced signaling cascade. As expected, RNF8 colocalizes with MDC1, NBS1, 53BP1, BRCA1, pATM and MCPH1, further lending credence to the potential role of RNF8 in the DNA damage response (**Supplementary Figure 1C**).

The DNA damage-induced focus formation of checkpoint proteins reflects their localization to chromatin structures at the vicinity of DNA breaks. Indeed, increased amount of RNF8 accumulated in the acid extractable fraction after IR treatment (**Figure**

1C). Moreover, the less-soluble fraction of RNF8 can be released by nuclease treatment (**Figure 1D**), suggesting that RNF8 accumulates at the chromatin upon DNA damage. Together, our studies suggest that RNF8 is a novel DNA damage responsive protein.

RNF8 acts downstream of H2AX and MDC1 following DNA damage

It is generally accepted that the phosphorylation of histone variant H2AX is the initial signal upon DNA lesion detection. γH2AX is required for the sustained localization of a number of DNA damage mediator/repair factors at chromatin regions at or near the sites of DNA damage (Paull et al., 2000). To delineate where RNF8 fits in the established DNA damage signaling cascade, we examined IRIF formation of RNF8 in a number of human or mouse cells with deficiencies in various DNA damage checkpoint proteins. Our anti-RNF8 antibody could not detect endogenous RNF8 in mouse embryonic fibroblasts (MEFs), so we used retroviral particles containing a RNF8 expression construct to infect these cells (**Figure 1E**). In sharp contrast to the control wild-type MEFs, no IR-induced RNF8 focus formation was observed in H2AX deficient MEFs or those reconstituted with the S139A phospho-mutant (**Figure 1E and Supplementary Figure 1D**). Likewise, RNF8 focus formation was also abrogated in MDC1 deficient cells. On the other hand, RNF8 relocalization to γ-H2AX containing foci is not noticeably affected in cells with BRCA1, 53BP1 or NBS1 deficiency (**Figure 1E**). These data suggest that RNF8 acts downstream of H2AX and MDC1 in the DNA damage responsive pathway.

The FHA, but not its RING domain, targets RNF8 to DNA breaks

The FHA domain is a phospho-protein binding module (Durocher et al., 2000; Li et al., 2000). **Figure 1F** shows that tagged wild-type RNF8 formed foci that co-localize with γH2AX following IR treatment. Similarly, foci formation can also be observed for the delRING mutant. On the other hand, the FHA deletion mutant (i.e. delFHA) failed to localize to γH2AX containing foci, suggesting that the FHA domain of RNF8 is important for targeting RNF8 to IR-induced DNA damage sites (**Supplementary Figure 1E**).

The FHA domain of RNF8 selects phospho-motifs similar to those recognized by tandem BRCT domains

FHA domains, like tandem BRCT domains, recognize amino acid sequences extending 3-4 residues around a central phosphorylated amino acid, with selection determined primarily by residues in the third C-terminal (+3) position (Durocher et al., 2000). However, in contrast to BRCT domains which recognize both pSer and pThr-containing sequences, FHA domains appear only to recognize pThr-containing motifs. We determined the optimal phosphopeptide motifs recognized by RNF8 FHA domain using pThr-oriented peptide library screening (**Figure 2A**). Intriguingly, the RNF8 FHA domain showed strong selection for Tyr and Phe in the +3 position. This selection for aromatic amino acids differs substantially from the acidic and aliphatic residue selection in the +3 position shown by all other FHA domains for which X-ray crystal structures are available (Durocher et al., 2000; Li et al., 2002). Instead, this selection for aromatic amino acids at +3 position closely resembles the optimal phosphopeptide motifs

recognized by the tandem BRCT domains of BRCA1 and MDC1 (Manke et al., 2003; Stucki et al., 2005; Yu et al., 2003).

To investigate the structural basis for this unusual motif selection, we used limited proteolysis to map the boundaries of the FHA domain, and solved the high-resolution structure of the RNF8 FHA:optimal phosphopeptide complex by X-ray crystallography at 1.35Å (**Supplementary Table 1**; the PDB code for the RNF8 FHA domain is 2PIE). The global fold of the RNF8 FHA domain is an 11 stranded b-sandwich with the phosphopeptide-binding surface comprised of residues in loops that connect the b-strands at one end of the sandwich (**Figure 2B**), similar to what has been previously observed in the crystal structures of the 11-stranded Rad53 and Chk2 FHA domains (Durocher et al., 2000; Li et al., 2002). The bound phospho-peptide is in an extended conformation with extensive contacts between the peptide backbone and side-chain and main chain atoms from the RNF8 FHA domain (**Figure 2C**).

Three structural features observed in the RNF8 FHA:phosphopeptide complex are distinct from other FHA domains: First, the RNF8 FHA domain contains two divergent loops and a C-terminal α-helical extension that cluster along one face of the domain, well removed from the phosphopeptide-interacting surface (**Figure 2B**, shaded red). This region is likely involved in phospho-independent interactions with potential substrates or with additional portions of the full-length RNF8 molecule. Second, the RNF8 FHA domain makes extensive direct contacts to the phosphate group, including a novel bidentate interaction involving Arg-61 that is not observed in any other FHA domain:phosphopeptide crystal structure (**Figure 2D**). Third, the selectivity for Tyr/Phe in the +3 position results from its interaction with a flat, mostly non-polar surface

relatively enriched in sulfur-containing amino acids (Cys-55, Met-58, Val-110 and Leu-112). Interestingly, the general character of the interaction between the +3 Tyr and the surface of the RNF8 FHA domain is strikingly similar to that observed between the +3 Tyr residue of a γH2AX pSer-containing phosphopeptide and the surface of the tandem BRCT domains of MDC1 critical for MDC1 foci formation (**Figure 2E and F**). On the other hand, the RNF8 FHA domain +3 interacting surface bears little resemblance to the analogous surfaces in other FHA domains (**Figure 2G-H**). Thus, it appears that the pThr-binding FHA domain of RNF8 has evolved to bind to similar motifs as those recognized by the BRCT domains of the foci-forming proteins BRCA1 and MDC1.

Phosphopeptide binding by the FHA domain is required for RNF8 foci formation

We directly investigated whether phospho-dependent binding was critical for IRIF formation of RNF8. We found that mutation of Arg-61 to Gln reduced FHA domain:phosphopeptide binding by over 160-fold (**Supplementary Figure 2A and B**). When the full-length RNF8 R61Q mutant protein was introduced into cells, no R61Q foci were observed after radiation damage (**Supplementary Figure 2C**), indicating that phospho-dependent binding is required for interaction between the RNF8 FHA domain and its upstream binding partner.

In an experiment with cell lysates, wild-type RNF8 could be pulled down with a phospho-Ser-containing peptide derived from γH2AX (**Supplementary Figure 2D**) but not with the control unphosphorylated peptide. This interaction was totally abolished in experiments with the delFHA or R61Q mutant proteins. Furthermore, consistent with the previous observation that Chfr does not form IRIF, Chfr did not bind to the phosphorylated H2AX peptide (**Supplementary Figure 2E**). Although RNF8 bound to

phospho-H2AX peptides in a pulldown experiment, we failed to detect any direct binding between the RNF8 FHA domain and a phospho-H2AX peptide by isothermal titration calorimetry (data not shown), raising the possibility that the RNF8:γH2AX interaction observed was indirect. Because the BRCT domains of MDC1 mediate its direct binding to phospho-H2AX, and MDC1 is required for RNF8 IRIF, we examined whether RNF8 interacts with MDC1. Intriguingly, the optimal motif for phospho-peptide binding to the RNF8 FHA domain is pTXXY/F (**Figure 2A**), and inspection of the MDC1 sequence reveals four potential ATM/ATR phophorylation sites that match this motif (T^{699}QCF, T^{719}QAF, T^{752}QPF and T^{765}QPF). One of these TQPF sites was recently reported to be phosphorylated following DNA damage in a large-scale proteomic study (Matsuoka et al., 2007). We therefore synthesized peptides containing each of these four putative phosphorylation sites and measured their binding to the RNF8 FHA domain. Three of the four bound with affinities comparable to the optimal peptide (**Supplementary Figure 2F-I**), while the fourth bound more weakly. We next generated a deletion mutant spanning residues 698-768 (Del) of MDC1 (**Figure 3A**) and showed that MDC1, but not Del, specifically bound to purified GST-RNF8 (**Figure 3B and 3C**). In addition, RNF8 co-precipitated with wild-type but not Del mutant of MDC1 *in vivo* (**Figure 3D**), further implicating these putative phosphorylation sites are required for the interaction between RNF8 and MDC1. A control experiment using the delFHA mutant of RNF8 confirms that this interaction also requires the FHA domain of RNF8 (**Figure 3E**). Similar results were obtained in reciprocal immunoprecipitation assays. Consistent with the role of MDC1 in mediating RNF8 accumulation at DNA damage sites, an increased amount of MDC1 bound to RNF8 after IR, which was abolished with prior phosphatase treatment (**Figure**

3F). Likewise, wild-type but not Del mutant of MDC1 restored RNF8 IRIF in MDC1-depleted HeLa cells (**Supplementary Figure3 A-B**). Collectively, these *in vitro* and *in vivo* results support a possible direct role of MDC1 in facilitating RNF8 localization, via a phospho-specific interaction conferred by the RNF8 FHA domain, to the chromatin following DNA damage.

Both the RNF8 FHA and RING domains are required for BRCA1 and 53BP1 IRIF

To further probe the role of RNF8 at DNA damage sites *in vivo*, we depleted RNF8 using two different siRNAs and tested whether the IRIF of a number of mediator/repair proteins RNF8 dependent. RNF8 knockdown did not affect γH2AX or MDC1 foci formation at DNA damage sites (**Figure 4A and Supplementary Figure 4A-C**), however, localization of 53BP1 and BRCA1 to foci was abrogated (**Figure 4A**), suggesting that RNF8 lies upstream of these DNA damage signaling mediator/effectors and facilitates the accumulation of these proteins to the sites of DNA damage.

The MDC1/RNF8 interaction experiments presented in **Figure 3** imply that MDC1 may interact with RNF8 and regulate RNF8-dependent events following DNA damage. MDC1 was previously shown to be required for IRIF formation of these checkpoint mediator proteins (Goldberg et al., 2003; Lou et al., 2003a; Stewart et al., 2003; also see **Supplemental Figure 4D**). Here, we examined whether the RNF8/MDC1 interaction is crucial for these events *in vivo*. As expected, ectopically expressed MDC1 restored the accumulation of BRCA1 and 53BP1 in response to IR in $MDC1^{-/-}$ MEFs. The MDC1 deletion mutation, which abolishes its interaction with RNF8, did not affect its own focus localization following IR but failed to restore the RNF8-dependent

concentration of BRCA1 and 53BP1 at the foci (**Figure 4B**), suggesting that the MDC1/RNF8 interaction is likely to be required for RNF8-dependent functions following DNA damage.

In order to further explore roles of the RNF8 FHA and RING domains in targeting 53BP1 and BRCA1 to foci, we knocked down RNF8 in HeLa cells using siRNF8#2 (**Supplementary Figure 4E**) and reintroduced full-length RNF8, delFHA or delRING using constructs containing silent mutations within the RNF8 coding sequence which rendered the reintroduced constructs resistant to the siRNA. Unlike the deletion mutants, reconstitution with full-length RNF8 restored 53BP1 and BRCA1 IRIF in cells depleted of endogenous RNF8 (**Figure 4C and Supplemental Figure 4F**). Thus, both the phosphopeptide-binding and the ubiquitin ligase activity of RNF8 are required for its function in mediating the accumulation of DNA damage checkpoint proteins at the sites of DNA damage.

RNF8 mediates IR-induced damage-associated ubiquitin conjugates

Our observation that IRIF formation of BRCA1 and 53BP1 requires the RNF8 RING domain suggests that the accumulation of these checkpoint proteins is dependent on protein ubiquitylation at the site of the damaged chromatin. The finding that DNA damage-associated ubiquitin conjugates can be visualized using the anti-Ubiquitin FK2 antibody (Morris and Solomon, 2004; Polanowska et al., 2006) is consistent with this hypothesis. If RNF8 is involved in the ubiquitylation of proteins at the damaged chromatin, H2AX and MDC1 deficiencies, which abrogate RNF8 accumulation at IRIF, might be expected to disrupt damage-dependent FK2 focus formation. This is indeed the

case (see **Supplementary Figure 5A-C**). Recently, the E2 ubiquitin conjugating enzyme UBC13 was also implicated in the ubiquitylation of protein(s) at the chromatin following DNA damage (Zhao et al., 2007). However, the E3 ligase, which provides substrate specificity, has yet to be identified. That RNF8 was demonstrated to interact with UBC13 for substrate ubiquitylation (Plans et al., 2006) prompted us to speculate that RNF8 and UBC13 might act in concert in the DNA damage-signaling cascade. In support of this speculation, we found that damage-associated ubiquitin conjugates were absent in either RNF8-depleted or UBC13-depleted cells (**Figure 5A and Supplementary Figure 5D)**. UBC13 depletion also suppressed the accumulation of 53BP1 and BRCA1 at IRIF, but does not affect focus formation of phospho-H2AX and MDC1 (**Supplementary Figure 5E**). In addition, RNF8 IRIF can be readily visualized in UBC13-depleted cells, indicating that the damage-dependent RNF8 localisation precedes UBC13 function in the DNA damage response. These data, together with previous reports, imply that RNF8 acts with UBC13 to exert a mediator role in the DNA damage-signaling cascade.

RNF8 mediates accumulation of the UIM-containing protein Rap80 at sites of DNA breaks

The ubiquitin-interacting motif (UIM) containing protein Rap80 has recently been shown to relocalise to γH2AX-containing foci in a UIM-dependent manner (Kim et al., 2007; Sobhian et al., 2007; Wang et al., 2007). We found that Rap80 focus formation was abolished in RNF8-depleted and UBC13-depleted cells (**Figure 5B)**, and that its localization requires both the RING and FHA domains of RNF8 (**Figure 5C-D**). Together these results strongly suggest that the ubiquitin conjugates, whose appearance at

foci we have shown to be dependent on both RNF8 and UBC13, might serve as a signal for Rap80 accumulation at the sites of DNA damage.

RNF8 is required for H2AX ubiquitylation following DNA damage

Because H2AX phosphorylation is essential for sustained accumulation of MDC1 and RNF8, which in turn is required for localization of other checkpoint proteins including the Rap80-BRCA1 complex and 53BP1 at DNA damage sites, we speculate that H2AX might be ubiquitylated in a RNF8-dependent manner. We first examined whether H2AX can be ubiquitylated *in vivo*. By overexpressing tagged H2AX and ubiquitin in the cell, we found that some of the tagged H2AX molecules were ubiquitylated (**Figure 6A**). Moreover, in HeLa cells stably expressing HA-tagged H2AX, we showed that H2AX ubiquitylation is regulated in an IR-dependent manner *in vivo*, and that depletion of RNF8 abolished the IR-induced H2AX ubiquitylation. Because of the pivotal role phosphorylated H2AX plays in the localization of checkpoint proteins at IRIF, we used an antibody against γH2AX to examine the state of H2AX ubiquitylation specifically in the phosphorylated form. While RNF8 deficiency does not affect IR-induced H2AX phosphorylation, slower migrating bands corresponding to ubiquitylated endogenous γH2AX species were observed in irradiated cells expressing RNF8 but were compromised in the RNF8 knockdown cells (**Figure 6C**). While RNF8 is clearly responsible for γH2AX di-ubiquitylation, RNF8 knockdown also appears to lower the levels of γH2AX mono-ubiquitylation. Downregulation of UBC13 also significantly reduced damage-induced ubiquitylation of γH2AX (**Supplementary Figure 6C**), supporting our hypothesis that RNF8 acts with UBC13 in promoting protein

ubiquitylation at or near DNA damage sites. In control experiments we have shown that our anti-phospho-H2AX antibody specifically recognizes phosphorylated H2AX species following DNA damage (**Figure 6D and 6E**). Together, these results point to a role for RNF8 in regulating γH2AX ubiquitylation in response to DNA damage.

Because H2AX phosphorylation is critical for RNF8 localization to sites of DNA breaks (**Supplementary Figure 1D**), we asked whether H2AX ubiquitylation is similarly compromised in cells expressing a non-phosphorylatable S139A H2AX mutant protein. Indeed, only H2AX deficient MEFs reconstituted with wild-type H2AX, but not those reconstituted with the H2AX S139A mutant, supported damage-dependent H2AX ubiquitylation (**Figure 6E**). Similarly, the RNF8-dependent H2AX ubiquitylation is also compromised in MDC1 deficient cells (**Supplementary Figure 6A**).

We also reconstituted H2AX-/- cells with H2AX K119/120R mutant. While this H2AX mutant abolished the constitutive mono-ubiquitylation of H2AX, cells expressing this mutant still showed damage-induced ubiquitin conjugates formation and IR-induced H2AX ubiquitylation (**Supplementary Figure 6D-E**), suggesting that IR-induced H2AX ubiquitylation is distinct from those constitutively mono-ubiquitylated H2AX species.

To further evaluate whether the chromatin-associated RNF8 phosphopeptide-binding and E3 ligase activities are required for H2AX ubiquitylation in response to IR, RNF8-depleted HeLa cells expressing siRNA-resistant full-length, delFHA or delRING versions of RNF8 were examined. As shown in **Figure 6F**, IR-induced H2AX ubiquitylation required both the FHA and RING domains of RNF8.

RNF8 participates in the G2/M checkpoint and loss of RNF8 renders cells sensitive to ionizing radiation

DNA damage checkpoints have evolved to maintain genomic stability by preventing cells with damaged DNA from entering mitosis. Because RNF8 enables the accumulation of multiple checkpoint proteins at the sites of DNA breaks, we tested the effect of RNF8 in IR-induced cell cycle arrest. While cells transfected with control siRNA displayed normal checkpoint activation, RNF8-depleted cells, like those depleted of BRCA1, failed to properly arrest at the G2/M checkpoint upon IR (**Figure 7A and Supplementary Figure 7A**). Moreover, restoration of the G2/M checkpoint required re-introduction of full-length RNF8 in RNF8-depleted cells (**Figure 7B and Supplementary Figure 7B)**. Finally, depletion of RNF8 also resulted in a notable increase in IR sensitivity (**Figure 7B and Supplementary Figure 7C**), further supporting a role of RNF8 in cellular response to DNA damage.

Discussion

In this study, we have uncovered a novel role of RNF8 in the DNA damage response. Our data strongly suggests that RNF8 channels the initial phosphorylation-dependent marks at DNA lesions to promote the accumulation of multiple checkpoint proteins, including Rap80, BRCA1 and 53BP1, which in turn, contribute to its putative role in maintaining genome integrity. As E3 ubiquitin ligase, RNF8 promotes protein ubiquitylation at sites of DNA breaks.

In eukaryotic cells where DNA is tightly packed, the chromatin structure impedes many of the activities that require access to the genetic materials. Despite our understanding of the roles of H2AX phosphorylation in the DNA damage response, it has only become evident recently that chromatin remodeling and other histone modifications also play important functions in this cellular process. Specifically, a role of the ATP-dependent chromatin-remodeling complexes, such as the INO80, SWR1, RSC, and SWI/SNF, and histone acetyltransferase complexes including Trrap-Tip60 complex have been implicated in DNA repair (Murr et al., 2006; Tsukuda et al., 2005). However, unlike those catalysed by the Trrap-Tip60 complex, the impaired loading of DNA checkpoint proteins observed in RNF8-depleted cells could not be counteracted by pre-incubation with sodium butyrate, chloroquine or hypotonic solution (unpublished results). We hypothesize that RNF8 may be required for the accumulation of checkpoint/repair proteins via a different mechanism, i.e. ubiquitylating proteins at the sites of DNA breaks. Indeed, RNF8 is pivotal for the accumulation of ubiquitin conjugates at the damaged chromatin, which depended on its FHA and RING domains. In support of the role of RNF8 in protein ubiquitylation at sites of DNA breaks, we show that the

phosphorylation-dependent RNF8 accumulation at γ-H2AX sites is responsible for the IR-induced H2AX di-ubiquitylation. The E3 ligase complex BRCA1-BARD1 has also been implicated to catalyse ubiquitin polymers at the damaged chromatin (Morris and Solomon, 2004; Polanowska et al., 2006; Yu et al., 2006). However, unlike RNF8 and UBC13, BRCA1-depletion did not compromise the IR-induced H2AX ubiquitylation (**Supplementary Figure 6B**), suggesting that BRCA1 accumulates at the sites of DNA breaks subsequent to the RNF8/UBC13-dependent H2AX ubiquitylation following DNA damage. Finally, we found that ubiquitylation events catalysed by RNF8 is independent of H2AX K119 and K120, illustrating that these damage-induced H2AX ubiquitination are RNF8-dependent but distinct from the constitutive mono-ubiquitylation of H2AX (**Supplementary Figure 6D-E**).

A scenario is now emerging in which ubiquitination serves as a post-translational modifier in the DNA damage-dependent signaling cascade (Huang and D'Andrea, 2006). Recent studies suggest a role of histone ubiquitination as a means to remodel the chromatin in order to facilitate the accumulation of DNA repair protein (Kapetanaki et al., 2006; Wang et al., 2006). In addition, mono-ubiquitylation of a number of proteins has been demonstrated to be responsible for protein-protein interactions (Garcia-Higuera et al., 2001; Matsushita et al., 2005; Pavri et al., 2006; Stelter and Ulrich, 2003; Taniguchi et al., 2002). Multiple ubiquitin moieties covalently attached via lysine 63 have also been reported to regulate and promote the accumulation of proteins involved in DNA repair (Hoege et al., 2002; Hofmann and Pickart, 1999). More recently, the ubiquitin interacting motif (UIM)-containing protein Rap80 was discovered to play a role in the BRCA1-dependent DNA damage response, serving as an adaptor for BRCA1

accumulation at sites of DNA breaks (Kim et al., 2007; Sobhian et al., 2007; Wang et al., 2007). Our observation that RNF8 mediates both the IRIF of conjugated ubiquitin and Rap80 at sites of DNA breaks implicates that Rap80 might associate with the damaged chromatin by tethering to certain FK2-reacting ubiquitylated protein(s). The fact that the IR-induced H2AX ubiquitylation is similarly compromised in RNF8-depleted cells implicates H2AX as a RNF8 substrate. Besides H2AX, H2A has also been shown to be a substrate of RNF8 in the accompanying paper (**Mailand et al., XXX**). Together these studies support a model that ubiquitin chains on H2A, H2AX and probably other RNF8 substrates might serve as important docking sites during the transduction of the DNA damage signal.

While the ubiquitin-interacting domain (UIM)-containing protein RAP80 is required for BRCA1 localization, RAP80 is dispensable for 53BP1 localization. It would be interesting to test whether any additional ubiquitin-binding protein would serve to tether 53BP1 to DNA damage sites via damage-associated ubiquitin conjugates. Given the role of histone ubiquitylation in chromatin remodeling, it is also plausible that the RNF8-dependent ubiquitylation events at the vicinity of DNA breaks may enhance the accessibility of 53BP1 to modified histones (Huyen et al., 2004; Sanders et al., 2004; Botuyan et al., 2006). In any case, based on the requirement of RNF8 RING domain, we propose that RNF8 facilitates the transduction of the initial phosphorylation-dependent DNA lesion signal by regulating H2A/H2AX ubiquitylation, and possibly other substrates, and thus control the localization of the Rap80-BRCA1 complex and other checkpoint proteins.

In summary, our study implicates a critical role of the E3 ubiquitin ligase RNF8 in supporting genome integrity by licensing the assembly of multiple checkpoint/DNA repair proteins at DNA lesions. The link between protein phosphorylation and ubiquitylation revealed in this study highlights the importance of post-translational modifiers as molecular switches that govern, amongst many cellular processes, the DNA damage response pathway in a stimulus-inducible manner. RNF8 is a key player involved in the cross-talk between different protein modifications, with its FHA domain required for its localization to DNA damage foci through a phosphorylation-dependent interaction, and its E3 ligase catalytic domain required for the further accumulation of Rap80, BRCA1 and 53BP1 (**Figure 7F**). The interplay between these two protein modification cascades may play an essential role in ensuring the proper execution of cellular response to DNA damage.

Experimental Procedures

Antibodies

The RNF8 polyclonal antibody was raised against a GST-RNF8 fusion protein and was affinity purified using an MBP-RNF8 column. Antibodies against the myc epitope, H2AX, γH2AX, BRCA1, MDC1, 53BP1, were previously described (Lou et al., 2003b; Yu et al., 2006). The anti-H3, anti-FK2 and anti-ORC2 antibodies were obtained from Upstate Cell Signaling. Anti-pATM (Ser1981), anti-GAPDH, and anti-HA, anti-UBC13 antibodies were purchased from Calbiochem, Chemicon, Covance and Anaspec respectively. Anti-actin and anti-Flag (M2) were obtained from Sigma.

Cell Culture and Transfection

293T cells were cultured in RPMI 1640 supplemented with 5% fetal calf serum (FCS), 5% bovine serum and 100 U/ml penicillin, and 100 μg/ml streptomycin and maintained in 5% CO_2 at 37°C. Cell transfection was performed using Lipofectamine 2000 (Invitrogen) following manufacturer's protocol.

Immunostaining procedure

To visualize IRIF, cells cultured on coverslips were treated with 10 Gy IR (1 Gy=100 Rads) followed by recovery for 6 hrs. Cells were then washed with PBS, incubated in 3% paraformaldehyde for 12 minutes and permeabilized in 0.5% triton solution for 5 minutes at room temperature. Samples were blocked with 5% goat serum and incubated with primary antibody for 60 minutes. Samples were washed and incubated with secondary

antibody for 60 minutes. Cells were then stained with DAPI to visualize nuclear DNA. The coverslips were mounted onto glass slides with anti-fade solution and visualized using a Nikon ECLIPSE E800 fluorescence microscope.

IR sensitivity, G2/M checkpoint assays and Chromatin fractionation

IR sensitivity and G2/M checkpoint assays were performed as described previously (Lou et al., 2003b). Preparation of chromatin fractions were described previously with modifications (Yu et al., 2006). Briefly, cells were harvested at indicated times after treatment and washed once with PBS. Cell pellets were subsequently resuspended in low salt permeabilization buffer (10mM HEPES pH7.4, 10mM KCl, 0.05% NP-40 and protease inhibitors) and incubated on ice for 10 min. Thereafter, nuclei were recovered and resuspended in 0.2M HCl. The soluble fraction was neutralized with 1 M Tris-HCl pH 8.0 for further analysis. For microccocal nuclease (MNase) treatment, nuclei recovered after low salt extraction was washed and resuspended in nuclease reaction buffer (10mM HEPES pH 7.4, 10 mM KCl, 0.5 mM MgCl2, 2 mM CaCl2). 10 U of nuclease was added and incubated for 30 min on ice. Thereafter, the insoluble fraction was treated essential as above to isolate the chromatin-bound proteins.

Figure Legends

Figure 1. RNF8 is involved in mammalian DNA damage response.

A) Localization of tagged RNF8 and Chfr in response to IR. Cells expressing Myc-tagged RNF8 or Chfr were irradiated and immunostained with anti-Myc and anti-pH2AX antibodies. **B**) Localization of endogenous RNF8 before and after IR treatment in 293T cells. Immunostaining experiments were performed using anti-RNF8 and anti-pH2AX antibodies. **C, D**) RNF8 relocalizes to chromatin fraction after IR (**C**), which is reversible following micrococcal nuclease treatment (**D**). Procedures were carried out as described in Methods and immunoblotting experiments were conducted using indicated antibodies. **E**) Genetic dependence of RNF8 relocalization following DNA damage. Deficient cells and their respective wild-type counterparts were infected with retrovirus expressing Flag-tagged RNF8. Immunostaining experiments were performed using anti-Flag and anti-γH2AX antibodies. F) The FHA domain, but not the RING domain, of RNF8 targets its localization to DNA damage foci. Cells expressing Flag-tagged wild-type or mutants of RNF8 were mock treated or irradiated and immunostaining were carried out using indicated antibodies.

Figure 2. Structural basis for phosphorylation-dependent binding by RNF8 FHA domain.

A) Amino acid selectivity values for the RNF8 FHA domain determined using the phosphothreonine-oriented degenerate peptide library MAXXXX-pT-XXXXAKKK, where X indicates all amino acids except Cys. Values $\geq$ 1.4 indicate moderate selection; values $\geq$ 2.0 indicate strong selection. **B**) Cartoon representation of the RNF8 FHA domain bound to the optimal phosphopeptide ELKpTERY. **C**) stereo view of the

phosphopeptide-binding surface. **D**) Close up of the phosphate binding pocket, with 2Fo-Fc density map contoured at 2σ. A bound water molecule is evident in the upper center. **E-G**) Molecular interaction surfaces of the RNF8:phosphopeptide complex, the MDC1 tandem BRCT domain:γ-H_2AX phosphopeptide complex, and the Rad53 FHA1:LEVpTEAD phosphopeptide complex. Peptide surfaces are contoured in salmon, protein surfaces are contoured in lime. In the RNF8 FHA domain (**E**), selection for Tyr over Phe in the +3 position likely results from a water-mediated contact between the Tyr hydroxyl and the backbone nitrogen of Leu-57. In the Rad53 FHA1 structure (**G**), an Arg residue from the FHA domain occupies the equivalent position as the peptide +3 Tyr in the RNF8 structure (dashed line). (**H**) Divergence in the phospho-amino acid +3 binding surfaces of the FHA domains of RNF8 and Rad53. The Cα traces of the FHA domains of the RNF8 FHA domain:phosphopeptide complex and the Rad53FHA1 domain:phosphopeptide complex were optimally aligned. The phosphopeptide +3 interacting region is shown in cartoon representation, with the RNF8 FHA domain shaded blue, and its bound phosphopeptide shaded cyan, while the Rad53 FHA1 domain is shaded yellow and its bound phosphopeptide is shaded green. The +3 Tyr residue in the RNF8 optimal phosphopeptide, and the +3 Asp in the Rad53 FHA1 optimal phosphopeptide are shown in stick representation. Note that the +3 Tyr binding site in RNF8 is occluded in the Rad53 FHA domain by an Arg residue that mediates selection for Asp in the +3 position.

Figure 3. RNF8 is localized to the sites of DNA damage via a FHA-dependent interaction with MDC1.

A) Schematic diagram showing full-length MDC1 (WT) and an internal deletion mutant (Del) of MDC1 that abolishes all four putative phosphorylation sites. **B**) Commassie staining of purified bacterially-expressed GST-RNF8 protein. **C**) Full length MDC1 but not the deletion mutant (Del) interacts with RNF8 in a pull-down assay. Lysates from 293T cells over-expressing Flag-tagged MDC1 or its deletion mutant were incubated with GST-RNF8 fusion protein immobilized on the glutathione agarose beads for 2 hours before washing and subsequent analysis by Western blotting with anti-Flag antibody. **D**) MDC1 but not Del mutant of MDC1 co-immunoprecipitates with RNF8. 293T cells were co-transfected with plasmids encoding myc-tagged RNF8 and plasmids encoding SBP-Flag-MDC1 or its deletion mutant. Lysates were incubated with streptavidin beads for 2 hr at 4°C. Thereafter beads were washed three times with NETN, isolates were separated by SDS-PAGE and analyzed by Western blotting using indicated antibodies. **E**) RNF8 interacts with MDC1 via its FHA domain. Experiments were conducted similar to that described in **D)** and immunoprecipitation and immunoblotting were carried out as indicated. **F**) 293T cells were irradiated (10 Gy; 1Gy=100 Rads) or left untreated and cell extract (NETN + 500 mM NaCl) was treated with or without lambda phosphatase prior to diluting and incubating with bacterially expressed 10 μg of GST-RNF8 protein for 2 hr at 4°C . The GST-RNF8 complex was separated by SDS-PAGE to evaluate the amount of endogenous MDC1 that bound specifically to RNF8.

Figure 4. RNF8 is required for accumulation of BRCA1 and 53BP1 at the sites of DNA damage.

A) HeLa cells were transfected twice with either RNF8 siRNAs or a non-targeting control siRNA. 48 hr after the second transfection, cells were treated with 10 Gy IR and recovered for 6 hours before they were fixed and permeabilized. Immunostaining experiments were performed as described in the Experimental Procedures. **B**) 53BP1 and BRCA1 IRIF formation are restored in MDC1 deficient cells reconstituted with full-length MDC1 but not with the deletion mutant of MDC1. Expression constructs encoding HA-tagged MDC1 (WT) or its deletion mutant (Del) were transiently transfected into MDC1 deficient MEFs. 24 hours post-transfection, cells were irradiated (10 Gy) and immuno-stained with indicated antibodies. **C**) HeLa cells depleted of endogenous RNF8 using siRNA#2 were infected with viruses encoding siRNA-resistant wild-type, delFHA or delRING mutant of RNF8. Infected cells were then irradiated and processed as described above to visualize protein localization as indicated.

Figure 5. RNF8 functions in concert with UBC13 and is important for IR-induced DNA damage-associated ubiquitin conjugates.

A) HeLa cells depleted of endogenous RNF8 or UBC13 were irradiated (10Gy) and immunostained with FK2 and γH2AX antibodies. **B**) IRIF of UIM-containing protein Rap80 is dependent on RNF8 and UBC13. **C**) IRIF of damage-associated ubiquitin and **D**) Rap80 foci formation requires RNF8 FHA and RING domains. HeLa cells infected with virus expressing siRNA-resistant full-length RNF8, delFHA or delRING were transiently transfected with siRNF8#2 to deplete endogenous RNF8. 48 hours after the second transfection, cells were fixed and immuno-stained with indicated antibodies.

Figure 6. RNF8 is required for H2AX ubiquitylation following DNA damage.

A) H2AX is ubiquitylated *in vivo*. 293T cells were transiently transfected with plasmids encoding myc-tagged ubiquitin with or without plasmids encoding SBP-Flag-H2AX. Immunoprecipitation and immunoblotting were carried out using indicated antibodies. Black arrow indicates doubly ubiquitylated species of H2AX, while grey arrow indicates mono-ubiquitinated H2AX. Multiple-ubiquitinated H2AX species are also pointed out. **B**) HeLa cells stably expressing HA-tagged H2AX were transfected with control siRNA or RNF8 siRNA were treated with 10 Gy or left untreated. Cells were harvested 1 hr post-irradiation. Cell lysates were prepared, separated by SDS-PAGE and blotted with indicated antibodies. **C**) HeLa cells transfected with control siRNA or RNF8 siRNA were treated as described (**B**) and immunoblotting experiments were carried out using indicated antibodies. **D**) IR-induced H2AX ubiquitylation in H2AX+/+ and H2AX-/- MEFs. Cell lysates prepared from wild-type or H2AX-/- cells before and after irradiation were immunoblotted with anti-H2AX and anti-pH2AX antibodies. **E**) IR-induced H2AX ubiquitylation requires H2AX phosphorylation. H2AX deficient MEFs stably expressing HA-tagged H2AX or S139A mutant of H2AX were treated with 0 Gy or 10 Gy and immunoblotting was performed using indicated antibodies. **F**) IR-induced H2AX ubiquitylation requires RNF8 FHA and RING domains. Experiments were carried out as that described in Fig. 5g/5h. Immunoblotting experiments were conducted with antibodies as indicated. Arrow indicates ubiquitylated species of H2AX that only appear after radiation in cells expressing wild-type RNF8.

Figure 7. RNF8 is required for G2/M checkpoint control and cell survival following ionizing radiation.

A) IR-induced G2/M checkpoint is defective in cells with RNF8 depletion and requires both the RNF8 FHA and RING domains. Summary of the percentages of cells stained positive with phospho-H3 antibody before and after IR treatment from three individual experiments. Error bars indicate standard deviation. HeLa cells were transfected with indicated siRNAs and percentages of mitotic cells before and after radiation were determined by FACS analysis as described in Experimental procedures. **B**) RNF8-depleted cells display increased radiation sensitivity as determined by colony formation assay. Figure represents value obtained from three separate experiments, each performed in triplicate. Error bars indicate standard deviation. **C**) A proposed model of the DNA damage responsive pathway involving RNF8. The relocalization of the Rap80-BRCA1 complex and 53BP1 requires RNF8-dependent protein ubiquitylation at the chromatin, whereas the accumulation of NBS1 at DNA damage sites is independent of RNF8.

Acknowledgements

We thank Duaa Mohammad and J. Vey for technical help, Dr. Andre Nussenzweig for providing valuable reagent, and Dr Jiri Lukas for the MDC1 construct and communicating unpublished results. Portions of this research were carried out at the Stanford Synchrotron Radiation Laboratory, a national user facility operated by Stanford University on behalf of the U.S. Department of Energy, Office of Basic Energy Sciences. This work was supported by grants from the National Institutes of Health (CA89239, CA92312 and CA100109 to J.C. and GM 60594 to M.B.Y.). J.C is a recipient of an Era of Hope Scholar award from the Department of Defence and a member of the Mayo Clinic Breast SPORE program (P50 CA116201). X.Y. is supported by the Developmental fund from the University of Michigan Cancer Center. The PDB code for the RNF8 FHA domain is 2PIE.

References

Bartkova, J., Horejsi, Z., Koed, K., Kramer, A., Tort, F., Zieger, K., Guldberg, P., Sehested, M., Nesland, J.M., Lukas, C., *et al.* (2005). DNA damage response as a candidate anti-cancer barrier in early human tumorigenesis. Nature *434*, 864-870.

Bassing, C.H., Suh, H., Ferguson, D.O., Chua, K.F., Manis, J., Eckersdorff, M., Gleason, M., Bronson, R., Lee, C., and Alt, F.W. (2003). Histone H2AX: a dosage-dependent suppressor of oncogenic translocations and tumors. Cell *114*, 359-370.

Botuyan, M.V., Lee, J., Ward, I.M., Kim, J.E., Thompson, J.R., Chen, J., and Mer, G. (2006). Structural basis for the methylation state-specific recognition of histone H4-K20 by 53BP1 and Crb2 in DNA repair. Cell *127*, 1361-1373.

Celeste, A., Difilippantonio, S., Difilippantonio, M.J., Fernandez-Capetillo, O., Pilch, D.R., Sedelnikova, O.A., Eckhaus, M., Ried, T., Bonner, W.M., and Nussenzweig, A. (2003). H2AX haploinsufficiency modifies genomic stability and tumor susceptibility. Cell *114*, 371-383.

Durocher, D., Taylor, I.A., D., S., Haire, L.F., Westcott, S.L., Jackson, S.P., Smerdon, S.J., and Yaffe, M.B. (2000). The molecular basis of FHA Domain:phosphopeptide binding specificity and implications for phosphodependent signaling mechanisms. Mol Cell.

Fernandez-Capetillo, O., Chen, H.T., Celeste, A., Ward, I., Romanienko, P.J., Morales, J.C., Naka, K., Xia, Z., Camerini-Otero, R.D., Motoyama, N., *et al.* (2002). DNA damage-induced G2-M checkpoint activation by histone H2AX and 53BP1. Nat Cell Biol *4*, 993-997.

Garcia-Higuera, I., Taniguchi, T., Ganesan, S., Meyn, M.S., Timmers, C., Hejna, J., Grompe, M., and D'Andrea, A.D. (2001). Interaction of the Fanconi anemia proteins and BRCA1 in a common pathway. Mol Cell *7*, 249-262.

Goldberg, M., Stucki, M., Falck, J., D'Amours, D., Rahman, D., Pappin, D., Bartek, J., and Jackson, S.P. (2003). MDC1 is required for the intra-S-phase DNA damage checkpoint. Nature *421*, 952-956.

Gorgoulis, V.G., Vassiliou, L.V., Karakaidos, P., Zacharatos, P., Kotsinas, A., Liloglou, T., Venere, M., Ditullio, R.A., Jr., Kastrinakis, N.G., Levy, B., *et al.* (2005). Activation of the DNA damage checkpoint and genomic instability in human precancerous lesions. Nature *434*, 907-913.

Hoege, C., Pfander, B., Moldovan, G.L., Pyrowolakis, G., and Jentsch, S. (2002). RAD6-dependent DNA repair is linked to modification of PCNA by ubiquitin and SUMO. Nature *419*, 135-141.

Hofmann, R.M., and Pickart, C.M. (1999). Noncanonical MMS2-encoded ubiquitin-conjugating enzyme functions in assembly of novel polyubiquitin chains for DNA repair. Cell *96*, 645-653.

Huang, T.T., and D'Andrea, A.D. (2006). Regulation of DNA repair by ubiquitylation. Nat Rev Mol Cell Biol *7*, 323-334.

Huyen, Y., Zgheib, O., Ditullio, R.A., Jr., Gorgoulis, V.G., Zacharatos, P., Petty, T.J., Sheston, E.A., Mellert, H.S., Stavridi, E.S., and Halazonetis, T.D. (2004). Methylated lysine 79 of histone H3 targets 53BP1 to DNA double-strand breaks. Nature *432*, 406-411.

Ito, K., Adachi, S., Iwakami, R., Yasuda, H., Muto, Y., Seki, N., and Okano, Y. (2001). N-Terminally extended human ubiquitin-conjugating enzymes (E2s) mediate the ubiquitination of RING-finger proteins, ARA54 and RNF8. Eur J Biochem *268*, 2725-2732.
Kapetanaki, M.G., Guerrero-Santoro, J., Bisi, D.C., Hsieh, C.L., Rapic-Otrin, V., and Levine, A.S. (2006). The DDB1-CUL4ADDB2 ubiquitin ligase is deficient in xeroderma pigmentosum group E and targets histone H2A at UV-damaged DNA sites. Proc Natl Acad Sci U S A *103*, 2588-2593.
Kim, H., Chen, J., and Yu, X. (2007). Ubiquitin-binding protein RAP80 mediates BRCA1-dependent DNA damage response. Science *316*, 1202-1205.
Li, J., Lee, G.I., Van Doren, S.R., and Walker, J.C. (2000). The FHA domain mediates phosphoprotein interactions. J Cell Sci *113 Pt 23*, 4143-4149.
Li, J., Williams, B.L., Haire, L.F., Goldberg, M., Wilker, E., Durocher, D., Yaffe, M.B., Jackson, S.P., and Smerdon, S.J. (2002). Structural and functional versatility of the FHA domain in DNA-damage signaling by the tumor suppressor kinase Chk2. Mol Cell *9*, 1045-1054.
Lou, Z., Chini, C.C., Minter-Dykhouse, K., and Chen, J. (2003a). Mediator of DNA damage checkpoint protein 1 regulates BRCA1 localization and phosphorylation in DNA damage checkpoint control. J Biol Chem *278*, 13599-13602.
Lou, Z., Minter-Dykhouse, K., Franco, S., Gostissa, M., Rivera, M.A., Celeste, A., Manis, J.P., van Deursen, J., Nussenzweig, A., Paull, T.T., *et al.* (2006). MDC1 maintains genomic stability by participating in the amplification of ATM-dependent DNA damage signals. Mol Cell *21*, 187-200.
Lou, Z., Minter-Dykhouse, K., Wu, X., and Chen, J. (2003b). MDC1 is coupled to activated CHK2 in mammalian DNA damage response pathways. Nature *421*, 957-961.
Mailand, N., Bekker-Jensen, S., Faustrup, H., Melander, F., Bartek, J., Lukas, C., and Lukas, J. (XXX) Cell XXX
Manke, I.A., Lowery, D.M., Nguyen, A., and Yaffe, M.B. (2003). BRCT repeats as phosphopeptide-binding modules involved in protein targeting. Science *302*, 636-639.
Matsuoka, S., Ballif, B.A., Smogorzewska, A., McDonald, E.R., 3rd, Hurov, K.E., Luo, J., Bakalarski, C.E., Zhao, Z., Solimini, N., Lerenthal, Y., *et al.* (2007). ATM and ATR substrate analysis reveals extensive protein networks responsive to DNA damage. Science *316*, 1160-1166.
Matsushita, N., Kitao, H., Ishiai, M., Nagashima, N., Hirano, S., Okawa, K., Ohta, T., Yu, D.S., McHugh, P.J., Hickson, I.D., *et al.* (2005). A FancD2-monoubiquitin fusion reveals hidden functions of Fanconi anemia core complex in DNA repair. Mol Cell *19*, 841-847.
Minor, W., Cymborowski, M., Otwinowski, Z., and Chruszcz, M. (2006). HKL-3000: the integration of data reduction and structure solution--from diffraction images to an initial model in minutes. Acta Crystallogr D Biol Crystallogr *62*, 859-866.
Morris, J.R., and Solomon, E. (2004). BRCA1 : BARD1 induces the formation of conjugated ubiquitin structures, dependent on K6 of ubiquitin, in cells during DNA replication and repair. Hum Mol Genet *13*, 807-817.
Murr, R., Loizou, J.I., Yang, Y.G., Cuenin, C., Li, H., Wang, Z.Q., and Herceg, Z. (2006). Histone acetylation by Trrap-Tip60 modulates loading of repair proteins and repair of DNA double-strand breaks. Nat Cell Biol *8*, 91-99.

Paull, T.T., Rogakou, E.P., Yamazaki, V., Kirchgessner, C.U., Gellert, M., and Bonner, W.M. (2000). A critical role for histone H2AX in recruitment of repair factors to nuclear foci after DNA damage. Curr Biol *10*, 886-895.
Pavri, R., Zhu, B., Li, G., Trojer, P., Mandal, S., Shilatifard, A., and Reinberg, D. (2006). Histone H2B monoubiquitination functions cooperatively with FACT to regulate elongation by RNA polymerase II. Cell *125*, 703-717.
Plans, V., Scheper, J., Soler, M., Loukili, N., Okano, Y., and Thomson, T.M. (2006). The RING finger protein RNF8 recruits UBC13 for lysine 63-based self polyubiquitylation. J Cell Biochem *97*, 572-582.
Polanowska, J., Martin, J.S., Garcia-Muse, T., Petalcorin, M.I., and Boulton, S.J. (2006). A conserved pathway to activate BRCA1-dependent ubiquitylation at DNA damage sites. Embo J *25*, 2178-2188.
Sanders, S.L., Portoso, M., Mata, J., Bahler, J., Allshire, R.C., and Kouzarides, T. (2004). Methylation of histone H4 lysine 20 controls recruitment of Crb2 to sites of DNA damage. Cell *119*, 603-614.
Sobhian, B., Shao, G., Lilli, D.R., Culhane, A.C., Moreau, L.A., Xia, B., Livingston, D.M., and Greenberg, R.A. (2007). RAP80 targets BRCA1 to specific ubiquitin structures at DNA damage sites. Science *316*, 1198-1202.
Stelter, P., and Ulrich, H.D. (2003). Control of spontaneous and damage-induced mutagenesis by SUMO and ubiquitin conjugation. Nature *425*, 188-191.
Stewart, G.S., Wang, B., Bignell, C.R., Taylor, A.M., and Elledge, S.J. (2003). MDC1 is a mediator of the mammalian DNA damage checkpoint. Nature *421*, 961-966.
Storoni, L.C., McCoy, A.J., and Read, R.J. (2004). Likelihood-enhanced fast rotation functions. Acta Crystallogr D Biol Crystallogr *60*, 432-438.
Stucki, M., Clapperton, J.A., Mohammad, D., Yaffe, M.B., Smerdon, S.J., and Jackson, S.P. (2005). MDC1 directly binds phosphorylated histone H2AX to regulate cellular responses to DNA double-strand breaks. Cell *123*, 1213-1226.
Sun, Z., Hsiao, J., Fay, D.S., and Stern, D.F. (1998). Rad53 FHA domain associated with phosphorylated Rad9 in the DNA damage checkpoint [see comments]. Science *281*, 272-274.
Takano, Y., Adachi, S., Okuno, M., Muto, Y., Yoshioka, T., Matsushima-Nishiwaki, R., Tsurumi, H., Ito, K., Friedman, S.L., Moriwaki, H., *et al.* (2004). The RING finger protein, RNF8, interacts with retinoid X receptor alpha and enhances its transcription-stimulating activity. J Biol Chem *279*, 18926-18934.
Taniguchi, T., Garcia-Higuera, I., Xu, B., Andreassen, P.R., Gregory, R.C., Kim, S.T., Lane, W.S., Kastan, M.B., and D'Andrea, A.D. (2002). Convergence of the fanconi anemia and ataxia telangiectasia signaling pathways. Cell *109*, 459-472.
Tsukuda, T., Fleming, A.B., Nickoloff, J.A., and Osley, M.A. (2005). Chromatin remodelling at a DNA double-strand break site in Saccharomyces cerevisiae. Nature *438*, 379-383.
Wang, B., Matsuoka, S., Ballif, B.A., Zhang, D., Smogorzewska, A., Gygi, S.P., and Elledge, S.J. (2007). Abraxas and RAP80 form a BRCA1 protein complex required for the DNA damage response. Science *316*, 1194-1198.
Wang, H., Zhai, L., Xu, J., Joo, H.Y., Jackson, S., Erdjument-Bromage, H., Tempst, P., Xiong, Y., and Zhang, Y. (2006). Histone H3 and H4 ubiquitylation by the CUL4-DDB-

ROC1 ubiquitin ligase facilitates cellular response to DNA damage. Mol Cell *22*, 383-394.
Ward, I.M., Minn, K., Jorda, K.G., and Chen, J. (2003). Accumulation of checkpoint protein 53BP1 at DNA breaks involves its binding to phosphorylated histone H2AX. J Biol Chem *278*, 19579-19582.
Yu, X., and Chen, J. (2004). DNA damage-induced cell cycle checkpoint control requires CtIP, a phosphorylation-dependent binding partner of BRCA1 C-terminal domains. Mol Cell Biol *24*, 9478-9486.
Yu, X., Chini, C.C., He, M., Mer, G., and Chen, J. (2003). The BRCT domain is a phospho-protein binding domain. Science *302*, 639-642.
Yu, X., Fu, S., Lai, M., Baer, R., and Chen, J. (2006). BRCA1 ubiquitinates its phosphorylation-dependent binding partner CtIP. Genes Dev *20*, 1721-1726.
Yu, X., Minter-Dykhouse, K., Malureanu, L., Zhao, W.M., Zhang, D., Merkle, C.J., Ward, I.M., Saya, H., Fang, G., van Deursen, J., *et al.* (2005). Chfr is required for tumor suppression and Aurora A regulation. Nat Genet *37*, 401-406.
Zhao, G.Y., Sonoda, E., Barber, L.J., Oka, H., Murakawa, Y., Yamada, K., Ikura, T., Wang, X., Kobayashi, M., Yamamoto, K., *et al.* (2007). A critical role for the ubiquitin-conjugating enzyme Ubc13 in initiating homologous recombination. Mol Cell *25*, 663-675.

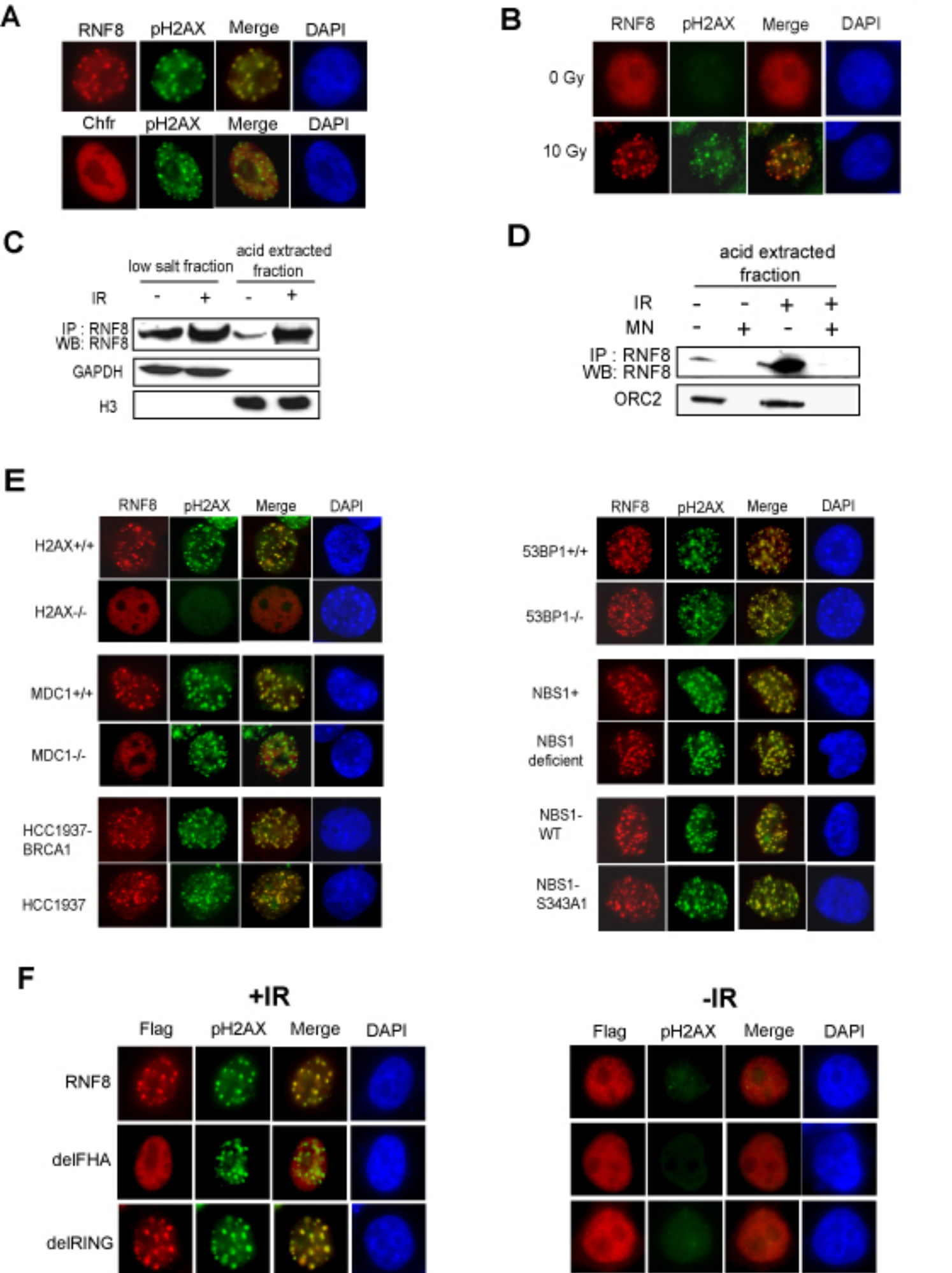
A
RNF8
pH2AX
Merge
DAPI
Chfr
pH2AX
Merge
DAPI
B
RNF8
pH2AX
Merge
DAPI
0 Gy
10 Gy
C
low salt fraction
acid extracted fraction
IR
- + - +
IP : RNF8
WB: RNF8
GAPDH
H3
D
acid extracted fraction
IR - - + +
MN - + - +
IP : RNF8
WB: RNF8
ORC2
E
RNF8
pH2AX
Merge
DAPI
H2AX+/+
H2AX-/-
MDC1+/+
MDC1-/-
HCC1937-BRCA1
HCC1937
53BP1+/+
53BP1-/-
NBS1+
NBS1 deficient
NBS1-WT
NBS1-S343A1
F
+IR
-IR
Flag
pH2AX
Merge
DAPI
RNF8
delFHA
delRING

A

RNF8 Motif Selectivity

-3	-2	-1	+1	+2	+3
E (1.6)	L (1.8)	K (1.4)	E (1.8)	X	**Y** (4.0)
L (1.5)	E (1.5)	E (1.4)	V (1.6)		**F** (2.9)
		I (1.4)	I (1.6)		
			R (1.5)		
			Q (1.4)		

B

C

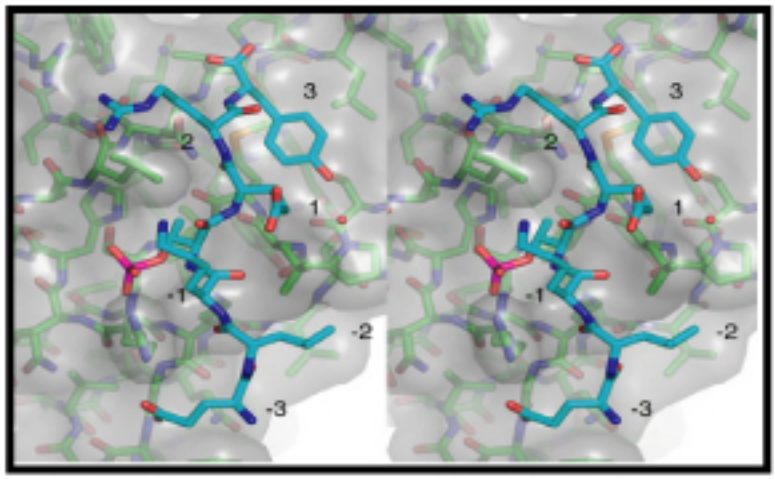

D

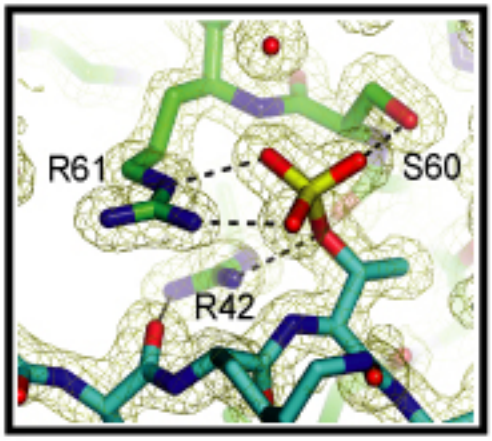

E

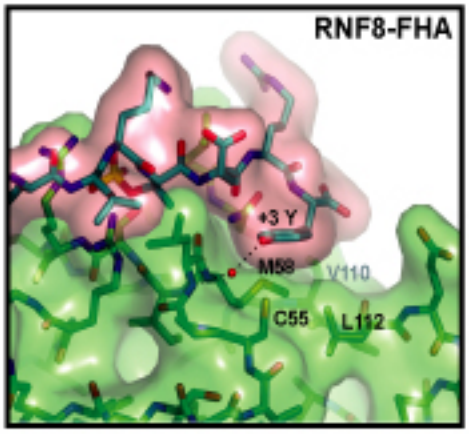

F

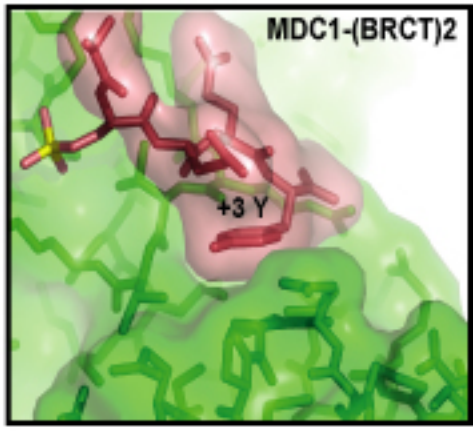

G

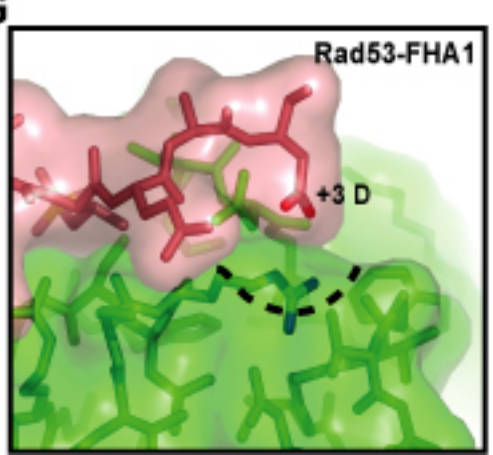

H

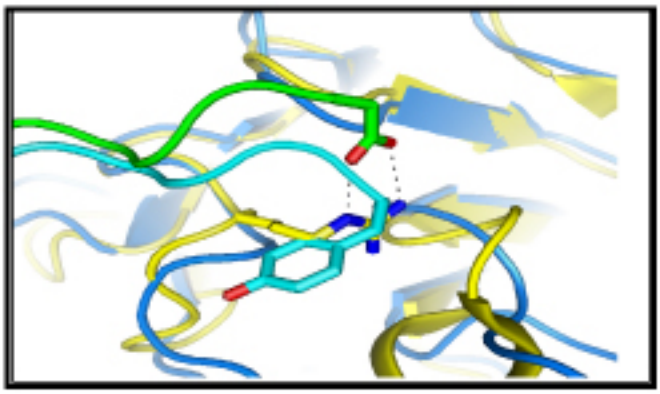

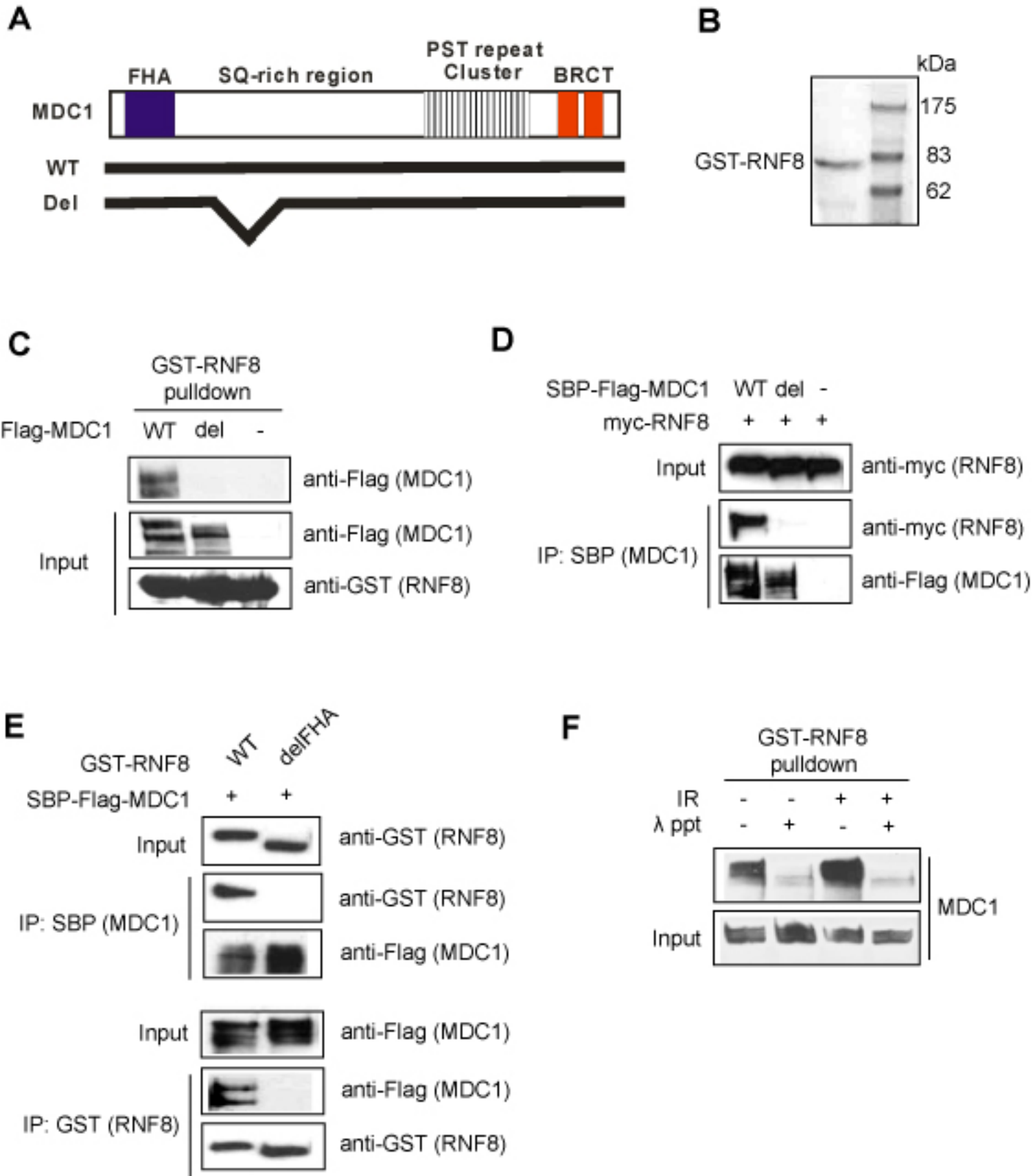
A
FHA
SQ-rich region
PST repeat Cluster
BRCT
MDC1
WT
Del
B
kDa
175
83
62
GST-RNF8
C
GST-RNF8 pulldown
Flag-MDC1 WT del -
anti-Flag (MDC1)
Input
anti-Flag (MDC1)
anti-GST (RNF8)
D
SBP-Flag-MDC1 WT del -
myc-RNF8 + + +
Input
anti-myc (RNF8)
IP: SBP (MDC1)
anti-myc (RNF8)
anti-Flag (MDC1)
E
GST-RNF8 WT delFHA
SBP-Flag-MDC1 + +
Input
anti-GST (RNF8)
IP: SBP (MDC1)
anti-GST (RNF8)
anti-Flag (MDC1)
Input
anti-Flag (MDC1)
IP: GST (RNF8)
anti-Flag (MDC1)
anti-GST (RNF8)
F
GST-RNF8 pulldown
IR - - + +
λ ppt - + - +
MDC1
Input

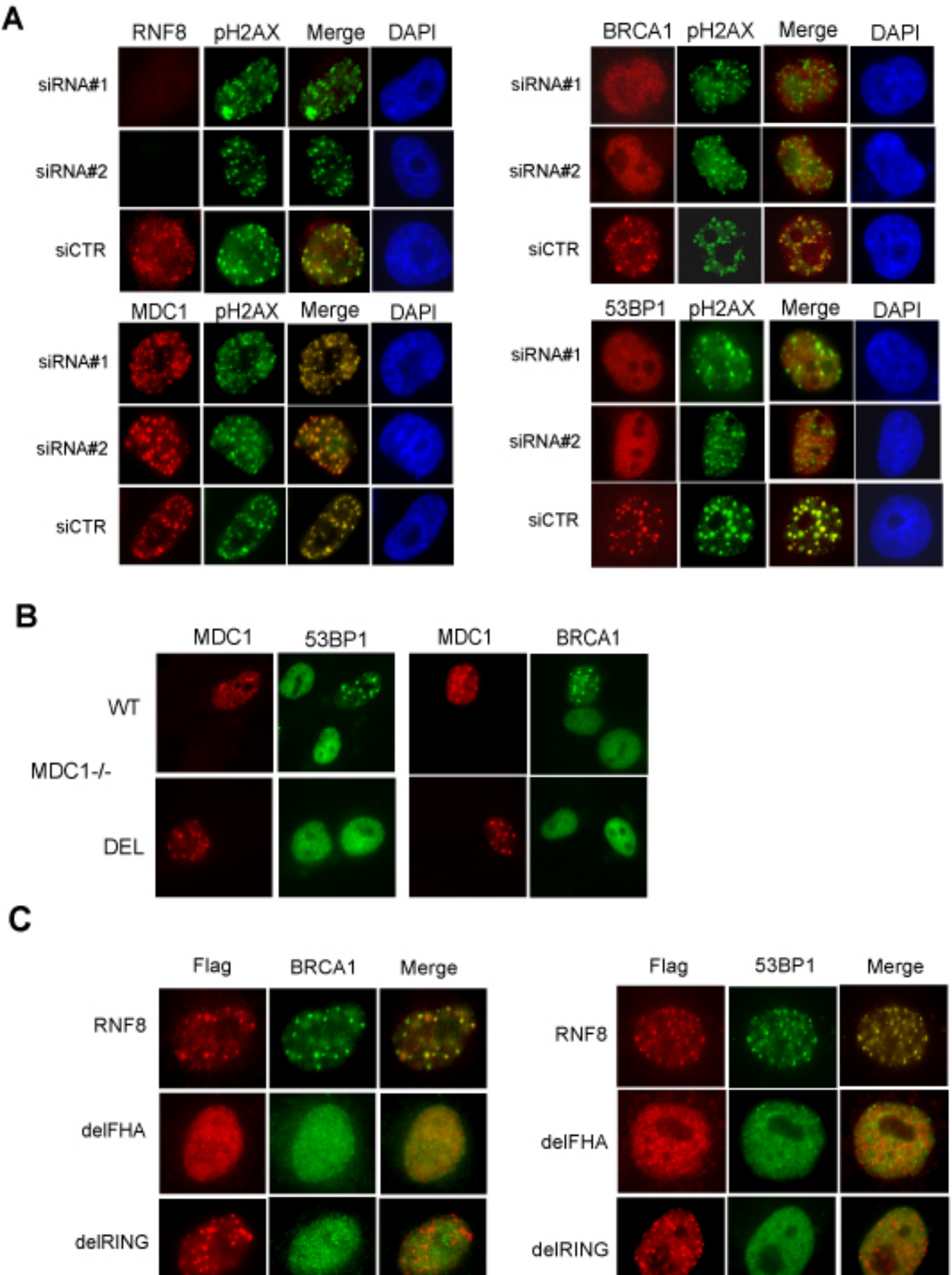
A
RNF8
pH2AX
Merge
DAPI
siRNA#1
siRNA#2
siCTR
BRCA1
pH2AX
Merge
DAPI
siRNA#1
siRNA#2
siCTR
MDC1
pH2AX
Merge
DAPI
siRNA#1
siRNA#2
siCTR
53BP1
pH2AX
Merge
DAPI
siRNA#1
siRNA#2
siCTR
B
MDC1
53BP1
MDC1
BRCA1
WT
MDC1-/-
DEL
C
Flag
BRCA1
Merge
RNF8
delFHA
delRING
Flag
53BP1
Merge
RNF8
delFHA
delRING

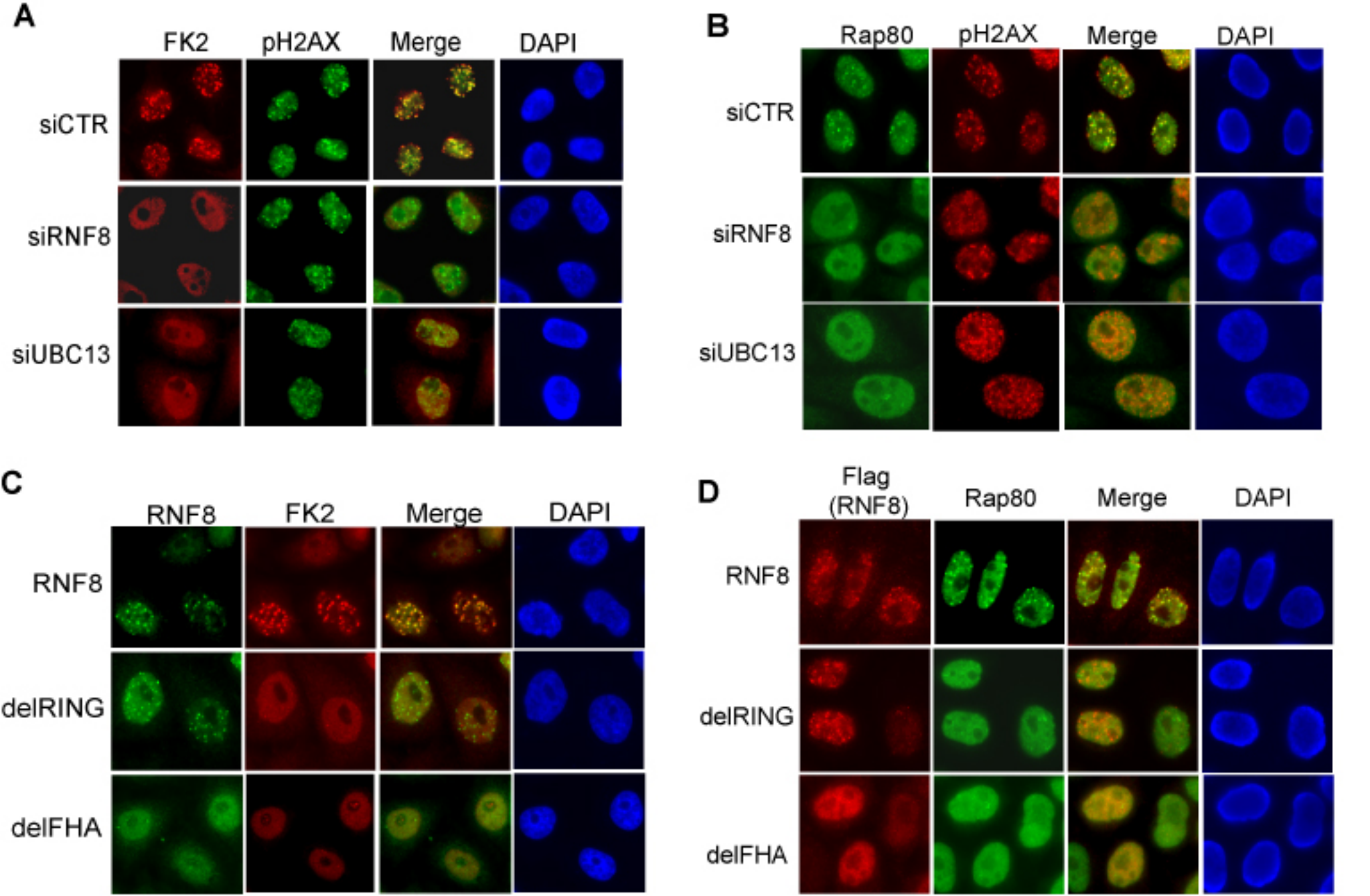
A
FK2
pH2AX
Merge
DAPI
siCTR
siRNF8
siUBC13
B
Rap80
pH2AX
Merge
DAPI
siCTR
siRNF8
siUBC13
C
RNF8
FK2
Merge
DAPI
RNF8
delRING
delFHA
D
Flag (RNF8)
Rap80
Merge
DAPI
RNF8
delRING
delFHA

Figure 6

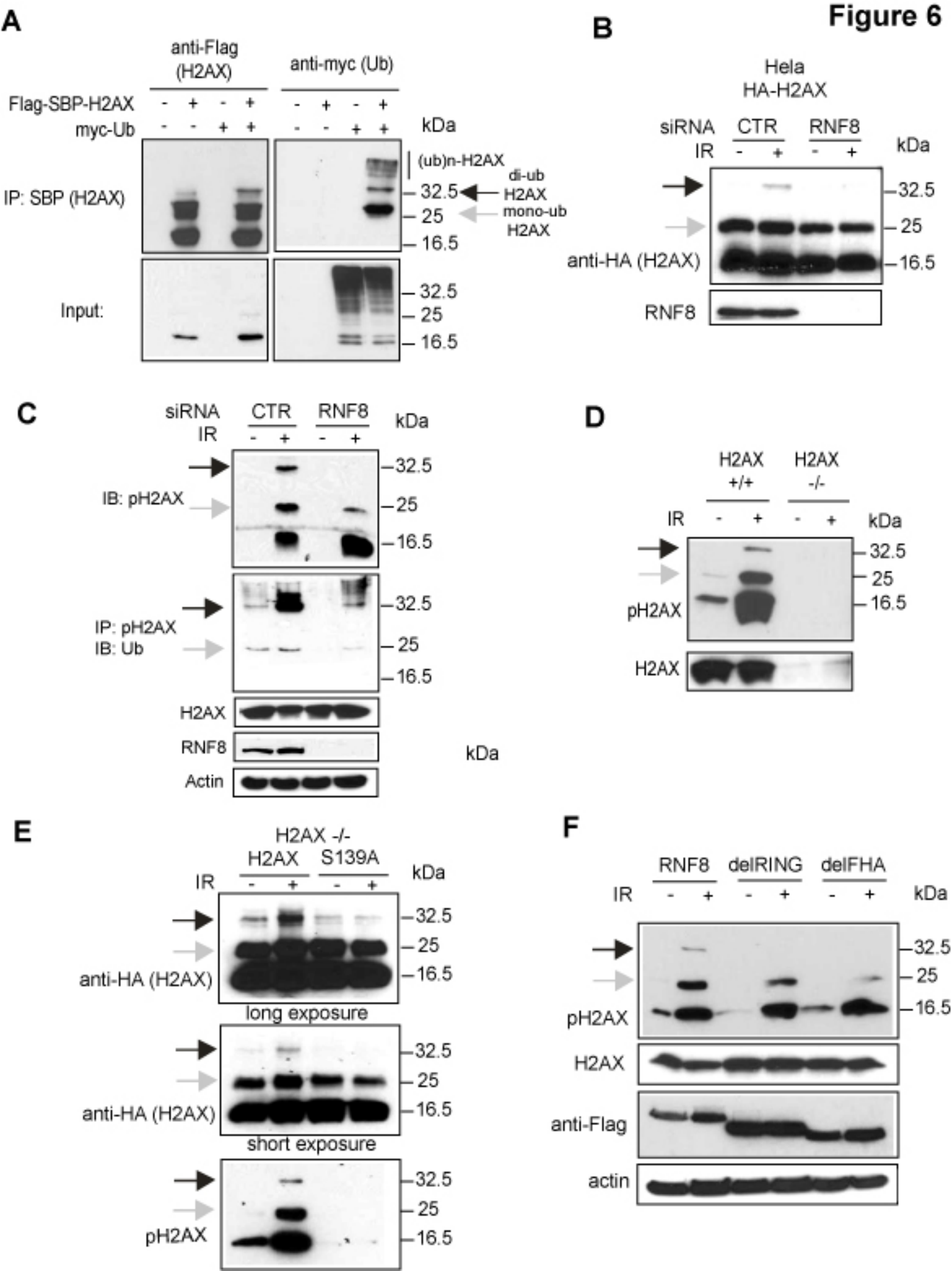
A
anti-Flag (H2AX)
anti-myc (Ub)
Flag-SBP-H2AX
myc-Ub
kDa
(ub)n-H2AX
di-ub H2AX
mono-ub H2AX
IP: SBP (H2AX)
32.5
25
16.5
Input:
B
Hela HA-H2AX
siRNA CTR RNF8
IR
kDa
anti-HA (H2AX)
RNF8
C
siRNA CTR RNF8
IR
kDa
IB: pH2AX
IP: pH2AX
IB: Ub
H2AX
RNF8
Actin
D
H2AX +/+
H2AX -/-
IR
kDa
pH2AX
H2AX
E
H2AX -/-
H2AX
S139A
IR
kDa
anti-HA (H2AX)
long exposure
short exposure
pH2AX
F
RNF8
delRING
delFHA
IR
kDa
pH2AX
H2AX
anti-Flag
actin

Figure 7

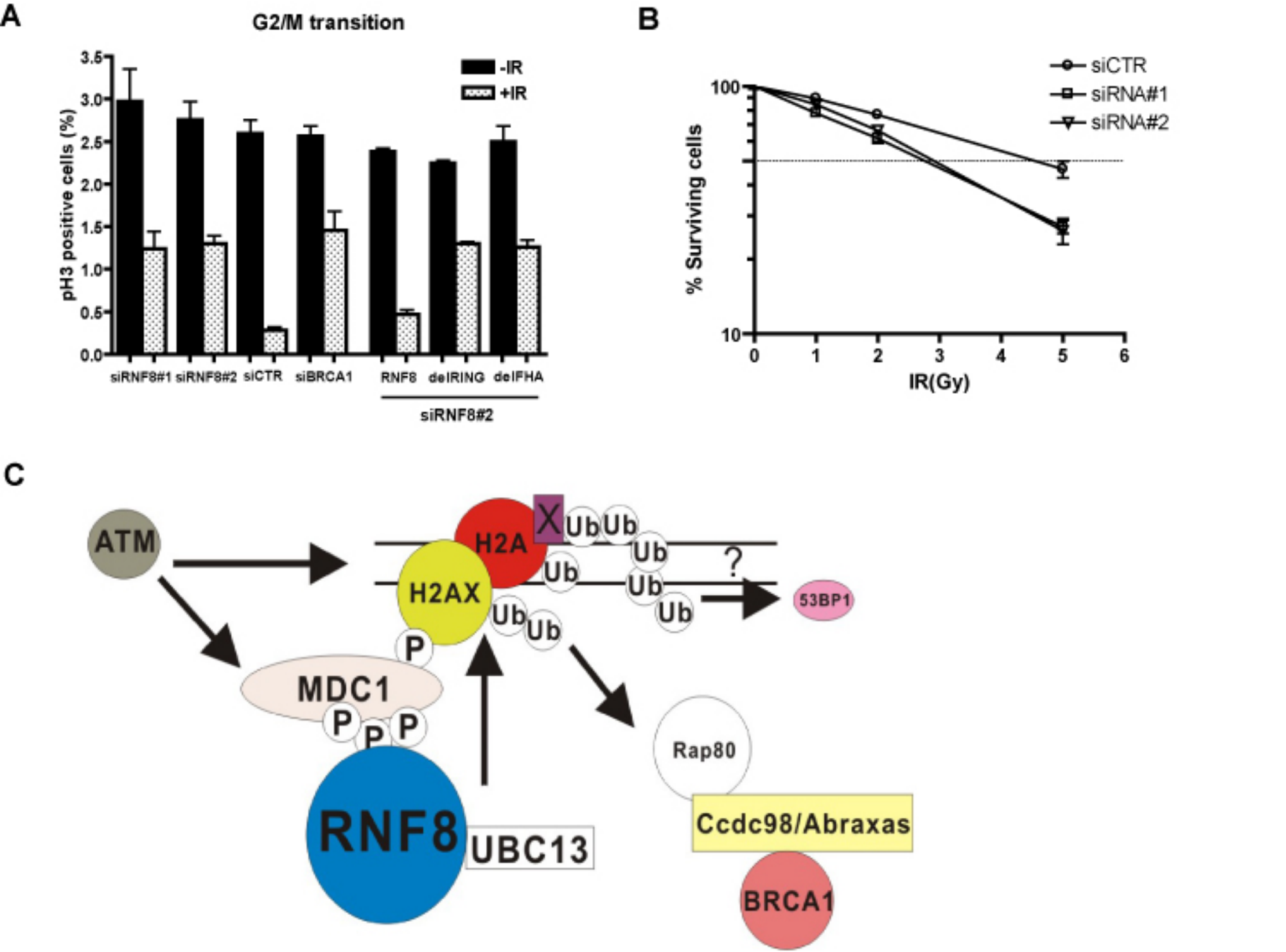
A
G2/M transition
pH3 positive cells (%)
-IR
+IR
siRNF8#1
siRNF8#2
siCTR
siBRCA1
RNF8
deIRING
deIFHA
siRNF8#2
B
% Surviving cells
IR(Gy)
siCTR
siRNA#1
siRNA#2
C
ATM
H2A
X
Ub
H2AX
P
MDC1
RNF8
UBC13
53BP1
Rap80
Ccdc98/Abraxas
BRCA1

Supplemental Experimental Procedures

Oriented peptide library screening

Combinatorial peptide library screening was performed using residues 1-211 of RNF8 fused to GST and analyzed as described previously (Manke et al., 2003).

FHA domain mapping by limited proteolysis

The RNF8 core FHA domain fragment (residues 13-146) was identified by limited proteolysis of the GST-RNF8 (1-211) fusion protein. Briefly, nucleotides corresponding to amino acids 1-211 in RNF8, including all of the FHA domain were subcloned into pGEX4T-1, and the GST-fusion protein expressed in E. coli BL21 cells. The tagged protein was purified on a glutathione-sepharose column (Amersham). 75 ng samples of purified protein (50 μL at 1.5 ng/ μL) were digested with trypsin (Sigma) using a protein:protease ratio of 50:1 (w/w). Duplicate experiments were carried out at room temperature and at 4 C. Samples for SDS-PAGE were collected at 15, 30, 60, and 180 minutes. The stable ~15 kDalton tryptic fragment produced was identified as amino acids 13-136 by a combination of electrospray mass spectroscopy and N-terminal amino acid sequencing by Edman degradation (MIT Biopolymers Lab).

Protein expression and purification for crystallography

Nucleotides encoding the tryptic core of the RNF8 FHA domain (residues 13-146) were cloned into a modified version of pET28a (Novagen). The fusion protein produced by the resulting expression vector contains an N-terminal His_6-tag followed by MBP with a Tev protease site between the MBP domain and the FHA domain. The presence of C-

terminal end of the MPB sequence, the Tev site and the proper FHA domain sequence was verified by DNA sequencing. The fusion protein was expressed in E.coli Rosetta 2 cells (Novagen) and purified by Ni-NTA affinity chromatography. Further purification with amylose bead affinity chromatography was followed by cleavage of the His_6-MBP from the FHA domain by incubation with His_6-tagged Tev protease. The His_6-MBP and protease were removed by passage back through a Ni-NTA column. The purified FHA domain was dialyzed into buffer containing 10 mM Tris pH 8.0, 10 mM NaCl and 1.5 mM DTT then concentrated to 27 mg/ml with an ultra-filtration concentrator (Millipore). Concentrated protein was aliquoted into 50 or 100 μL volumes, flash frozen in LN_2 and stored at -80 C.

Protein-peptide complex crystallization, structure solution and refinement

A phosphopeptide with the optimal sequence for binding the RNF8 FHA domain (ELKpTERY) was synthesized using N-α-FMOC amino acids and standard BOP/HOBt coupling chemistry, and purified by reverse phase HPLC. Purified RNF8 FHA stock was thawed and the optimal phosphopeptide was added at a 2:1 molar excess for batch crystallization, which were performed in 4 mM Tris-HCl pH 8.0, 4 mM NaCl and 0.5 mM DTT at 4ºC. Crystals were obtained over several days and screened at 130 K using a MicroMax 007-HF rotating anode generator with VariMax HR optics and a RAXIS-IV detector (Rigaku). For data collection, crystals were briefly washed with 30% glycerol and frozen in liquid nitrogen. The crystals belong to the space group $C222_1$ with a= 34.7 Å, b= 76.0 Å and c= 121.1 Å. Datasets were collected at 2.5 Å and 1.7 Å resolution using a home source, and at 1.35 Å resolution at SSRL beamline BL9-2. Data were integrated,

scaled and processed using HKL2000 (Minor et al., 2006). A 2.5 Å data set from the rotating anode was used to solve the structure by molecular replacement using PHASER (Storoni et al., 2004). The search model was the first of 20 models in the ensemble comprising the NMR structure of the domain (PDB 2CSW). Each asymmetric unit of the crystal contains one FHA domain- peptide complex. A 1.7 Å data set collected on the rotating anode was used for the initial refinement. The same crystal was later used to collect a 1.35Å data set at SSRL beamline BL9-2. The 1.35 Å data set was missing many strong reflections at low to moderate resolution, so the two reduced data sets from the crystal were merged using Scalepack to produce the data set used for high resolution refinement. R_{sym} for this data set are limited by the resolution of the anode data. The model was built with Coot and refined using Refmac 5.0-Arp/Warp from the CCP4 suite. A summary of the crystallographic statistics is shown in **Supplementary Table1**.

Recombinant RNF8 FHA R61Q mutant protein

The R61Q mutation was produced in the pET28a expression system using the QuickChange mutagenesis kit (Stratagene) and verified by DNA sequencing. Mutant FHA domain was purified by the same method as the wild type domain with the addition of gel filtration on a Superose-12 column as a final step.

Isothermal Titration Calorimetry

Calorimetry measurements were performed on the wild-type and R61Q mutant FHA domains using a VP-ITC microcalorimeter (MicroCal Inc.). Experiments involved 10 μL injections of peptide solutions (150 μM) into a sample cell containing 15 μM RNF8-FHA

domain in 25mM Tris/HCl (pH 8.0), 200mM NaCl. Thirty injections were performed with a spacing of 240s and a reference power of 25 μCal/s. Binding isotherms were plotted and analyzed using Origin Software (MicroCal Inc.)

SiRNA

SiRNAs targeting RNF8, UBC13 and a non-targeting control siRNA were purchased from Dharmacon. SiRNA transfection was performed according to the manufacturer's protocol. Sequences of siRNA#1 and siRNA#2 against RNF8 are 5' AGA AUG AGC UCC AAU GUA UUU 3' and 5' CAG AGA AGC UUA CAG AUG UUU 3', respectively. siRNA against UBC13 was 5' GCA CAG UUC UGC UAU CGA UUU 3'. BRCA1 and MDC1 siRNA was described previously (Kim et al., 2007; Lou et al., 2003).

Construction of wild-type and mutant RNF8

Site-directed mutagenesis was performed according to standard procedure to obtain delFHA, delRING, and R61Q mutants of RNF8. DNA fragments containing wild-type RNF8 or various mutants were subsequently cloned into the pDONR201 vector using Gateway Technology (Invitrogen). For transient expression of RNF8 and its mutants, the corresponding fragments in the entry vectors were transferred into a Gateway compatible destination vector which harbors an N terminal triple-epitope tag (S protein tag, Flag epitope tag and Streptavidin binding peptide tag).

Construction of SiRNA-resistant wild-type and mutant RNF8

Site-directed mutagenesis was performed according to standard procedure to generate silent mutations within RNF8 coding region that is targeted by RNF8 siRNA#2. Sequences of the primers used are 5' ACT CTT CAG CAT CTC AGA GGA GGT TAC AGA TGT TTA AGG TGA CCA TG 3' and 5' ACC TTA AAC ATC TGT AAC CTC CTC TGA GAT GCT GAA GAG TTT G 3'.

Construction of siRNA resistant MDC1 and its deletion mutant

Site-directed mutagenesis was used to generate the internal deletion mutant of MDC1 using primers 5' AAG ATC TGG ACC TAC AAG CTG ACA CGC ACC TTG AGG CCT AT G 3' and 5' AGG CCT CAA GGT GCG TGT CAG CTT GTA GGT CCA GAT CTT CAG 3'. SiRNA-resistant MDC1 construct was generated similarly using primers 5' AGA CAG AGC AAT CCA GTG AGT CTT TGA GGT GTA ACG TGG AGC CAG TAG 3' and 5' ACT GGC TCC ACG TTA CAC CTC AAA GAC TCA CTG GAT TGC TCT GTC TCC TCC 3'.

Culture of MEFs and retroviral infection

Mouse embryonic fibroblasts (MEFs) derived from various knockout strains were cultured in DMEM supplemented with 15% FCS and 100 U/ml penicillin, and 100 μg/ml streptomycin and maintained in 5% CO_2 at 37°C. For viral particle packaging, BOSC23 cells were transiently transfected with the pclampho and expression constructs. Viral supernatant was collected 48 hours post-transfection and was used for infection. Stable pools of infected MEFs were selected in the presence of 2 μg/ml puromycin.

References

Kim, H., Chen, J., and Yu, X. (2007). Ubiquitin-binding protein RAP80 mediates BRCA1-dependent DNA damage response. Science *316*, 1202-1205.

Lou, Z., Minter-Dykhouse, K., Wu, X., and Chen, J. (2003). MDC1 is coupled to activated CHK2 in mammalian DNA damage response pathways. Nature *421*, 957-961.

Manke, I.A., Lowery, D.M., Nguyen, A., and Yaffe, M.B. (2003). BRCT repeats as phosphopeptide-binding modules involved in protein targeting. Science *302*, 636-639.

Minor, W., Cymborowski, M., Otwinowski, Z., and Chruszcz, M. (2006). HKL-3000: the integration of data reduction and structure solution--from diffraction images to an initial model in minutes. Acta Crystallogr D Biol Crystallogr *62*, 859-866.

Storoni, L.C., McCoy, A.J., and Read, R.J. (2004). Likelihood-enhanced fast rotation functions. Acta Crystallogr D Biol Crystallogr *60*, 432-438.

Supplemental Figure Captions

Supplementary Figure 1 A) Schematic diagram showing protein domain structure of Chfr and RNF8. Sequence alignment of the FHA domains of Chfr and RNF8 is also presented. **B**) Characterization of RNF8 antibody. Whole cell extracts (WCE) were prepared from HeLa cells transfected with control siRNA or RNF8 siRNA. Immunoprecipitation and immunoblotting with anti-RNF8 polyclonal antibody were performed as indicated. **C**) RNF8 foci colocalize with those of γH2AX, MDC1, 53BP1, NBS1, pATM, MCPH1 and BRCA1 following DNA damage. **D**) H2AX phosphorylation is required for damage-dependent RNF8 localisation at sites of DNA breaks. H2AX-deficient MEFs reconstituted with wild-type or S139A mutant of H2AX were infected with retrovirus expressing Flag-tagged RNF8. 72 hours post-infection cells were irradiated (10 Gy) or left untreated. Thereafter, cells were fixed and immunostained using indicated antibodies. **E**) Summary of wild-type or mutant RNF8 in IR-induced focus formation.

Supplementary Figure 2. A specific interaction between RNF8 FHA domain and phospho-peptide is important for its IR-induced foci formation. (**A**) Binding of wild-type RNF8 FHA domain to its optimal phosphopeptide. The binding of RNF8 FHA domain (residues 13-146) to its optimal phosphopeptide ELKpTERY was measured by isothermal titration calorimetry. Analysis of the data revealed a single binding site with a Kd = 3.5 ± 0.4 μM. (**B**) The R61Q mutation dramatically reduces phosphopeptide binding by the RNF8 FHA domain. Binding of the RNF8 R61Q mutant FHA domain to

the phosphopeptide ELKpTERY was measured by isothermal titration calorimetry. The best-fit analysis revealed a Kd of ~ 565 μM. **C**) The FHA R61Q mutation abolishes RNF8 relocalization to DNA damage sites. Cells transfected with plasmids encoding Myc-tagged R61Q mutant of RNF8 were mock treated or irradiated (10 Gy). Immunostaining experiments were performed using anti-Myc and anti-pH2AX antibodies. **D**) The FHA deletion mutant and R61Q point mutation disrupt the binding of RNF8 to the pH2AX peptide. 293T cells were transiently transfected with plasmids encoding Myc-tagged RNF8 or its deletion mutant. 24 hr post transfection cell lysates were prepared and incubated with 10 μg of pH2AX peptide for 2 hours before adding streptavidin beads for another 1 hour. Thereafter, pH2AX-containg complex was isolated, separated on SDS-PAGE and immunoblotted with indicated antibodies. **E**) RNF8 but not Chfr binds to the pH2AX peptide. Lysates from 293T cells expressing myc-tagged RNF8 or Chfr were incubated with 10 μg of pH2AX peptide for 2 hours before adding streptavidin beads for another 1 hour. Thereafter, pH2AX complex was isolated, separated on SDS-PAGE and analyzed by immunoblotting using anti-myc antibodies. **F-I**) The RNF8 FHA domain shows significant binding affinities for four putative phosphorylation sites on MDC1. Calorimetry measurements were performed on the MBP-RNF8 FHA domain using a VP-ITC microcalorimeter (MicroCal Inc.) essentially as described in Methods except that the buffer used contained 1 mM beta-mercaptoethanol. The phospho-peptides correspond to residues **F**) 695-702*, **G**) 715-722*, **H**) 748-758 **I**) 760-769 on MDC1. *Note: c-terminal A replaces more hydrophobic residues in actual MDC1 sequence for enhanced solubility.

Supplementary Figure 3. MDC1 but not its deletion mutant facilitates RNF8 IRIF formation. HeLa cells were transfected twice with MDC1 siRNA. **A**) Cell lysate was harvested and separated by SDS-PAGE to quantify MDC1 depletion. **B**) 24 hour post transfection either the siRNA resistant wild-type (WT) MDC1 or its deletion mutant (Del) was introduced into these MDC1-depleted cells. Cells were irradiated (10 Gy), fixed, permeabilised and immunostained with antibodies as indicated.

Supplementary Figure 4. RNF8 is required for local accumulation of BRCA1 and 53BP1 at the sites of DNA damage**.** Procedures were carried out as described in Methods and Figure 4a legend. Immunostaining were performed using indicated antibodies in **A)** and immunoblotting shown in **B)** indicates that depletion of RNF8 does not affect protein expression levels of MCPH1, BRCA1 or 53BP1. **C**) RNF8 depletion does not affect NBS1 IRIF formation. **D**) MDC1 is required for IRIF formation of BRCA1 and 53BP1. MDC1+/+ or MDC1-/- MEFs were irradiated (10Gy) and thereafter immuno-stained with indicated antibodies. **E**) Validation of siRNA-resistant RNF8 construct**.** 293T cells were co-transfected with Flag-tagged SiRNA-resistant tagged RNF8, myc-tagged RNF8 together with control siRNA or RNF8-specific siRNA#1 or siRNA#2. Cell lysates were prepared 24 hours post-transfection to evaluate the expression levels of RNF8 proteins using antibodies as indicated. **F)** IRIF formation of BRCA1 and 53BP1 requires both RNF8 FHA and RING domains. Procedures were carried out as described in Methods.

Supplementary Figure 5. A-C) H2AX (**A**), phospho-H2AX (**B**) and MDC1 (**C**) are all required for IRIF formation of DNA damage-associated ubiquitin conjugates. Wild-type

cells, H2AX-/- cells, H2AX-/- cells reconstituted with wild-type or S139A mutant of H2AX or MDC1-/- cells were irradiated and co-immunostained with anti-ubiquitin FK2 antibody and anti-H2AX antibody (**A, B**) or anti-pH2AX antibodies (**C**). **D**) Validation of siRNA targeting UBC13. HeLa cells was transfected with control siRNA or UBC13 siRNA. Cell lysates were prepared 24 hours post-transfection to evaluate the expression level of endogenous UBC13. Immunoblotting using antibody to Actin is included as loading control. **E**) IRIF formation of 53BP1 and BRCA1 is abolished in UBC13-depleted cells. HeLa cells transfected with control siRNA (siCTR) or UBC13 siRNA (siUBC13) were irradiated and immunostained with indicated antibodies.

Supplementary Figure 6. A-C) IR-induced H2AX ubiquitylation is dependent on MDC1, RNF8 and UBC13 but not BRCA1. **A**) MDC1 deficient cells or its wildtype counterpart were irradiated (10 Gy) or left untreated. Chromatin fractions were prepared 1 hr post-treatment to examine H2AX ubiquitylation using antibodies as indicated. Chromatin extracts prepared from HeLa cells were used as controls. Black arrow indicates doubly ubiquitylated species of H2AX, while grey arrow indicates mono-ubiquitinated H2AX. A non-specific band recognized by the anti-pH2AX antibody in extracts prepared from mouse cells is indicated by an asterisk (*). **B-C**) HeLa cells were transfected twice with indicated siRNAs and harvested 48 hours post-transfection. Chromatin fractions were separated by SDS-PAGE and blotted with pH2AX antibody (upper panels). Immunoblotting with indicated antibodies in the lower panels are included as controls. IR-dependent H2AX ubiquitylation requires RNF8 and UBC13 (**B, C**), but not BRCA1 (**B**). **D-E**) H2AX K119R mutation does not affect IR-dependent FK2

IRIF (**D**) or RNF8-dependent H2AX ubiquitylation (**E**). H2AX deficient cells were reconstituted with HA-tagged H2AX K119/120R mutant. Immunostaining and immunoblotting procedures are the same as that described for H2AX deficient MEFs reconstituted with wild-type or the S139A phosphomutant H2AX.

Supplementary Figure 7. **A**) IR-induced G2/M checkpoint is defective in cells with RNF8 depletion. HeLa cells were transfected with indicated siRNAs and percentages of mitotic cells before and after radiation were determined by FACS analysis as described in Experimental procedures. **B**) RNF8-dependent G2/M checkpoint control requires its FHA and RING domains. HeLa cells infected with viruses expressing siRNA-resistant full-length RNF8, delFHA or delRING mutant of RNF8 were transfected with siRNF8#2 to deplete endogenous RNF8. Cells were fixed and FACS analyses were conducted as described in Experimental procedures. **C**) Expression levels of RNF8 in HeLa cells treated with control siRNA or RNF8 siRNAs were assessed using anti-RNF8 antibodies.

Supplementary Figure 1

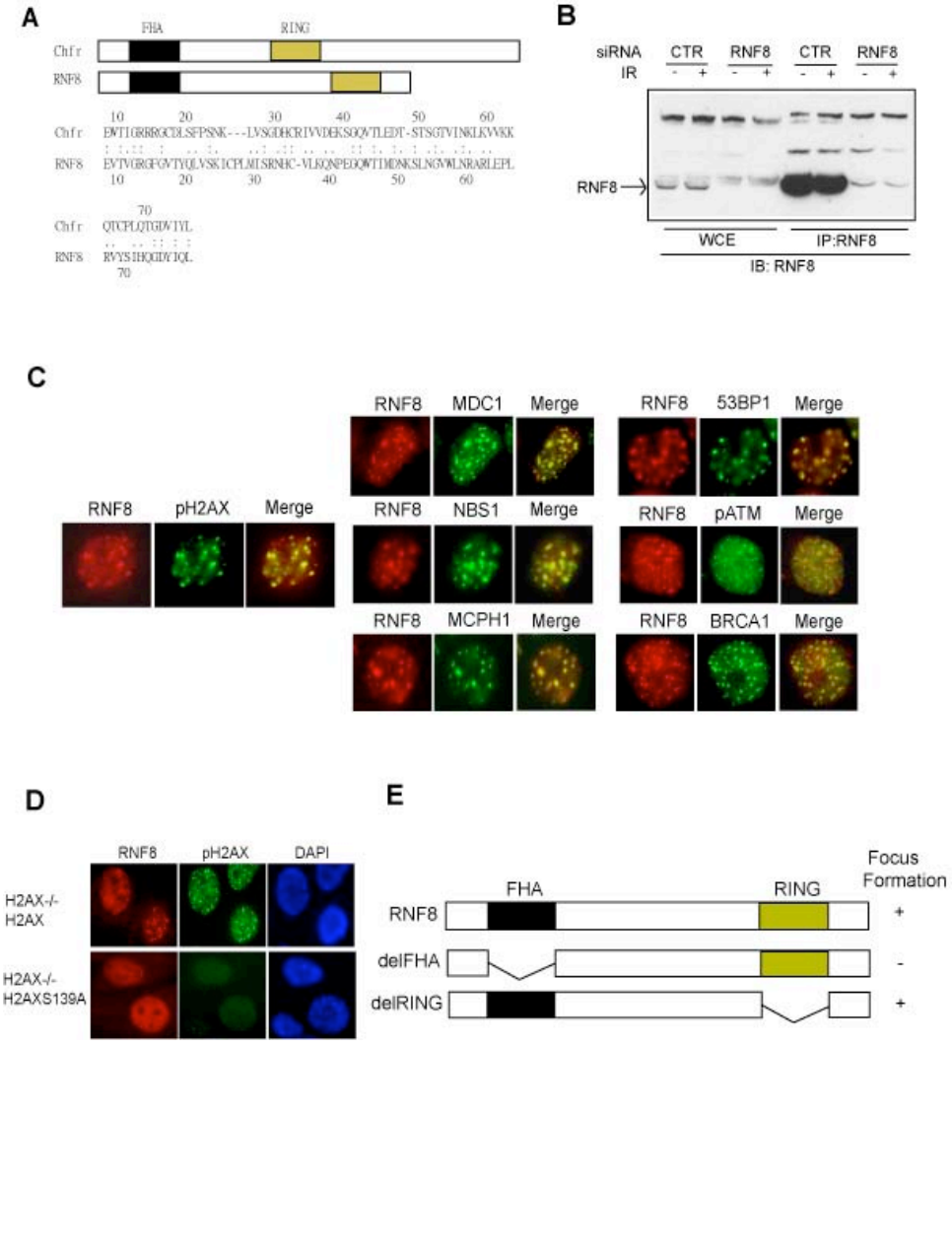

Supplementary Figure 2

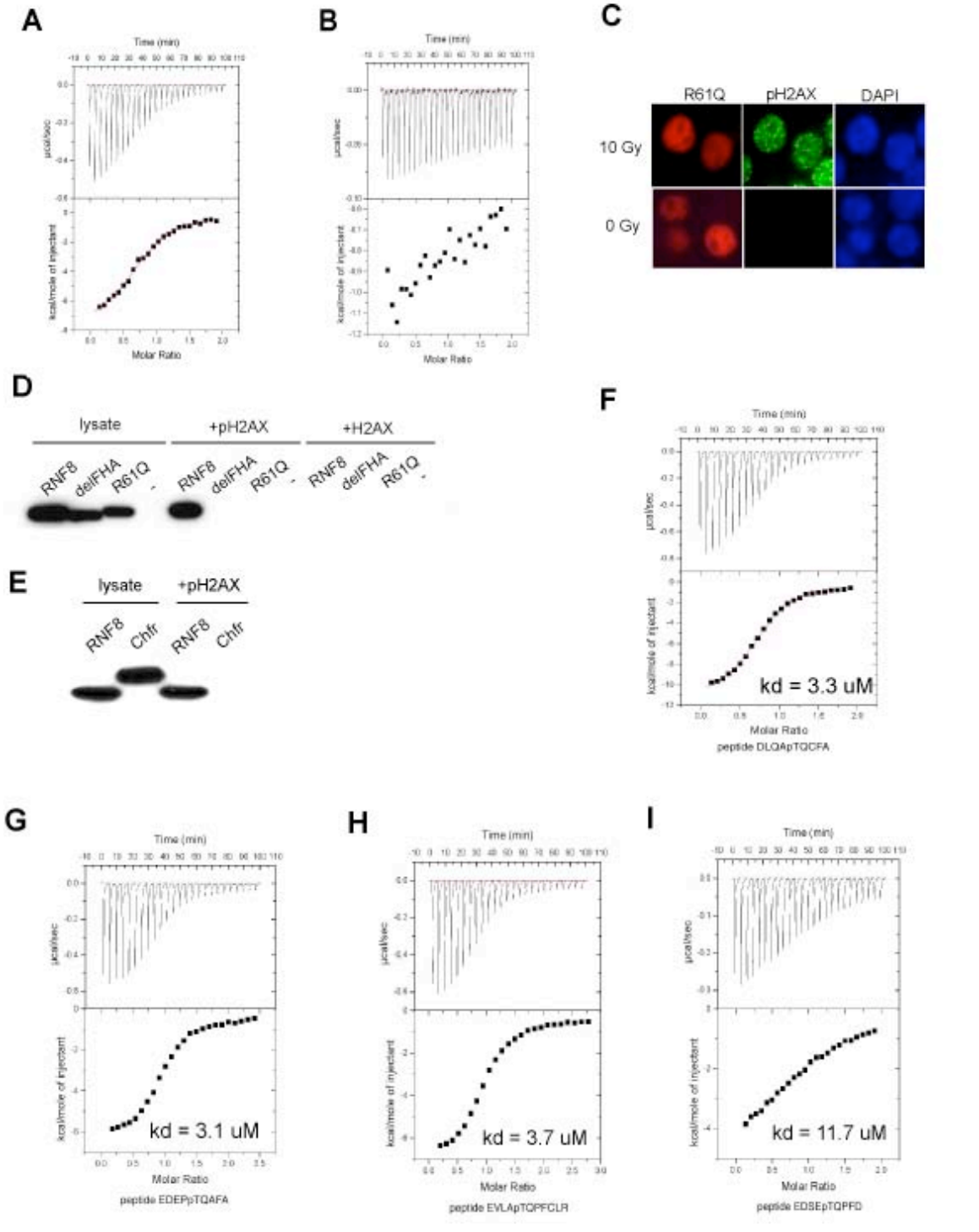

Supplementary Figure 3

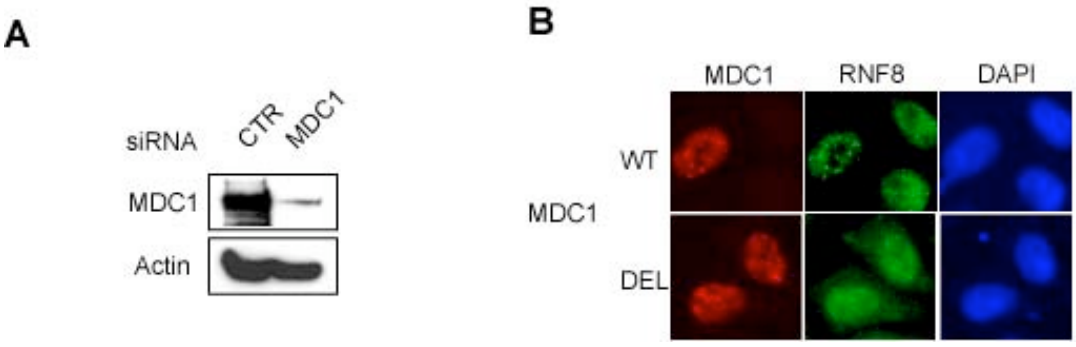

Supplementary Figure 4A-B

A

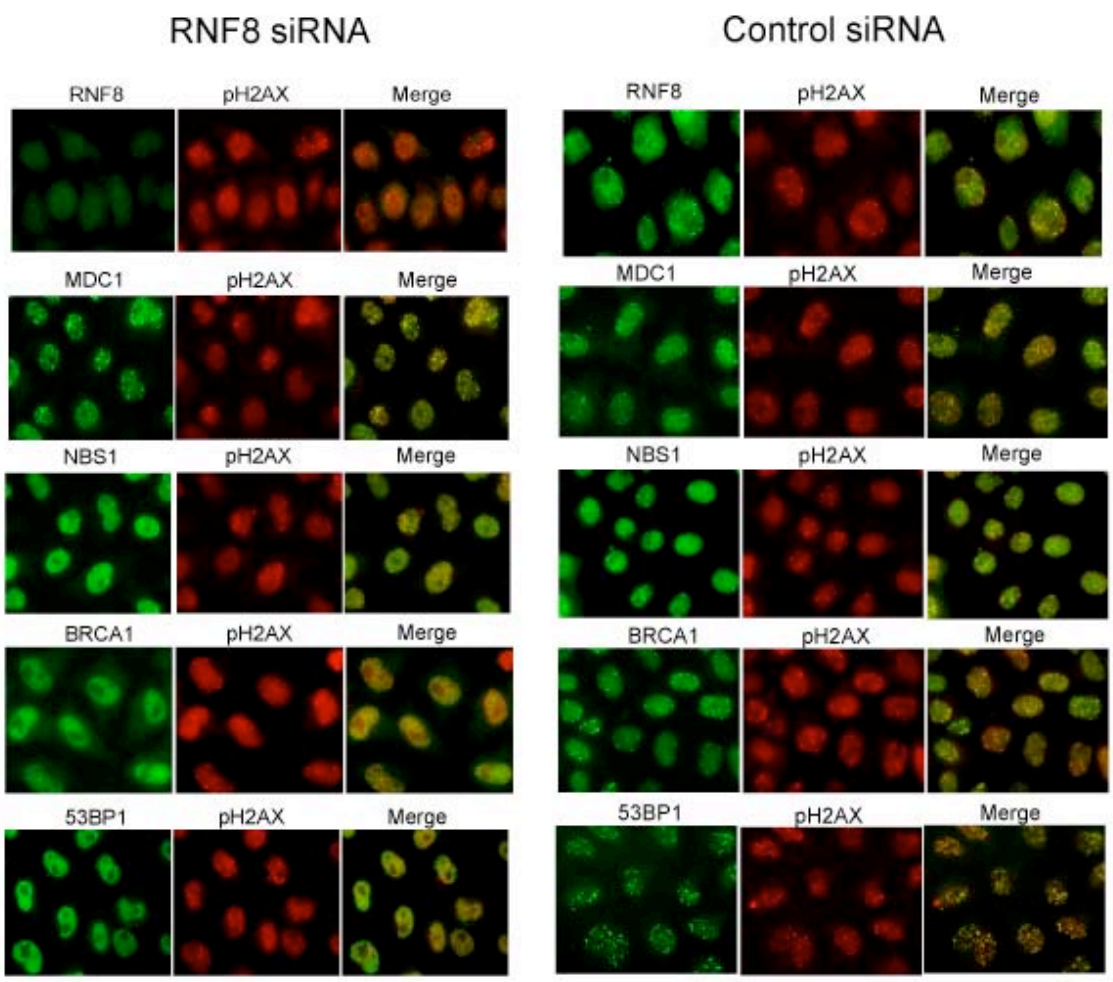

B

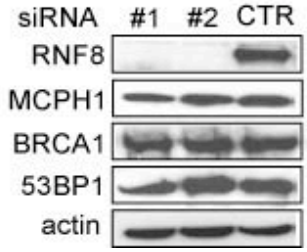

Supplementary Figure 4C-F

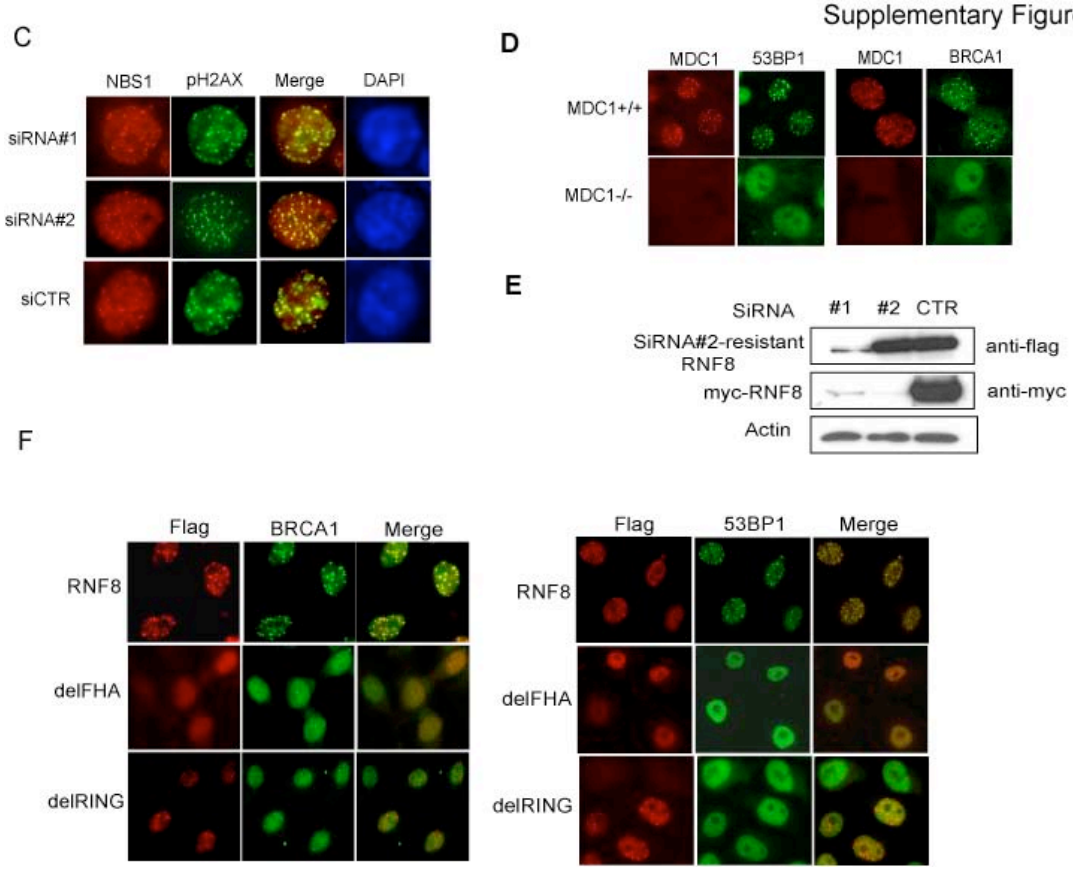

Supplementary Figure 5A-C

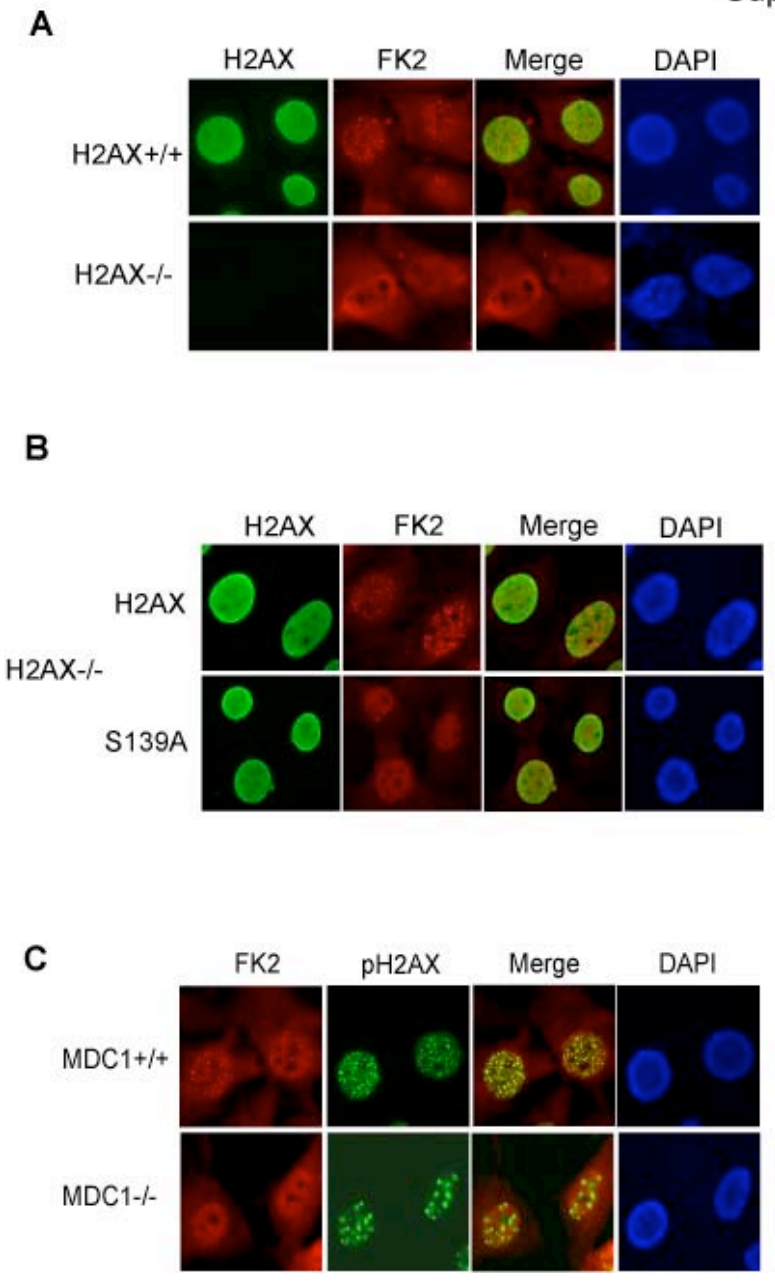

Supplementary Figure 5D-E

D

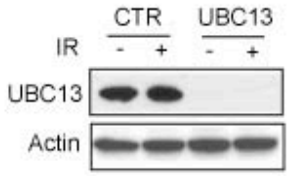

E

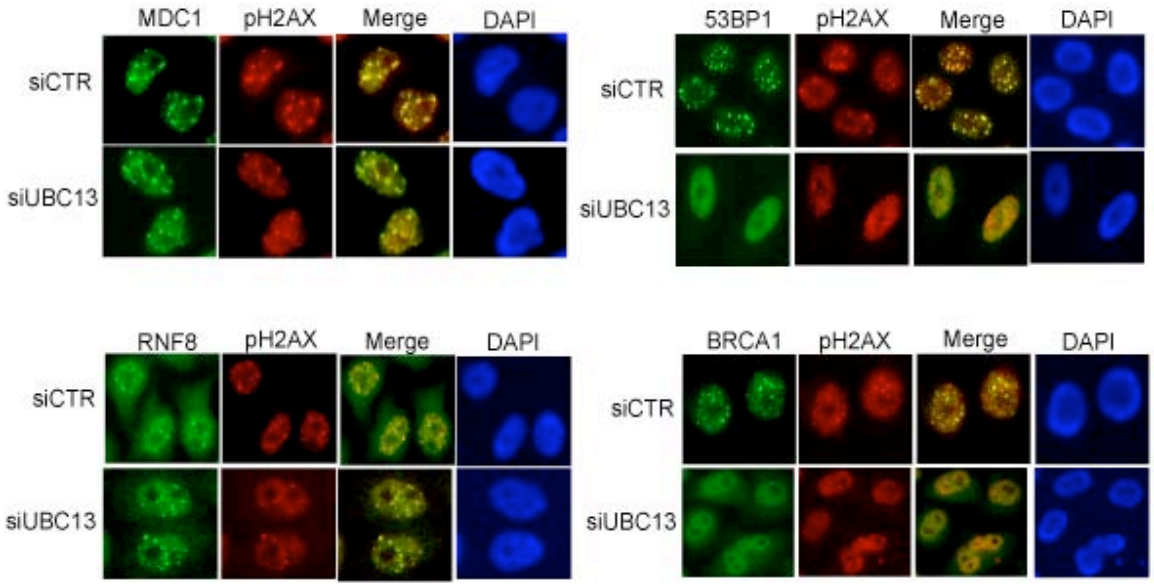

Supplementary Figure 6

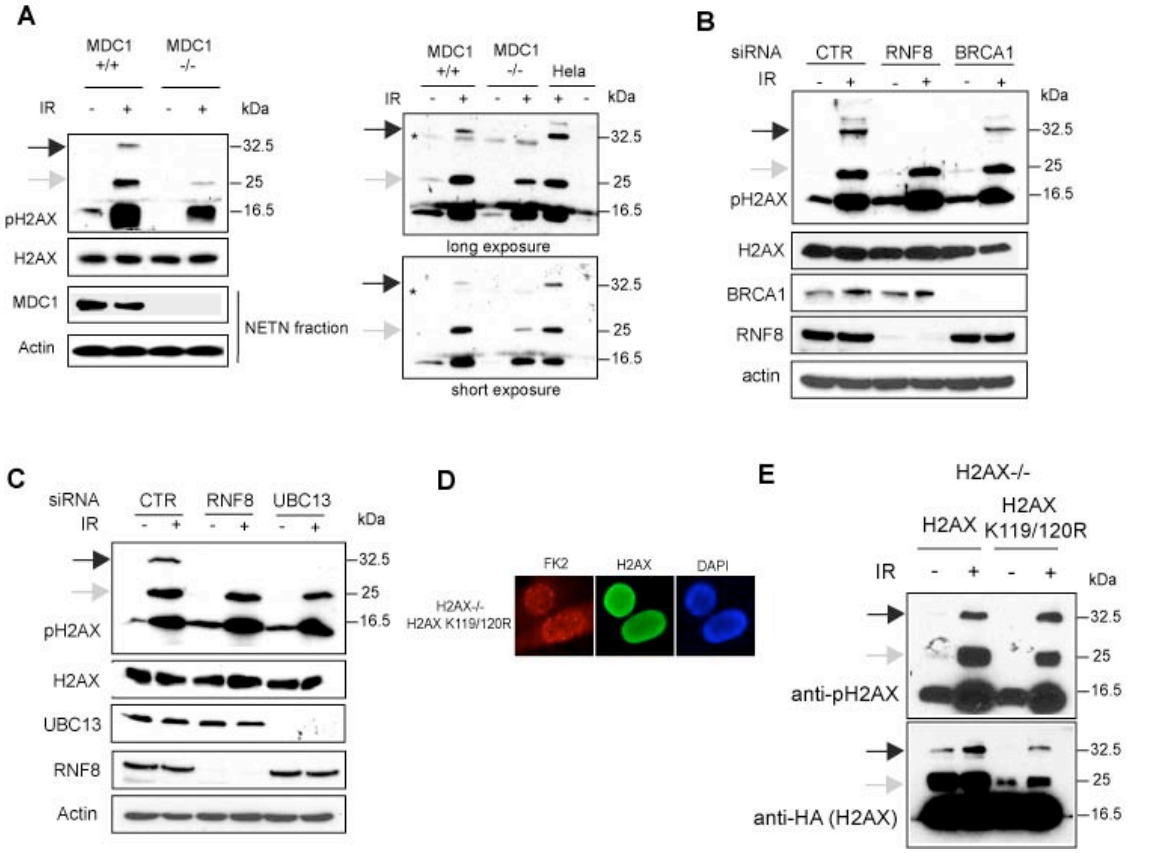

Supplementary Figure 7

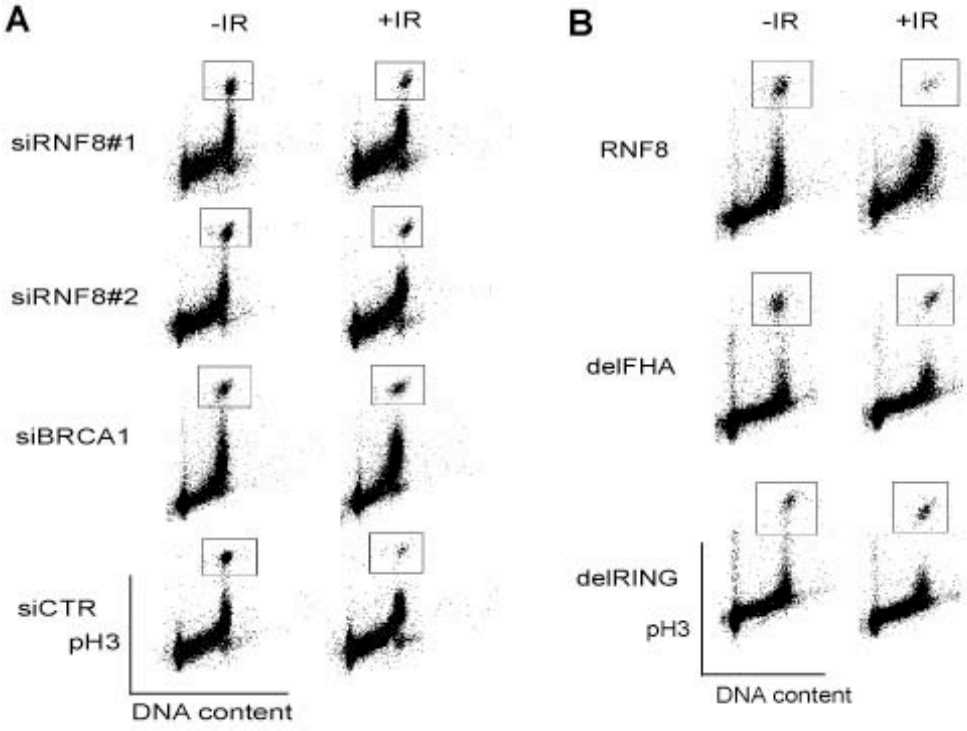

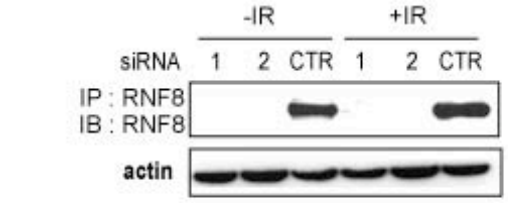

Supplemental Table 1 Crystallographic data collection and refinement

Data Collection

Data sets	anode	beamline	merged
Wavelength (Å)	1.54178	0.97946	
Resolution (Å)	50-1.7	50-1.35	50-1.35
R_{sym} (%)	4.9 (27.9)	5.2 (35.9)	5.6 (16.4) *
Completeness (%)	98.4 (86.0)	91.9 (99.9)	99.9 (99.7)
# observations	102108	217157	
# unique hkl	17966	33048	33838
average I/σ	22.8 (3.0)	21.1 (3.7)	24.7 (3.7)

values in parenthesis are for the high resolution shell
1.76 – 1.70 Å for Anode data set
1.40 – 1.35 Å for the Beamline data set

Refinement

Protein atoms	1239
Water molecules	180
Rwork	0.195
Rfree	0.215
RMS deviations	
bonds (Å)	0.007
angles (degrees)	1.31

$R_{sym} = \Sigma_h\Sigma_j |I_j(h) - \langle I(h)\rangle| / \Sigma_h\Sigma_j \langle I(h)\rangle$, where $I_j(h)$ is the j^{th} reflection of index h and $\langle I(h)\rangle$ is the average intensity of all observations of I(h)

$R_{work} = \Sigma_h |F_{obs}(h) - F_{calc}(h)| | / \Sigma_h |F_{obs}(h)|$, calculated over the 95% of the data in the working set. R_{free} equivalent to R_{work} except calculated over the 5% of the data assigned to the test set